

Titre: Re-engineering of superalloy power shaft for turbine engine
Title:

Auteur: Roberto Grassi
Author:

Date: 2004

Type: Mémoire ou thèse / Dissertation or Thesis

Référence: Grassi, R. (2004). Re-engineering of superalloy power shaft for turbine engine
Citation: [Mémoire de maîtrise, École Polytechnique de Montréal]. PolyPublie.
<https://publications.polymtl.ca/8414/>

 **Document en libre accès dans PolyPublie**
Open Access document in PolyPublie

URL de PolyPublie: <https://publications.polymtl.ca/8414/>
PolyPublie URL:

**Directeurs de
recherche:** Marek Balazinski, & Ioan Sasu
Advisors:

Programme: Non spécifié
Program:

UNIVERSITÉ DE MONTRÉAL

**RE-ENGINEERING OF SUPERALLOY POWER SHAFT
FOR TURBINE ENGINE**

**ROBERTO GRASSI
DÉPARTEMENT DE GÉNIE MÉCANIQUE
ÉCOLE POLYTECHNIQUE DE MONTRÉAL**

**MÉMOIRE PRÉSENTÉ EN VUE DE L'OBTENTION
DU DIPLÔME DE MAÎTRISE ÈS SCIENCES APPLIQUÉES
(GÉNIE MÉCANIQUE)**

Août 2004

©Roberto Grassi, 2004.



Library and
Archives Canada

Published Heritage
Branch

395 Wellington Street
Ottawa ON K1A 0N4
Canada

Bibliothèque et
Archives Canada

Direction du
Patrimoine de l'édition

395, rue Wellington
Ottawa ON K1A 0N4
Canada

Your file *Votre référence*
ISBN: 978-0-494-47667-3
Our file *Notre référence*
ISBN: 978-0-494-47667-3

NOTICE:

The author has granted a non-exclusive license allowing Library and Archives Canada to reproduce, publish, archive, preserve, conserve, communicate to the public by telecommunication or on the Internet, loan, distribute and sell theses worldwide, for commercial or non-commercial purposes, in microform, paper, electronic and/or any other formats.

The author retains copyright ownership and moral rights in this thesis. Neither the thesis nor substantial extracts from it may be printed or otherwise reproduced without the author's permission.

AVIS:

L'auteur a accordé une licence non exclusive permettant à la Bibliothèque et Archives Canada de reproduire, publier, archiver, sauvegarder, conserver, transmettre au public par télécommunication ou par l'Internet, prêter, distribuer et vendre des thèses partout dans le monde, à des fins commerciales ou autres, sur support microforme, papier, électronique et/ou autres formats.

L'auteur conserve la propriété du droit d'auteur et des droits moraux qui protègent cette thèse. Ni la thèse ni des extraits substantiels de celle-ci ne doivent être imprimés ou autrement reproduits sans son autorisation.

In compliance with the Canadian Privacy Act some supporting forms may have been removed from this thesis.

While these forms may be included in the document page count, their removal does not represent any loss of content from the thesis.

Conformément à la loi canadienne sur la protection de la vie privée, quelques formulaires secondaires ont été enlevés de cette thèse.

Bien que ces formulaires aient inclus dans la pagination, il n'y aura aucun contenu manquant.


Canada

UNIVERSITÉ DE MONTRÉAL
ÉCOLE POLYTECHNIQUE DE MONTRÉAL

Ce mémoire intitulé:

**RE-ENGINEERING OF SUPERALLOY POWER SHAFT
FOR TURBINE ENGINE**

présenté par : GRASSI Roberto

**en vue de l'obtention du diplôme de: Maîtrise ès sciences appliquées
a été dûment accepté par le jury d'examen constitué de:**

M. BARON, Luc, Ph.D., président

M. BALAZINSKI, Marek, Ph.D., membre et directeur de recherche

M. SASU, Ioan, Ph.D., membre et codirecteur de recherche

M. TURENNE, Sylvain, Ph.D., membre

ACKNOWLEDGEMENT

I would like to thank my co director Ioan Sasu who welcomed me at Pratt & Whitney Canada. I am grateful for his support by means of funding and encouragement. The successful completion of this work was not possible without his useful ideas and interest in my work. From Pratt & Whitney Canada, I also want to underline the support received from the stress analysis specialist Abdel Fattah Elsayaf, the material specialist Isabelle Bacon and the dynamic analysis specialist Yves Fournier.

Special thanks are due to Professor Marek Balazinski for critical suggestions and comments. His dedication in teaching and enthusiasm inspired me to start exploring the field of manufacturing.

I am grateful to my colleagues Acher Igal Abenhaim and Marius Petean, whose company made my studies at École Polytechnique de Montréal a very joyful experience.

Last but most important, I want to thank my parents, Rosa and Nazzareno, my grandmother Antonia and aunt Teresa along with my brother Claudio and my girlfriend Chayma, for listening to my problems and being able to provide me with constructive comments.

Finally, I want to dedicate this work to my grandfather Eugenio, who always believed in my capacities. Even if he's not in this world anymore, he's still present in me.

ABSTRACT

This thesis deals with the re-engineering of the superalloy power shaft for the PW307 turbofan engine of Pratt & Whitney Canada (PWC). The objectives of the project are to lower the machining time and material removal, fix the concentricity problem between the inside and outside diameters of the shaft and overcome the difficulties of machining Inconel 718.

As explained in the bibliographical review, it is known that a power shaft can be manufactured by friction welding two different materials. Moreover, since the current power shaft is made from Inconel 718, and this material can be flow formed, it represents another manufacturing opportunity.

This thesis is composed of four chapters. In the first chapter, a bibliographic review presents the basic notions on the shafts for aeronautics and automotive, it covers the superalloy materials for high temperatures and explains the different manufacturing technologies for assembling and cold forming. In the second chapter, the problem statement and context is described along with the objectives and motivation of the project. In chapter three, the actual design and manufacturing technique used to make the power shaft are detailed. In the last chapter, there is an explanation of an optimization technique developed for the design of the shaft; new design configurations as well as manufacturing techniques that are proposed to make the new shaft and tests. Finally, the conclusion states the achievements of the projects as well as the future work suggestions.

To prove the possibility of the new design configurations, analytical analyses have been done and are included in chapter four. For the manufacturing technique retained for this project, tests are taking place for inertia welding and a contract proposal was received for the flow forming technique. In conclusion, using friction welding or the flow forming technique, great cost reduction of the power shaft's manufacturing will be achieved and

thanks to the computer program performing the design optimization, weight reduction of the power shaft is accomplished.

RÉSUMÉ

Ce mémoire traite de la ré-ingénierie de l'arbre de transmission de puissance en super alliage pour la turbosoufflante PW307 de Pratt & Whitney Canada. Les objectifs du projet sont de diminuer le temps d'usinage et la quantité de matière à enlever, régler le problème de concentricité entre les diamètres intérieurs et extérieurs de l'arbre, et surmonter les difficultés d'usinage de l'Inconel 718.

Comme expliqué dans la revue bibliographique, on sait qu'un arbre de transmission de puissance peut être fabriqué en soudant par friction deux matériaux différents. De plus, étant donné que l'arbre actuel est fait d'Inconel 718, et que ce matériau peut être formé par fluotournage, ceci représente une autre option de fabrication.

Ce mémoire se compose de quatre chapitres. Dans le premier chapitre, une revue bibliographique présente les notions de base sur les arbres pour l'aéronautique et le domaine de l'automobile, d'ailleurs il traite des matériaux en super alliage pour les températures élevées et explique les différentes technologies de fabrication pour assembler et former à froid. Dans le deuxième chapitre, le problème et le contexte du projet sont décrits avec les objectifs et la motivation du projet. Au chapitre trois, la technique de conception et de fabrication actuelle, qui est employée pour faire l'arbre de transmission de puissance sont détaillée. Dans le dernier chapitre, on retrouve l'explication d'une technique d'optimisation du design qui a été développée, des nouveaux designs de l'arbre ainsi que les techniques de fabrication proposées et des essais. À la fin, les plus importantes conclusions du projet sont présentés avec des suggestions pour travaux futurs.

Pour démontrer le potentiel de ces nouveaux designs, des analyses ont été faites et sont incluses dans le chapitre quatre. Pour les techniques de fabrication retenues pour ce

projet, des essais ont eu lieu pour la soudure par friction et une proposition de contrat a été reçue pour la technique de fluotournage.

En conclusion, l'utilisation de la soudure par friction ou le fluotournage permet une grande réduction des coûts de fabrication de l'arbre de transmission de puissance tandis que l'optimisation de la forme par le logiciel d'optimisation du design permet une importante diminution de la masse totale de la pièce.

CONDENSÉ EN FRANÇAIS

Pratt et Whitney Canada (PWC) est un pionnier dans la conception et la fabrication de petites et moyennes turbosoufflantes à gaz. Pour maintenir sa position de leader mondial, PWC doit continuellement réduire ses coûts de fabrication et améliorer la qualité de ses produits afin de les offrir à des prix concurrentiels. Dans ce contexte, l'innovation technologique devient une priorité. En conséquence, il est essentiel d'être à jour avec les technologies de fabrication, en s'assurant toujours que celles utilisées sont les meilleures technologies disponibles.

Introduction

La pièce faisant l'objet de ce projet est l'arbre de transmission de puissance de la turbosoufflante PW307 de PWC. L'arbre a une forme complexe et il est difficile à fabriquer. PWC a suggéré d'analyser la soudure par friction et le fluotournage comme techniques pour aider à la fabrication de cet arbre.

Dans une turbosoufflante, deux sections peuvent être distinguées. Le devant de la turbosoufflante où l'air entre, représentant la section froide et l'arrière de la turbosoufflante, où la combustion a lieu, définissant la section chaude. Lorsque la turbosoufflante PW307 est en fonction, il y a une grande différence de température à travers sa longueur, entre la section froide et chaude, qui va de 534F° à 928 F°.

Une revue de littérature des arbres de transmission de puissance, des matériaux en superalliage et des technologies de fabrication, est détaillée au chapitre 1. Au chapitre 2 on retrouve la définition du problème et le contexte du projet. Le chapitre 3 inclut de l'information sur les techniques de conception et de fabrication qui sont actuellement employées pour fabriquer l'arbre. Au chapitre 4, la réingénierie de l'arbre est détaillée et les résultats des essais sont analysés. À la fin, les plus importantes conclusions du projet sont présentées avec des suggestions pour des travaux futurs.

Revue de littérature

Comme mentionné, la revue de littérature présente les technologies de fabrication des arbres de transmission de puissance et les matériaux en superalliages qui sont employés pour les fabriquer. De plus, une revue des articles, sur la soudure par friction et le fluotournage, est détaillée.

Après une recherche sur des articles couvrant l'arbre de transmission de puissance pour une turbosoufflante, il est possible de déclarer que relativement peu de recherches et développements ont été publiés sur ce sujet jusqu'à ce moment. Le seul article qui va vraiment en détail sur la fabrication d'un arbre de transmission de puissance pour une turbosoufflante est l'article de J.A. Miller et de J.J. O'Connor (1980) [1]. Cet article explique comment un arbre de transmission de puissance pour une turbosoufflante Lycoming T55 est soudé par friction et faisceau d'électrons. L'arbre est construit d'une seule pièce rigide et fabriquée en utilisant trois aciers différents, chacun choisi selon l'endroit et la fonction. Bien que les articles sur les arbres de transmission de puissance pour une turbosoufflante soient presque inexistantes, quelques articles sur la fabrication des arbres latéraux pour les voitures ont été retenus. Ces articles sont très intéressants parce que les problématiques sont similaires. P. Amborn, H. Frielingsdorf, S.K. Ghosh et K. Greulich (1995) [2], ont présenté une comparaison générale des divers processus qui sont appliqués aux techniques courantes et nouvelles pour la fabrication des arbres latéraux modernes pour les voitures. Dans un autre article, P. Amborn, S.K. Ghosh et I.K. Leadbetter (1997) [3], font une revue d'ensemble des principaux développements dans la conception et la fabrication des arbres latéraux pour les voitures et regardent plus spécifiquement les conditions requises pour les arbres tubulaires et monobloc.

D.G. Backman et J.C. Williams (1992) [4] présentent dans leur article un résumé des développements des matériaux structuraux pour les moteurs d'avions. M. Rahman,

W.K.H. Seah et T.T. Teo (1997) [5] discutent des conditions d'usinabilité de l'Inconel 718. Ce dernier est un alliage à base de nickel à haute résistance thermique, qui joue un rôle de plus en plus important dans le développement et la fabrication des moteurs aéronautiques pour les avions à réaction. J. Albrecht (1999) [6] a comparé le comportement en fatigue des alliages à base de titane et nickel. Particulièrement dans les applications aérospatiales, les alliages en titane sont en concurrence avec les alliages en nickel, car les alliages en titane ont l'avantage d'avoir une densité plus faible. E.O. Ezugwu, J. Bonney et Y. Yamane (2003) [7] donnent une vue d'ensemble de l'usinabilité des alliages pour les moteurs aéronautiques.

M. Soucail et Y. Bienvenu (1996) [8] expliquent la dissolution à l'équilibre de la phase γ' dans un superalliage à base de nickel, lorsqu'elle a chauffé rapidement comme dans le cas du soudage par friction. Y. Yamashita, T. Yoshida et K. Fujita (1998) [9] ont fait une recherche sur l'application de la soudure par friction sur des joints de matériaux différents pour les usines d'énergie électrique. L'article de M. Preuss, J.W.L. Pang, P.J. Withers et G.J. Baxter (2002) [10] décrit une étude quantitative de la microstructure des tubes en superalliage à base de nickel, qui sont joint avec une soudure par friction. M. Preuss, J.W.L. Pang, P.J. Withers et G.J. Baxter (2002) [11], ont écrit un article sur les gradients microstructuraux élevés, qui ont été observés dans les assemblages de tubes de superalliage à base nickel, soudées par friction. Dans l'article de L. D'Alvise, E. Massoni et S.J. Walløe (2002) [12], il est expliqué comment faire l'analyse par éléments finis du procédé de soudure par friction entre des matériaux différents.

L'article de M. Jahazi et de G. Ebrahimi (2000) [13] étudie les influences des paramètres de fluotournage et de l'état de la microstructure sur la qualité et les propriétés mécaniques de l'acier D6ac (0.43C – 0.74Mn – 0.26Si – 1.0Cr – 0.59Ni – 0.96Mo – 0.1V – 0.01Al – 0.01P – 0.003S). H. Näegel, H. Wörner et M. Hirschvogel (2000) [14] démontrent l'importance pour un fournisseur de combiner les opérations de formage et d'usinage. K.S. Lee et L. Lu (2001) [15] ont présenté une étude sur le fluotournage de tubes

cylindrique utilisant un mécanisme de roulement. Dynamics Machines Works (www.flowforming.com) sont des leaders en fluotournage. Après des années de fluotournage d'Inconel 718, ils affirment que le fluotournage offre aux concepteurs la possibilité d'explorer des propriétés en tension très élevées et des grains très raffinés suites à un traitement thermique.

Définition du problème

L'arbre de transmission de puissance de la turbosoufflante PW307 a un profil externe complexe et son centre est évidé par perçage. Actuellement, l'arbre est fabriqué à partir d'une barre ronde d'Inconel 718. La gamme de fabrication présente les problèmes suivants :

1. 80% de la matière doit être enlevée;
2. le contrôle de la concentricité, entre les diamètres internes et externes de l'arbre, est complexe;
3. il est difficile d'usiner l'Inconel 718.

En plus de ces problèmes techniques, le coût de fabrication des arbres devrait être diminué afin de demeurer concurrentielle sur les marchés internationaux.

L'objectif principal de ce projet est d'explorer des solutions aux problèmes techniques, qui viennent d'être mentionnés, de même que de diminuer les coûts de fabrication. Afin de réaliser ces buts, l'approche adoptée n'est pas seulement basée sur un changement de technologie de fabrication, mais aussi sur la maîtrise et la modification du design actuel de l'arbre de transmission de puissance. Il est essentiel de changer et d'adapter le design de l'arbre pour pouvoir employer différentes technologies de fabrication qui n'étaient pas convenable avec le design original. Si on veut réaliser un arbre avec des meilleures performances et à prix raisonnable, la conception doit être intégrée avec la fabrication.

Puisque le design de l'arbre sera modifié, un autre objectif de ce projet est de s'assurer que le nouveau design sera optimal. La technique d'optimisation consiste à maximiser l'utilisation du matériau dans l'arbre, en d'autres termes, éviter que des sections soient surdimensionnées, ce qui résulterait en un excès de poids. Pour faciliter cette optimisation, un logiciel a été développé. Ainsi, les objectifs pour ce qui concerne le design de l'arbre sont les suivants :

1. Concevoir une technique d'optimisation du design de l'arbre;
2. Développer un logiciel, qui intègre cette technique d'optimisation.

Avant de lancer le projet, PWC a suggéré des techniques de fabrication pour faciliter l'usinage de l'arbre de puissance. Les techniques conseillées sont les suivantes : technique de soudage par friction pour fabriquer un arbre de transmission multi matériaux et la technique de fluotournage.

Design et fabrication de l'arbre de transmission de puissance de la turbosoufflante PW307

Le profil extérieur d'un arbre est déterminé par les composantes de la turbosoufflante qui sont assemblés sur l'arbre et de l'espace disponible entre celui-ci et les composantes voisines. Cependant, le profil intérieur dépend des analyses en contraintes et en dynamique ainsi que de la technique d'usinage pour évider le centre de l'arbre.

L'analyse des contraintes est effectuée par un logiciel de PWC conçu à cette fin. P0889 est un logiciel d'analyse des contraintes d'un arbre écrit en Fortran 77. Il est employé pour déterminer les contraintes et la durée de vie de la plupart des arbres de PWC. Fondamentalement, il y a sept types d'analyses disponibles: l'analyse en fatigue olygocyclique et vibratoire, précession gyroscopique, perte de lame de soufflante (analyse de chargement ultime), impact d'un grand oiseau (analyse de chargement ultime), impact d'un oiseau moyen (analyse de chargement limite), perte de lame de

turbine (analyse de chargement ultime), couple de saisie (analyse de chargement ultime). Afin d'être acceptable, chaque analyse doit générer des facteurs de design plus petit que la valeur acceptable propre à chacune. Les facteurs de design générés sont proportionnels à la vie en nombre de cycles. Lorsqu'un facteur de design correspond à la valeur acceptable, la vie en nombre de cycles correspond à la vie en nombre de cycles garantie. Pour une turbosoufflante, un cycle représente une mission qui va du décollage jusqu'à l'atterrissage d'un avion. Pour la turbosoufflante PW307, la vie en nombre de cycles garantie est de 20 000 cycles. Pour l'analyse en fatigue olygocyclique et vibratoire, le facteur de design correspond à la contrainte élastique équivalente de la fatigue vibratoire dérivant des forces appliquées divisées par la contrainte de limite élastique du matériau de l'arbre. Ce facteur de design ne doit pas être plus grands que 1.0 pour que la section soit acceptable. Pour l'analyse gyroscopique de précession, le facteur de design représente la contrainte gyroscopique équivalente en fatigue vibratoire divisée par la contrainte permise en fatigue vibratoire. Ce facteur de design doit être sous la valeur de 1.0 pour que la section soit approuvée. Le facteur de design pour les analyses de charge ultime, qui est la contrainte plastique effective divisée par la contrainte ultime en tension, peut être au-dessus de 1.0, s'il peut être comparé aux résultats d'essais expérimentaux. Pour l'arbre de la turbosoufflante PW307, la valeur exigée est 1.34 pour la perte de lame de compresseur et 1.6 pour les impacts de grands oiseaux et cela pour les premières 7 sections de concentration de contraintes de l'arbre. Le facteur de design pour les analyses de charge limite, qui correspond au rapport de la contrainte élastique maximum divisée par la limite élastique du matériau, peut être au-dessus de 1.0 s'il peut être comparé aux résultats d'essais expérimentaux. Pour l'arbre de la turbosoufflante PW307 la valeur exigée est de 1.7 pour l'impact d'oiseau moyen.

Quand un nouveau design d'arbre de transmission de puissance est conçu, une étape importante pour son approbation finale est la vérification des vitesses critiques, de la manœuvre en état d'équilibre, de la réponse non équilibrée, ainsi que la réponse transitoire de l'arbre lors d'impacts avec des lames ou des oiseaux. Afin de valider un

arbre de transmission de puissance, le logiciel P0571 prend soin de vérifier toutes les analyses mentionnées. En général, avant d'exécuter le programme P0571, la manipulation de quelques données doit être faite. Premièrement, les modèles 3D de chacune des composantes du système dynamique sont transformés en points avec une fonction dans CATIAV4 qui a été spécifiquement créée à cette fin. Par la suite, ces points sont traités dans un logiciel spécial de PWC (NASBEAM) qui génère un fichier compatible avec NASTRAN, qui sera utilisé comme fichier d'entrée dans le programme P0571.

Pour avoir un arbre qui est dynamiquement acceptable, l'énergie de déformation sur l'arbre de transmission de puissance ne devrait pas être plus de 50% de toute l'énergie de déformation. Une autre contrainte est que le troisième mode de fréquence naturelle devrait se produire à une vitesse correspondant à 120% de la vitesse maximale de la turbosoufflante (dans notre cas 11 000 t/min). Un exemple de fichier qui est généré par le logiciel P0571 est disponible en annexe à la section 8.

Ré ingénierie de l'arbre de transmission de puissance de la turbosoufflante PW307

Ce qui suit est le noyau du projet constituant ma contribution personnelle. Dans la première partie, l'aspect de conception est discuté après quoi, les techniques de fabrication qui ont été retenues sont expliquées.

Débutant par l'aspect de la conception, l'optimisation du design est concentrée sur le profil intérieur de l'arbre, qui représente la partie la plus difficile à usiner. Le profil intérieur dépend des analyses en contraintes et en dynamique ainsi que de la technique d'usinage pour éviter le centre de l'arbre. Pour maintenir les choses simples, l'extérieur de l'arbre de transmission de puissance est gardé tel quel. Il serait trop long pour les fins de ce projet de commencer à vérifier la possibilité de modifier le profil extérieur de l'arbre à cause de trop inconnus.

En observant l'analyse en fatigue olygocyclique et vibratoire de l'arbre actuel faite avec le logiciel P0889, il est possible de noter que toutes les sections de concentration de contraintes ont des facteurs de design, qui correspondent à la contrainte équivalente divisée par la contrainte permise du matériau, inférieur à 1.0 et sont donc tous acceptables. Cependant, la plus part des valeurs sont beaucoup plus petites que 1.0, ce qui signifie qu'il y a un excès de matériau et ces sections sont plus fortes que requises. Cela peut également être remarqué si on observe les valeurs des cycles de vie pour les sections qui sont plus fortes que requis. Il est possible de voir le lien parce que ces résultats sont de 1 000 000 cycles ce qui représente une vie infinie et donc excèdent de beaucoup les 20 000 cycles garantis par PWC pour cette turbosoufflante. Entre les valeurs des facteurs de design et les cycles de vie, il est également possible de noter une corrélation qui est inversement proportionnelle. Plus la valeur des facteurs de design est proche de 1.0, plus la durée de vie est voisine de 20,000 cycles. La technique d'optimisation est basée sur l'agrandissement du diamètre intérieur des sections de concentration de contraintes, là où la valeur du facteur de design est beaucoup plus basse de 1.0. Ceci aura comme effet de rapprocher le facteur à 1.0 et par le fait même aux 20,000 cycles de vie. Si on applique ces techniques à toutes les sections dont la valeur du facteur de design est beaucoup plus petite que 1.0, il est possible de diminuer le poids de l'arbre de transmission de puissance de 5.472 livres. Pour supporter ce résultat, une analyse dynamique avec le logiciel P0571 a été faite. Puisque l'optimisation des sections a été faite manuellement et était très longue, on a décidé de développer un logiciel qui pourrait le faire automatiquement. Le logiciel P0889 pour l'analyse des contraintes d'un arbre a été écrit en FORTRAN77. Il a été décidé ainsi de développer le nouveau logiciel dans le même langage pour pouvoir boucler sur le logiciel P0889 sans avoir à le modifier. Ce nouveau logiciel "P0889opt" va permettre de rendre l'optimisation répétable et augmenter considérablement la vitesse de l'optimisation.

Comme mentionné dans l'introduction, PWC a suggéré l'utilisation de la soudure par friction et la technique de fluotournage pour fabriquer cet arbre. Suite à la revue de

littérature, il est possible de dire que la soudure par friction est recommandée dans l'article de J.A. Miller et J.J. O'Connor (1980) [1] et P. Amborn, H. Frielingsdorf, S.K. Ghosh et K. Greulich (1995) [2], alors que l'article de P. Amborn, S.K. Ghosh et d'I.K. Leadbetter (1997) [3] appui la technique de fluotournage pour les arbres cylindriques.

Lors de la soudure par frottement, une des pièces est attachée à une unité entraînée par un moteur, alors que l'autre pièce est retenue (Figure I). La pièce entraînée par le moteur est tournée à une vitesse constante prédéterminée. Les pièces à souder sont rapprochées, et une force est appliquée. De la chaleur est générée pendant que les surfaces en contact se frottent. Ceci continue pendant un temps prédéterminé ou jusqu'à quand une distance de l'avancement d'une pièce dans l'autre est atteinte. Ensuite, l'entraînement est cessé, et la pièce tournante est arrêtée par l'application d'une force. La force de la soudure par friction est maintenue ou augmentée pendant un temps prédéterminé après la que la rotation du moteur ait cessé.

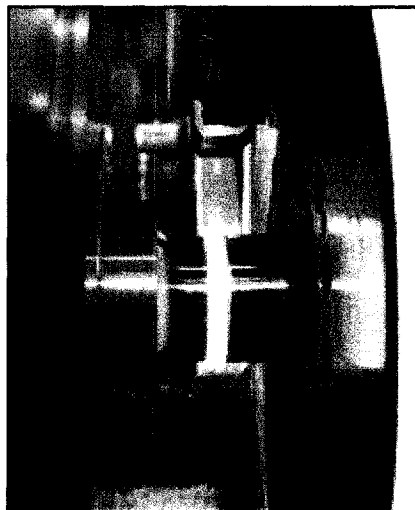


Figure I: Déplacement du matériau à l'état plastique lors du soudage par frottement

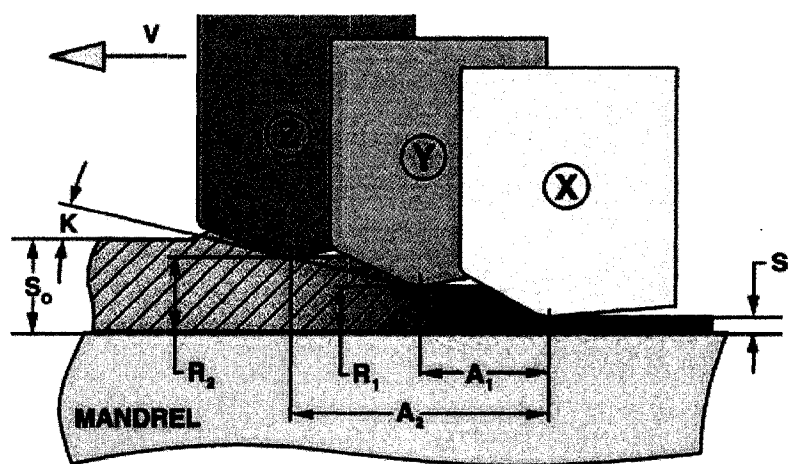
En analysant les températures d'opération de la turbosoufflante, on peut constater que seulement la section de l'arbre de transmission de puissance, qui est soumise à 928F°, a vraiment besoin de l'Inconel 718. Ceci représente seulement 21% (11.125" sur 53.125") de l'arbre. Après cette analyse, il est possible de conseiller l'Inconel 718 pour la section à

928F° et un acier pour le reste. Ceci est réalisable avec l'utilisation de la soudure par friction, qui permet de souder des matériaux de natures différentes. Puisque PWC n'utilise que des matériaux qui ont été caractérisés par eux, CPW245 (17-22A) et HCM3 sont des aciers qui pourraient être employés pour faire la section froide de l'arbre.

Avant de commencer les tests en laboratoire, des analyses de contraintes par le logiciel P0889 ont été faites sur différentes configurations d'arbres multi-matériaux. Les configurations proposées sont les suivantes: CPW245 et Inconel 718, HCM3 et Inconel 718, CPW245 et HCM3 et Inconel 718. De plus pour garantir que ces configurations multi-matériaux respectent aussi les spécifications dynamiques, des analyses par le logiciel P0571 ont aussi été effectuées. Toutes les configurations permettent des diminutions de poids grâce à la technique d'optimisation du design, et des réductions des coûts d'usinage par le remplacement de l'Inconel 718 avec des aciers. La configuration qui a été retenue est celle du CPW245 avec Inconel 718. Cette configuration permet la meilleure réduction des coûts d'usinage (3957 \$) et une diminution du poids acceptable (2.308 livres). Présentement, des tests sont en cours sur le soudage par friction du CPW245 avec l'Inconel 718 et les tests de traction faits sur les éprouvettes sont encourageants étant donné que l'éprouvette ne casse pas à la soudure mais plutôt du côté du CPW245. Bientôt, un prototype de l'arbre sera fait.

La deuxième option de fabrication est le fluotournage. Cette technique se fait par l'application d'une puissance uniforme en compression sur le diamètre extérieur d'une pièce cylindrique, en utilisant une combinaison de forces axiales et radiales à partir de trois rouleaux commandés numériquement et situés à 120 degrés autour de la circonférence de la pièce. Chacun des trois rouleaux a une géométrie spécifique pour assurer son rôle particulier dans le processus de formage. La position des rouleaux est décalée axialement et radialement un par rapport à l'autre (Figure II). Le métal est comprimé et plastifié au-dessus de sa limite élastique et s'écoule dans la direction axiale sur un mandrin. La pièce, les rouleaux et le mandrin tournent tous en même temps. Pour

les tests, "Dynamic Machine Works" a été contacté et ils ont soumissionné sur le fluotournage de l'arbre de transmission de puissance de la turbosoufflante PW307 de PWC. Suites à plusieurs discussions et différentes versions des dessins de la pièce, ils ont garanti que la pièce aurait la section centrale de l'arbre aux dimensions finies. C'est-à-dire, juste les deux bouts devraient être tournés et fraisés pour avoir l'arbre correspondant au dessin original à l'exception de quelques dimensions des rayons intérieurs, qui seraient modifiées à cause de certains problèmes d'écoulement du matériel lors du fluotournage.



(Rollers shown on the same plane for clarity)

R1 R2	Radial roller offset	S0	Starting wall thickness
A1 A2	Axial roller offset	S1	Finished wall thickness
K	Preform lead angle	V	Direction of feed

Figure II: Position des rouleaux pour le fluotournage

Conclusion

En utilisant la technique de soudure par friction, il est possible de faire un arbre de transmission de puissance fait de différents matériaux, chacun choisi pour sa fonction. On a établi avec des analyses analytiques de contraintes et en dynamique que l'arbre multi-matériaux soudé par friction est réalisable. En outre, quelques essais de soudure de frottement ont confirmé lors de tests de traction que l'échantillon casse du côté du

matériau plus faible mais jamais à la soudure. Par conséquent, la possibilité d'avoir un arbre de transmission de puissance multi-matériaux est envisageable.

Les avantages d'avoir un arbre multi-matériaux sont énormes. Il faut seulement de légers changements dans le processus de fabrication et aucun investissement dans les équipements, si le soudage par friction est sous-contracté. La longueur de perçage du centre de l'arbre est plus petite étant donné qu'on a deux pièces et le CPW245 a une usinabilité meilleure que celle de l'Inconel 718. Il y a donc moins de problèmes de concentricité entre les diamètres intérieurs et extérieurs. De plus, il y a moins de difficultés pour usiner l'Inconel 718 sur une longueur plus petite (11.125”).

Après avoir étudié le travail déjà effectué par “Dynamic Machine Works” sur le fluotournage de l'Inconel 718, on leur a demandé de soumissionner sur le fluotournage de l'arbre de transmission de puissance de la turbosoufflante PW307. “Dynamic Machine Works” a garanti que la pièce aurait la section centrale de l'arbre aux dimensions finies et que seulement les deux bouts devraient être tournés et fraisés pour avoir l'arbre correspondant au dessin original. En conséquence, un prototype d'arbre de transmission de puissance fait par fluotournage représentera une nouvelle façon de faire et une innovation dans l'industrie aéronautique.

Avec le fluotournage, l'enlèvement de matière serait inexistant et le temps d'usinage serait considérablement réduit. En outre, les problèmes de concentricité entre les diamètres intérieurs et extérieurs disparaîtraient parce qu'ils ne dépendraient plus du perçage du centre de l'arbre. Avec le fluotournage, la concentricité des diamètres dépend de la finition et les tolérances du mandrin utilisé, ce qui est plus facile à contrôler.

Le développement de la technique d'optimisation pour la conception de l'arbre de transmission de puissance s'est avéré un succès et ceci permettra de toujours s'assurer que le matériau de l'arbre est employé à sa capacité maximale tout en respectant les

spécifications requises pour les contraintes. De plus, cette optimisation permettra de s'assurer que le poids de l'arbre soit minimal. Suite à ce succès, un logiciel exécutant la technique d'optimisation a été développé afin de faciliter et accélérer cette opération.

En conclusion, l'utilisation de la soudure par friction et le fluotournage permet de grandes réductions des coûts de fabrication de l'arbre de transmission de puissance de la turbosoufflante PW307 de PWC. Grâce au logiciel d'optimisation du design, une diminution du poids de l'arbre est réalisable.

Dans l'avenir, il est très important de terminer les essais de soudure par friction ainsi que ceux pour le fluotournage, et de fabriquer les premiers prototypes pour chacune des solutions. Ensuite, les deux prototypes devraient être testés sur un banc d'essai simulant l'arbre en opération dans la turbosoufflante. La prochaine étape serait un test dans la turbosoufflante PW307 pour les prototypes ayant passé avec succès les tests sur banc d'essai. En conclusion, une étude des coûts serait exigée pour mettre en application la solution dans la chaîne de production.

CONTENTS

ACKNOWLEDGEMENT.....	IV
ABSTRACT.....	V
RÉSUMÉ	VII
CONDENSÉ EN FRANÇAIS	IX
CONTENTS.....	XXII
LIST OF FIGURES	XXIV
LIST OF TABLES	XXIX
LIST OF SYMBOLES.....	XXX
LIST OF EQUATIONS.....	XXXI
LIST OF APPENDIX	XXXII
INTRODUCTION.....	1
CHAPTER 1. LITERATURE REVIEW	2
1.1 POWER SHAFT FOR TURBINE ENGINE.....	2
1.2 SUPERALLOY MATERIALS FOR HIGH TEMPERATURES.....	19
1.3 MANUFACTURING TECHNOLOGIES	25
1.3.1 Assembling techniques	25
1.3.2 Cold forming techniques.....	26
1.4 LITERATURE REVIEW CONCLUSIONS	27
CHAPTER 2. PROBLEM STATEMENT AND CONTEXT.....	29
2.1 OBJECTIVES	30
2.2 MOTIVATION	31
CHAPTER 3. ACTUAL SHAFT	32
3.1 SHAFT DESIGN	32
3.1.1 P0889 Shaft Analysis Program	32
3.1.2 Dynamic analysis of the power shafts	38
3.2 SHAFT MANUFACTURING.....	41
3.2.1 Manufacturing operations summary	41

3.2.2	Manufacturing operations list	44
CHAPTER 4. SHAFT RE-ENGINEERING		46
4.1	SHAFT DESIGN OPTIMIZATION.....	46
4.1.1	Optimization technique.....	46
4.1.2	Development of P0889opt Automated Shaft Analysis Program	57
4.2	NEW MANUFACTURING TECHNOLOGIES	64
4.1.1	Friction welded shaft.....	64
4.1.2	Flow-formed shaft.....	96
CONCLUSION		107
REFERENCES.....		109

LIST OF FIGURES

Figure I: Déplacement du matériau à l'état plastique lors du soudage par frottement..	XVII
Figure II: Position des rouleaux pour le fluotournage	XIX
Figure 1.1: Shaft assembly. J.A. Miller and J.J. O'Connor (1980) [1].....	2
Figure 1.2: Solution for bar shaft. P. Amborn, H. Frielingsdorf, S.K. Ghosh and K. Greulich (1995) [2]	4
Figure 1.3: Bar shaft drilled and friction-welded. P. Amborn, H. Frielingsdorf, S.K. Ghosh and K. Greulich (1995) [2]	5
Figure 1.4: Monobloc tube shaft outside/inside cylindrical (uniform wall thickness). P. Amborn, H. Frielingsdorf, S.K. Ghosh and K. Greulich (1995) [2].....	5
Figure 1.5: Monobloc tube shaft outside cylindrical - inside stepped (Thick/thin wall thickness). P. Amborn, H. Frielingsdorf, S.K. Ghosh and K. Greulich (1995) [2]	6
Figure 1.6: Monobloc tube shaft, outside contour stepped with different wall thickness. P. Amborn, H. Frielingsdorf, S.K. Ghosh and K. Greulich (1995) [2].....	6
Figure 1.7: Monobloc tube shaft outside contour multi-stepped (Thick-thin thickness). P. Amborn, H. Frielingsdorf, S.K. Ghosh and K. Greulich (1995) [2].....	8
Figure 1.8: Both drive shafts ends welded to multi-stepped middle section (Thick/thin wall thickness). P. Amborn, H. Frielingsdorf, S.K. Ghosh and K. Greulich (1995) [2]	9
Figure 1.9: Improvement of shaft performance, capacity, weight and behavior. P. Amborn, S.K. Ghosh and I.K. Leadbetter (1997) [3]	10
Figure 1.10: Influence of the tube wall thickness on natural bending frequency. P. Amborn, S.K. Ghosh and I.K. Leadbetter (1997) [3]	11
Figure 1.11: Influence of length of tube shaft on natural bending frequency. P. Amborn, S.K. Ghosh and I.K. Leadbetter (1997) [3].....	12
Figure 1.12: Examples of shaft designs and their weight, natural bending frequency and torsion stiffness. P. Amborn, S.K. Ghosh and I.K. Leadbetter (1997) [3].....	13
Figure 1.13: Press layout. P. Amborn, S.K. Ghosh and I.K. Leadbetter (1997) [3]	14

Figure 1.14: The principle of rotary swaging process. P. Amborn, S.K. Ghosh and I.K. Leadbetter (1997) [3]	15
Figure 1.15: Thick - Thin swaging steps for monobloc tubular shafts. P. Amborn, S.K. Ghosh and I.K. Leadbetter (1997) [3].....	16
Figure 1.16: Hydraulic expansion formed tube shaft with swaged ends. P. Amborn, S.K. Ghosh and I.K. Leadbetter (1997) [3].....	16
Figure 1.17: Hydraulic expansion in a flexible die. P. Amborn, S.K. Ghosh and I.K. Leadbetter (1997) [3]	17
Figure 1.18: Combination of hydraulic expansion with rotary swaging. P. Amborn, S.K. Ghosh and I.K. Leadbetter (1997) [3].....	18
Figure 1.19: Universal copy roll technology. P. Amborn, S.K. Ghosh and I.K. Leadbetter (1997) [3]	18
Figure 1.20: Weight-specific LCF comparison of IMI 834 and IN 718. J. Albrecht (1999) [6].....	21
Figure 1.21: Weight-related macrocrack propagation, comparison of IMI 834 and IN 718. J. Albrecht (1999) [6].....	22
Figure 1.22: Evaluation of materials use in aerogas turbines. E.O. Ezugwu, J. Bonney and Y. Yamane (2003) [7]	24
Figure 2.1: PW307 power shaft	29
Figure 3.1: PW307 engine cross section with operational temperatures	32
Figure 3.2: Feature dimension definition (external fillet) – PWC P0889 Shaft Analysis Program Engineering and Software Manual [16]	34
Figure 3.3: Feature dimension definition (internal fillet) - PWC P0889 Shaft Analysis Program Engineering and Software Manual [16]	35
Figure 3.4: PW307 Power Shaft	41
Figure 3.5: Mollart Gun Drill Machine.....	42
Figure 3.6: SAUPAL Ultrasonic Inspection Machine	42
Figure 3.7: Fellows Gear Shaper	43
Figure 4.1: PW307 power shaft stress concentration sections.....	47

Figure 4.2: Results of LCF/HCF Analysis for PW307 actual power shaft (Equiv/Allow)	48
Figure 4.3: Results of LCF/HCF Analysis for PW307 actual power shaft (Life Cycles)	48
Figure 4.4: Results of LCF/HCF Analysis for PW307 optimized power shaft (Equiv/Allow)	51
Figure 4.5: Results of LCF/HCF Analysis for PW307 actual power shaft (Life Cycles)	52
Figure 4.6: Results of LCF/HCF Analysis for Actual VS Optimized (Equiv/Allow)	53
Figure 4.7: Results of LCF/HCF Analysis for Actual VS optimized (Life Cycles)	54
Figure 4.8: Optimization weight savings per section for PW307 power shaft.	55
Figure 4.9: PW307 Actual power shaft with data prompted when running P0889 Shaft analysis program	61
Figure 4.10: Phase 1 - Low temp interface heat cycle by spinning one component against another stationary component.	65
Figure 4.11: Phase 2 - Solid forging cycle showing displaced plastic state material when final axial forging force is applied	66
Figure 4.12: Phase 3 - Plastic state flashing is removed easily, even for hardenable materials that would otherwise require grinding	66
Figure 4.13: Multi material power shaft - CPW245 & Inconel 718	69
Figure 4.14: Results of LCF/HCF Analysis for PW307 multi material power shaft (Equiv/Allow) - CPW245&Inconel 718	70
Figure 4.15: Results of LCF/HCF Analysis for PW307 multi material power shaft (Life Cycles) - CPW245&Inconel 718	70
Figure 4.16: Optimization weight savings per section for PW307 multi material (CPW245&Inconel 718) power shaft.	71
Figure 4.17: Multi material power shaft - HCM3 & Inconel 718	73
Figure 4.18: Results of LCF/HCF Analysis for PW307 multi material power shaft (Equiv/Allow) - HCM3&Inconel 718	74
Figure 4.19: Results of LCF/HCF Analysis for PW307 multi material power shaft (Life Cycles) - HCM3&Inconel 718	74

Figure 4.20: Optimization weight savings per section for PW307 multi material (HCM3&Inconel 718) power shaft.....	75
Figure 4.21: Multi material power shaft – CPW245 up to section 9, HCM3 up to section 22 and Inconel 718 to the end.....	77
Figure 4.22: Results of LCF/HCF Analysis for PW307 multi material power shaft (Equiv/Allow) - CPW245 up to section 9, HCM3 up to section 22 and Inconel 718 to the end.....	78
Figure 4.23: Results of LCF/HCF Analysis for PW307 multi material power shaft (Life Cycles) - CPW245 up to section 9, HCM3 up to section 22 and Inconel 718 to the end.....	79
Figure 4.24: Multi material power shaft – CPW245 up to section 14, HCM3 up to section 22 and Inconel 718 to the end.....	80
Figure 4.25: Results of LCF/HCF Analysis for PW307 multi material power shaft (Equiv/Allow) - CPW245 up to section 14, HCM3 up to section 22 and Inconel 718 to the end.....	81
Figure 4.26: Results of LCF/HCF Analysis for PW307 multi material power shaft (Life Cycles) - CPW245 up to section 14, HCM3 up to section 22 and Inconel 718 to the end.....	81
Figure 4.27: Multi material power shaft – CPW245 up to section 19, HCM3 up to section 22 and Inconel 718 to the end.....	82
Figure 4.28: Results of LCF/HCF Analysis for PW307 multi material power shaft (Equiv/Allow) - CPW245 up to section 19, HCM3 up to section 22 and Inconel 718 to the end.....	83
Figure 4.29: Results of LCF/HCF Analysis for PW307 multi material power shaft (Life Cycles) - CPW245 up to section 19, HCM3 up to section 22 and Inconel 718 to the end.....	83
Figure 4.30: CPW245 test piece configuration for friction welding	86
Figure 4.31: Inconel 718 test piece configuration for friction welding	86
Figure 4.32: CPW245 Test piece for friction welding.....	87

Figure 4.33: Inconel 718 Test piece for friction welding	87
Figure 4.34: IW1 - First test pieces pair being friction welded	88
Figure 4.35: IW1 - First test pieces pair being friction welded (section cut)	89
Figure 4.36: IW1 - Met section of first friction weld	90
Figure 4.37: IW2 - Met section of second friction weld.....	90
Figure 4.38: IW1 - Interface of the weld after tensile test	91
Figure 4.39: IW1 - Profile of the weld after tensile test	92
Figure 4.40: IW2 - Interface of the weld after tensile test.....	92
Figure 4.41: IW2 - Profile of the weld after tensile test	93
Figure 4.42: Vickers hardness test on sample 4-1 - stress relieved for 2 hours.....	94
Figure 4.43: Tension test results for sample 4-1	94
Figure 4.44: Tensile test on sample 4-1 - stress relieve for 2 hours	95
Figure 4.45: Etched sample 4-1 - stress relieved for 2 hours.....	95
Figure 4.46: Longitudinal carriage with roller housing.....	97
Figure 4.47: Position of the rollers	97
Figure 4.48: Mandrel	98
Figure 4.49: Forward flow forming	99
Figure 4.50: Reverse flow forming.....	99
Figure 4.51: Flow forming accuracy.....	100
Figure 4.52: Preform 100X etched.....	102
Figure 4.53: Flow formed 100X etched.....	103
Figure 4.54: Flow formed 700X etched.....	104
Figure 4.55: Flow formed Inconel 718. Preform on the right.....	105
Figure 4.56: Flow formed Inconel 718 micro inch finish in the ID.....	105

LIST OF TABLES

Table 1.1: Nominal chemical compositions for several recent turbine disk and blade superalloy. Only major alloying elements have been included in the tabulation. D.G. Backman and J.C. Williams (1992) [4]	19
Table 1.2: Commercially available nickel-based alloys. E.O. Ezugwu, J. Bonney and Y. Yamane (2003) [7]	24
Table 3.1: Design Factors Summary	36
Table 3.2: Analysis values requirements for P0889 Shaft analysis program.	38
Table 3.3: PW307 power shaft critical speeds.....	40
Table 4.1: Geometrical description of section 16 for the actual power shaft.	49
Table 4.2: Optimized geometrical description of section 16 (Inside diameter is increased to 2.2950").	50
Table 4.3: PW307 optimized power shaft critical speeds.....	56
Table 4.4: CPW245 & Inconel 718 multi material power shaft critical speeds	72
Table 4.5: HCM3 & Inconel 718 multi material power shaft critical speeds	76
Table 4.6: Power shaft configurations with machining cost savings and weight savings	85
Table 4.7: Properties of flow formed Inconel 718 after solution & aging heat treatment	102

LIST OF SYMBOLES

CPW245: Low-alloy heat resistant steel 0.9Cr – 0.5Mo – 0.3V (0.40-0.50C).

Equiv/Allow: Equivalent stress over allowable stress.

EWI: Edison Welding Institute, 1250 Arthur E. Adams Dr. Columbus, OH 43221-3585.

HCM3: Low-alloy 3.25Cr – 0.55Mo – 0.55Mn – 0.20V – 0.20Ni – 0.22Si – 0.39C – Fe balance.

Inconel 718: Corrosion and heat resistant nickel alloy 52.5Ni – 19Cr – 3Mo – 5Cb – 0.90Ti – 0.5Al – 18Fe.

LCF-HCF: Low cycle and high cycle fatigue.

PWC: Pratt & Whitney Canada

PW307: Pratt & Whitney Canada Turbofan Engine

P0889: Shaft Analysis Program - Engineering and Software Manual

P0571: Computing file P0571. Whirl speed analysis of coaxial shafts.

P0889opt: Automated shaft analysis program.

Ra: The arithmetic average of the deviations up and down from the mean line. The leveling of the peaks to fill the valleys represents the mean line.

LIST OF EQUATIONS

Equation 1.1: Critical rotary frequency equation.....	7
Equation 1.2: Spring coefficient equation	7

LIST OF APPENDIX

APPENDIX I	112
APPENDIX II	118
APPENDIX III	123
APPENDIX IV	128
APPENDIX V	129
APPENDIX VI	135
APPENDIX VII.....	144
APPENDIX VIII	147
APPENDIX IX	152
APPENDIX X.....	158

INTRODUCTION

Pratt & Whitney Canada (PWC) is a pioneer in the design and manufacturing of small and medium gas turbines. To maintain its position as a world leader, PWC must continuously reduce manufacturing costs and improve the quality of its products in order to offer them at competitive prices. In this context, technological innovation becomes a priority. Consequently, it is essential to be in line with today's manufacturing technologies, and to always wonder if the technologies that are being used at PWC are the best ones available on the market.

The part being analyzed in this project is the power shaft of the PW307 turbofan engine of PWC. The shaft has a complex shape and its manufacturing is difficult to achieve. PWC suggested the use of friction welding technique and the flow-forming technique as possibilities to manufacture this shaft.

In a turbofan engine, two sections can be distinguished. The front end of the engine, where the air enters, represents the cold section. The back end of the engine, where the combustion takes place, is the hot section. This PW307 engine has a large operation temperature difference across its length, between the cold and hot sections, that goes from 534F° to 928 F°.

A bibliographic review of power shafts, superalloy materials and manufacturing technologies is detailed in chapter 1, and in chapter 2 the problem statement and context of the project are explained. Chapter 3 includes information on the actual design and manufacturing techniques that are currently used to make the power shaft. In chapter 4, the re-engineering of the shaft is explained and testing results are examined. Finally, a conclusion is presented with future work suggestions.

CHAPTER 1. LITERATURE REVIEW

This chapter presents a review of power shaft manufacturing technologies and superalloy materials that are used to manufacture them. In addition, the chapter focuses on friction welding and flow-forming of work pieces of tubular section.

1.1 POWER SHAFT FOR TURBINE ENGINE

Following an extended research on articles covering power shafts for turbine engines, it is possible to state that little research and development has ever been published on this subject. Books on gas turbine engines were also consulted, but they do not focus on the design or manufacturing of the power shaft.

The only article that really gives details on the manufacturing of a power shaft is the article by J.A. Miller and J.J. O'Connor (1980) [1]. This paper explains how a power shaft for the Lycoming T55 turbine engine is friction and electro beam welded. The power shaft was a rigid one-piece construction that was manufactured using three different steels, each selected for its location and function. Figure 1.1 presents the configuration of this power shaft.

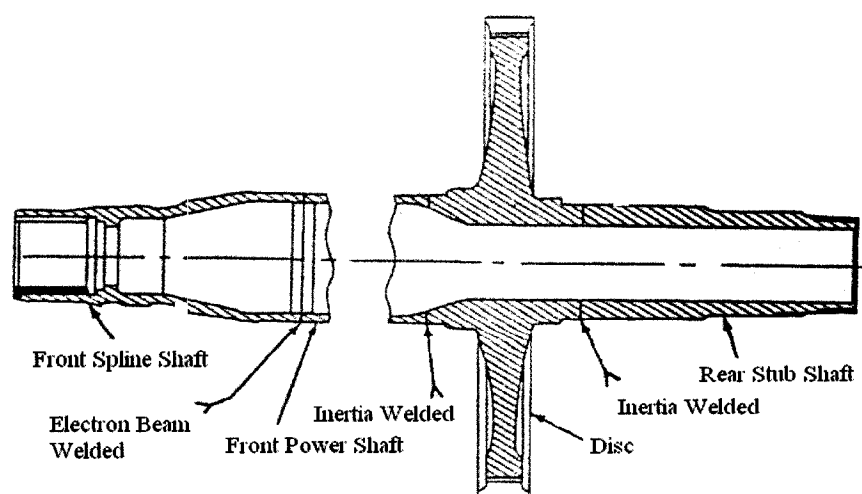


Figure 1.1: Shaft assembly. J.A. Miller and J.J. O'Connor (1980) [1]

These shafts have accumulated almost 400 000 hours of service to date and there has not been a single service problem recorded. This design is a significant improvement over the mechanically joined assembly, both in performance and reliability. It had been proven that critical aircraft engine rotating components can be made by modern welding procedures, and that their quality can be verified by available nondestructive testing techniques.

Although articles on power shafts for turbine engines are almost non-existent, some papers on the manufacturing of side-shafts for passenger cars were found. These articles are very interesting because the problems are similar even if the industries are different.

P. Amborn, H. Frielingsdorf, S.K. Ghosh and K. Greulich (1995) [2] presented a general comparison of various processes that are applied to current and new techniques for the manufacturing of modern side-shafts for cars. The complex processes consider the technological demands on a side-shaft, their influence on the design, material, manufacturing processes and heat-treatment, i.e., the total manufacturing. The various shaft configurations are outlined below:

- bar shaft
- drilled Bar Shaft
- friction Welded Drive Shaft
- both Driveshaft Ends Backwards Extruded and Friction Welded
- monobloc Tube Shaft Outside / Inside Cylindrical (Uniform Wall Thickness)
- monobloc Tube Shaft Outside Cylindrical – Inside Stopped (Thick / Thin Wall Thickness)
- monobloc Tube Shaft Outside Contour Stepped with Different Wall Thickness
- monobloc Tube Shaft Outside Contour Multi-Stepped with Different Wall Thickness

- both Drive Shaft Ends to Welded Multi-Stepped Middle Section

The *bar shaft* is the most cost effective version (see Fig. 1.2). It can be manufactured cheaper than tubular shaft and also the manufacturing operations are more cost effective than when a tubular material is employed. The main disadvantage of a bar shaft is the weight.

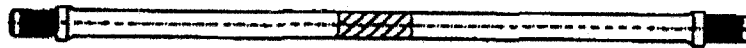


Figure 1.2: Solution for bar shaft. P. Amborn, H. Frielingsdorf, S.K. Ghosh and K. Greulich (1995) [2]

The simplest way to reduce the weight of a bar shaft is to remove the material by boring which is less important for the torque transmission. In some cases the *drilled bar shaft* is more cost effective than to use a thick walled tube with a relatively small outer diameter.

In order to reduce the rotating weight of the bar shaft on one hand and to influence the vibration behavior on the other, drive shafts were originally designed consisting of two welded parts of different lengths. This configuration is the *friction-welded shaft*. One side has an area with a small diameter for the spline application, and on the other side an enlarged diameter (see Fig. 1.3). Usually, the section with enlarged diameter of the longer part is bored. The diameter of the bore depends on the required torque transmission and the outer diameter of this section. After boring the longer part the ends with large diameter of both parts are machined, and afterwards, friction welded.



Figure 1.3: Bar shaft drilled and friction-welded. P. Amborn, H. Frielingsdorf, S.K. Ghosh and K. Greulich (1995) [2]

Similar to the friction welded shaft, another design consists of *both drive shaft ends being backwards extruded and then friction welded*. The difference consists in the cold forming of the material instead of machining it.

To avoid the drilling of a bar shaft, a possible configuration is the *monobloc tube shaft with outside/inside cylindrical profile* (uniform wall thickness). The difference of this version compared with the drilled bar shafts is that the required outside contour is manufactured by cold forming and not by machining. The wall thickness along the shaft is nearly constant (see Fig. 1.4). The parent and un-machined material fibers is a further advantage of this version. As a result, a monobloc tube shaft with the same outside contour as the drilled bar shaft can transmit a higher torque and offers a better endurance. This type of monobloc tube shaft is simple, cost effective and also weight saving design.

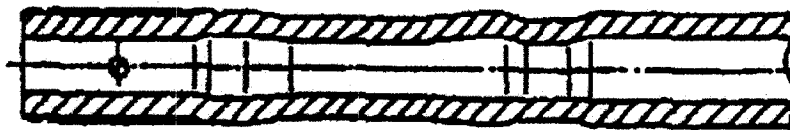


Figure 1.4: Monobloc tube shaft outside/inside cylindrical (uniform wall thickness). P. Amborn, H. Frielingsdorf, S.K. Ghosh and K. Greulich (1995) [2]

In cases of more severe demands concerning weight-reduction and constant torque and endurance specifications, it is necessary to change the wall thickness along the shaft (see Fig. 1.5) in order to have a *monobloc tube shaft with cylindrical outside and stepped*

inside. Due to the torque input to the shaft ends which is characterized by stress concentration, the wall thickness in the spline area is designed thicker than in the sections with homogenous stress distribution. For this application the cold forming technologies such as drawing, swaging, etc. are used.

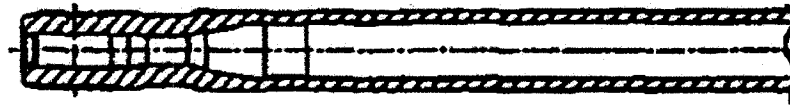


Figure 1.5: Monobloc tube shaft outside cylindrical - inside stepped (Thick/thin wall thickness). P. Amborn, H. Frielingsdorf, S.K. Ghosh and K. Greulich (1995) [2]

For optimal lightweight construction, enhanced mechanical requirements concerning stiffness and for special vibration situations it is necessary to increase significantly the outer diameter of the tube shaft in the section of homogeneous stress distribution (see Fig. 1.6). The *monobloc tube shaft with outside contour stepped and different wall thickness* allows the shape of the shaft to be optimized depending on the interdependence of the outer diameter and the wall thickness.



Figure 1.6: Monobloc tube shaft, outside contour stepped with different wall thickness. P. Amborn, H. Frielingsdorf, S.K. Ghosh and K. Greulich (1995) [2]

Vibration requirements force the designer to realize a natural bending frequency as high as possible. The natural bending frequency is a function of the mass and the stiffness against bending.

$$n_k = \frac{1}{2\pi} \sqrt{\frac{C_q}{m}}$$

Equation 1.1: Critical rotary frequency equation

where:

n_k = critical rotary frequency (Hz)

C_q = spring-coefficient for elastic lateral oscillation (N/m)

m = mass (kg)

In order to reach high natural bending frequencies, it is advantageous, in accordance with the above-mentioned formula to choose the spring coefficient C_q as large as possible.

$$C_q = \frac{48EI}{l^3} = \frac{48E\pi(D^4 - d^4)}{l^3 64}$$

Equation 1.2: Spring coefficient equation

where:

E = Elastic modulus (Pa)

I = Geometrical moment of inertia (m⁴)

l = Length of the shaft (m)

D = Outer diameter (m)

d = Inner diameter (m)

Therefore the outer diameter should be as large as possible and the inner diameter needs to be optimized depending on the mass-effect.

Often the room for drive shafts is very limited and it is necessary to design the shaft close to the available space under consideration of the movement of the shafts during operation. This can be achieved by designing sections along the shaft with different outer diameters having a *monobloc tube shaft contour multi-stepped*. Depending on the available manufacturing technologies, the whole contour and the transmission area are fixed. The manufacturing technologies ‘drawing’ and ‘swaging’ require cylindrical sections with smooth transition areas (see Fig. 1.7). On the contrary, the expansion technology allows other contours for these shafts.

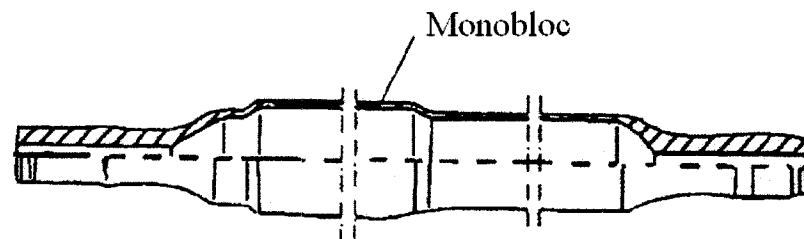


Figure 1.7: Monobloc tube shaft outside contour multi-stepped (Thick-thin thickness). P. Amborn, H. Frielingsdorf, S.K. Ghosh and K. Greulich (1995) [2]

The last shaft configuration is the same as the one previously described, except that the shaft is manufactured from a simple tube, whereby for this one the end sections are manufactured separately (e.g. by cold extrusion, forging, etc) and afterwards welded to the middle section (see Fig. 1.8). The advantage to have both drive shaft ends welded to a multi-stepped middle section is that the end sections can be made from material with greater strength.

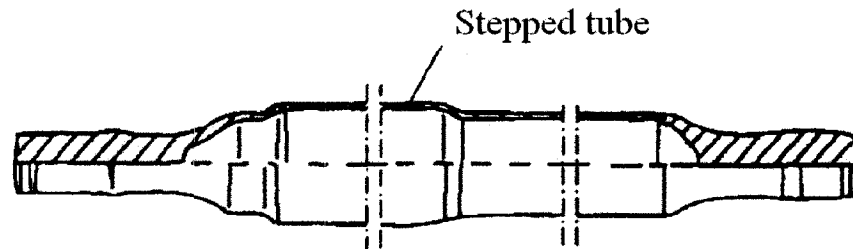


Figure 1.8: Both drive shafts ends welded to multi-stepped middle section (Thick/thin wall thickness). P. Amborn, H. Frielingsdorf, S.K. Ghosh and K. Greulich (1995) [2]

In another paper, P. Amborn, S.K. Ghosh and I.K. Leadbetter (1997) [3], made an overview of some major developments in the design and manufacture of automotive side shafts and specifically look at the most important requirements for Monobloc Tubular Shafts. The advantages and disadvantages of different cold forming technologies for the different types of Monobloc Tubular Shafts are discussed and some new processes, such as spline drawing, are briefly described.

In terms of design, increased competition amongst car manufacturers led to higher and lighter specifications for car components, particularly related to their influence on fuel economy, noise, vibration, harshness, etc. When solid bar shafts are used, vibratory difficulties have been resolved by using dampers or masses, but of course this is determinant to fuel economy. This conflict between reduction of vibration and decrease in fuel economy was overcome by the introduction of friction welded tube shafts (see Fig. 1.9).

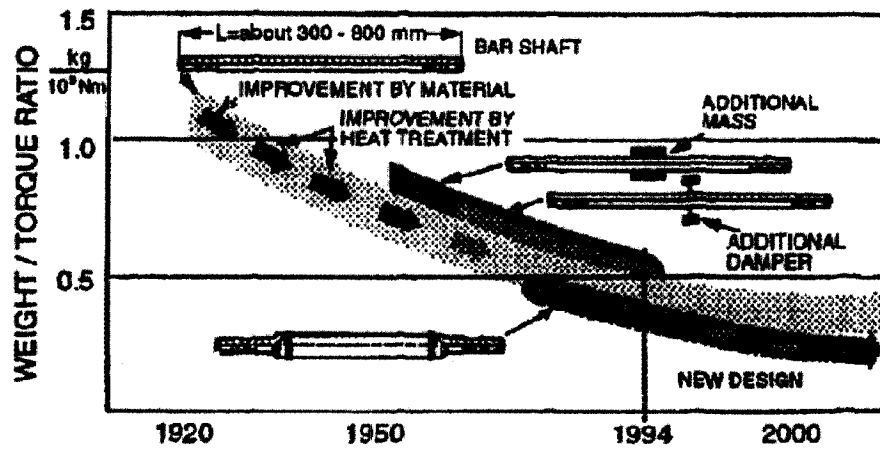


Figure 1.9: Improvement of shaft performance, capacity, weight and behavior. P. Amborn, S.K. Ghosh and I.K. Leadbetter (1997) [3]

Noise, vibration, harshness, lightweight and torsion stiffness place apparently conflicting requirements on the shaft design. As an example, lightweight requires a low wall thickness (see Fig. 1.10), whereas torsion stiffness improves with thicker walls.

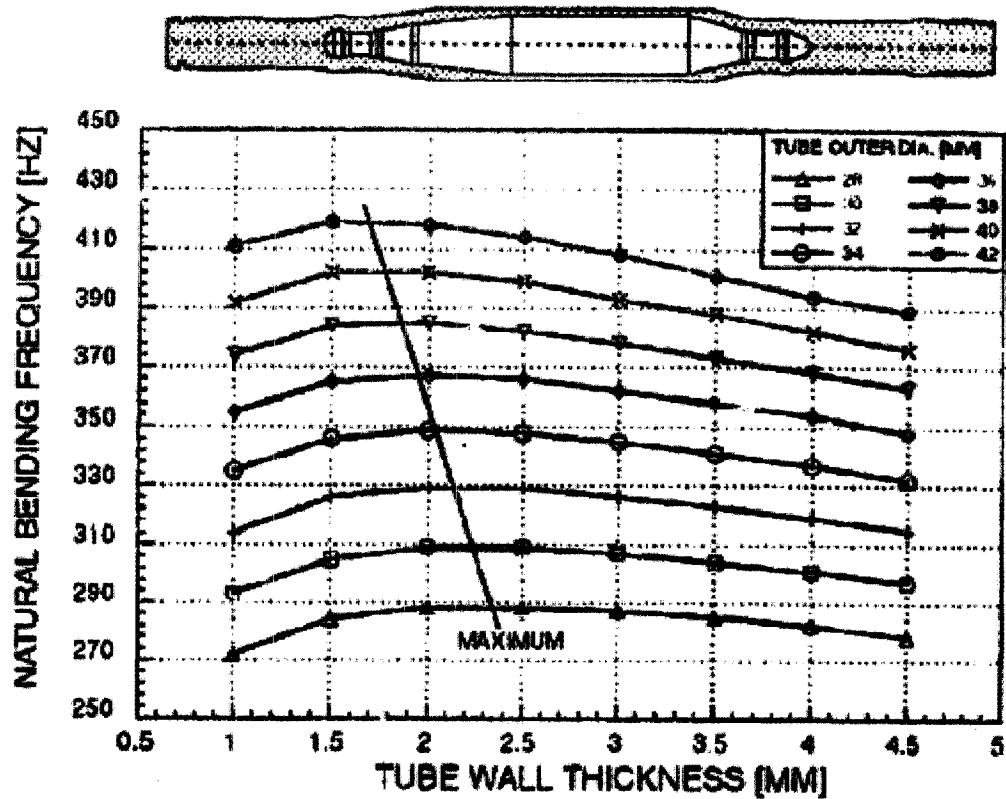


Figure 1.10: Influence of the tube wall thickness on natural bending frequency. P. Amborn, S.K. Ghosh and I.K. Leadbetter (1997) [3]

Similarly, thinner walls than those giving the needed stiffness are necessary to achieve the required bending frequency. It is therefore essential that designers of monobloc tubular shaft understand these interactions and can then optimize the tube outer diameter and wall thickness in order to achieve the specific vibration and torsion requirements for any given vehicle (see Fig. 1.11).

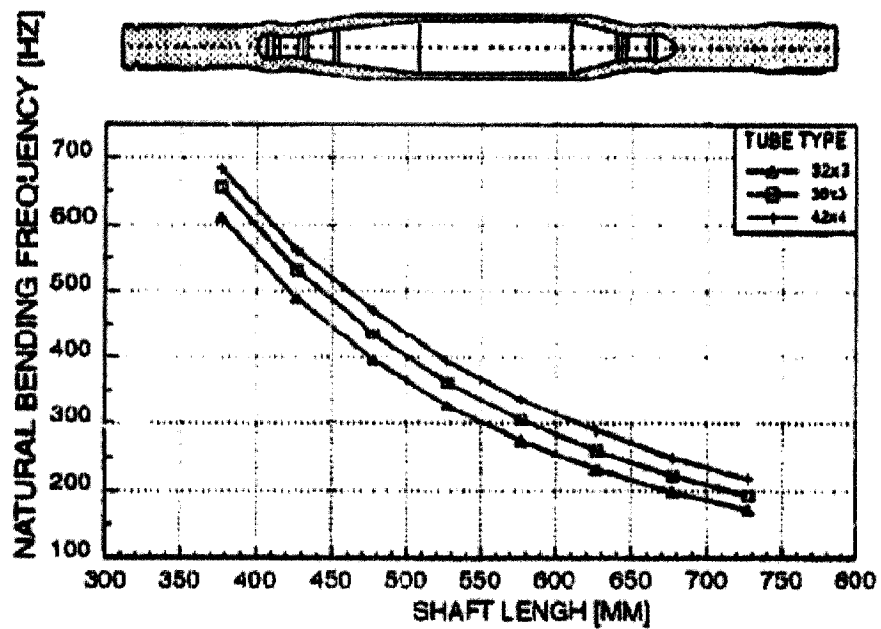


Figure 1.11: Influence of length of tube shaft on natural bending frequency. P. Amborn, S.K. Ghosh and I.K. Leadbetter (1997) [3]

Some examples of the different designs used to achieve these requirements under different application are shown in figure 1.12.

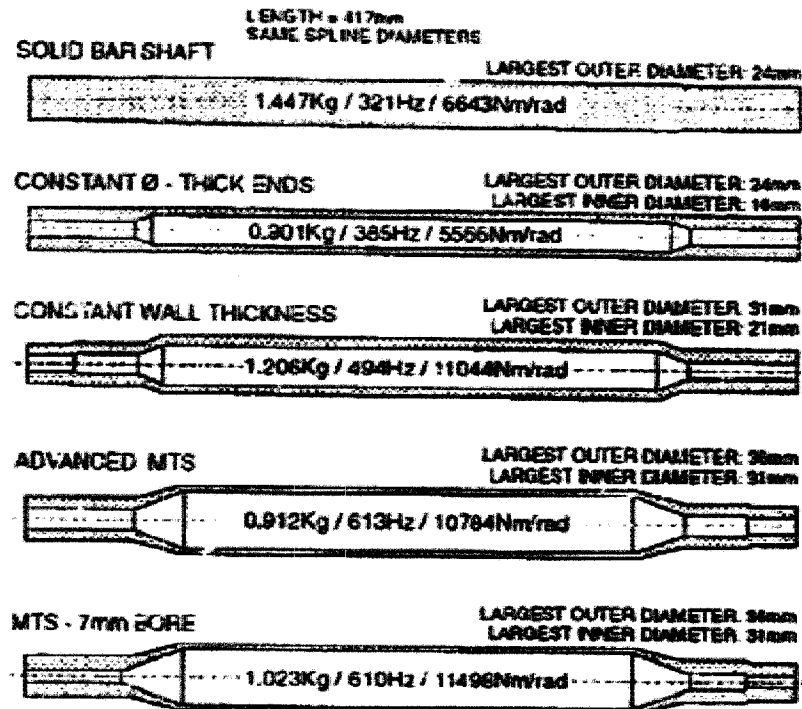


Figure 1.12: Examples of shaft designs and their weight, natural bending frequency and torsion stiffness. P. Amborn, S.K. Ghosh and I.K. Leadbetter (1997) [3]

Rolling technology can be only used for bar shafts and for monobloc tubular shafts which have a nearly solid cross section in the spline area. For those with larger inner diameter at the shaft ends, spline drawing technology has to be used, because the stresses generated by spline rolling would otherwise destroy the tube ends. The spline drawing process is a simple forming technique using hydraulic pressure to force the shaft end into a carbide steel die, see figure 1.13.

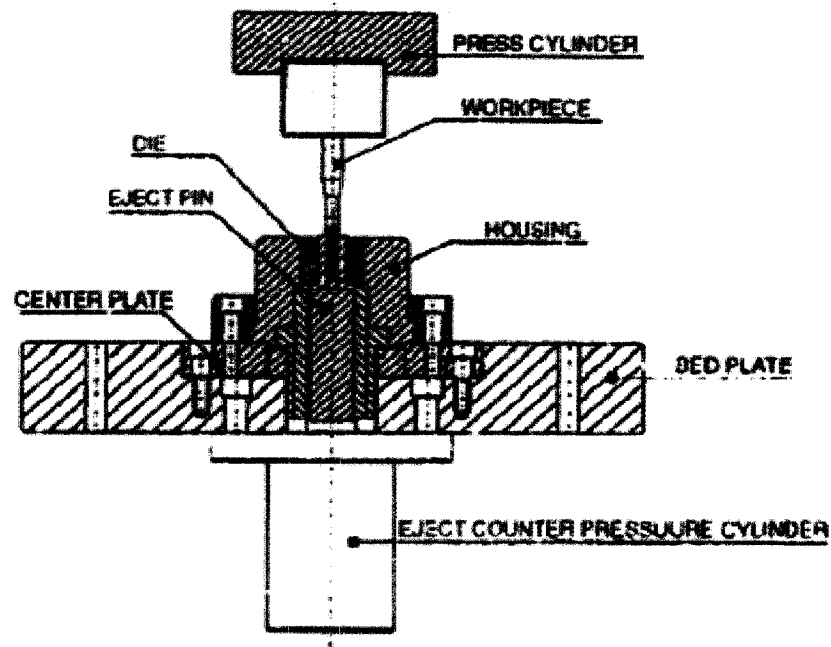


Figure 1.13: Press layout. P. Amborn, S.K. Ghosh and I.K. Leadbetter (1997) [3]

Rotary swaging is an old technique, which is now increasingly used for precision forming of tube shafts instead of turning. There are different swaging machine types on the market but the main functional differences are between feed swaging over a mandrel and recess swaging (see Fig. 1.14).

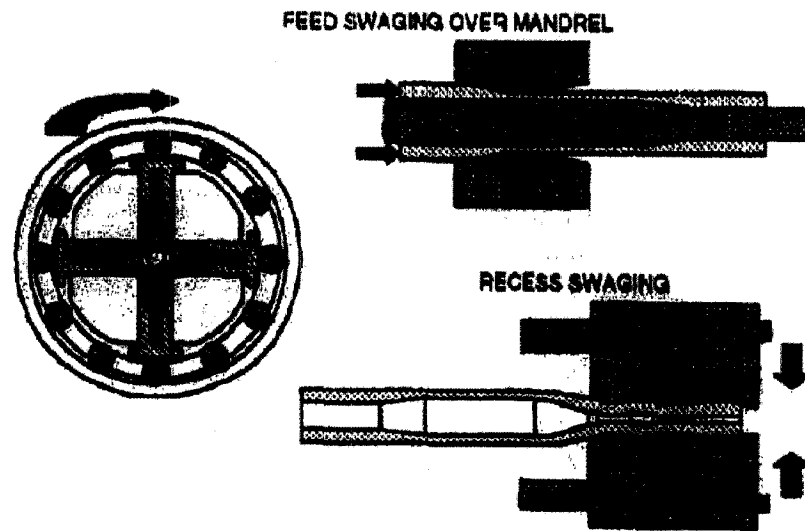


Figure 1.14: The principle of rotary swaging process. P. Amborn, S.K. Ghosh and I.K. Leadbetter (1997) [3]

To achieve the necessary high fatigue strength, small inner diameters are necessary at the tube ends. If the deformation ratio used to produce these small diameters is excessive, cracks can occur on the inner surface, which then decrease the fatigue and strength by a factor of 10 or more. To avoid such damages, careful attention has to be given to the material selection, not only to the composition of the alloying elements present but also to the cleanliness and initial hardness. The tube should also be formed in the softest condition.

In some cases, very high torsion stiffness requirements can lead to shaft designs with a high wall thickness in the center section. In such cases, feed swaging over a mandrel is not necessary, and the shaft ends can be produced in a way similar to that shown in figure 1.15, step IV and V.

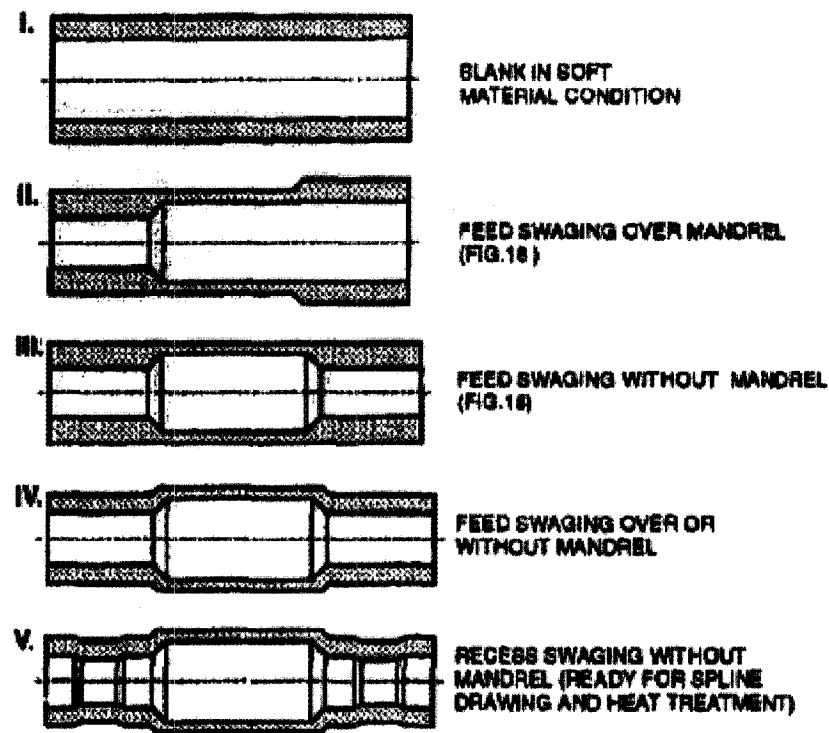


Figure 1.15: Thick - Thin swaging steps for monobloc tubular shafts. P. Amborn, S.K. Ghosh and I.K. Leadbetter (1997) [3]

Another technique used to manufacture a monobloc tubular shaft is the hydraulic expansion of tubes. The main advantage of this technology is the ability to form the tube centre area to any desired shape. Additionally, it has the flexibility to adjust the diameter and wall thickness along the length of the shaft (see Fig. 1.16).



Figure 1.16: Hydraulic expansion formed tube shaft with swaged ends. P. Amborn, S.K. Ghosh and I.K. Leadbetter (1997) [3]

Using very high fluid pressure (up to 10,000 bar), high axial forces and a fully automated operation control, the tube section can be deformed to any desired axisymmetric shape. Depending on the value of the axial forces, the tube wall thickness can be readily increased or decreased (see Fig. 1.17).

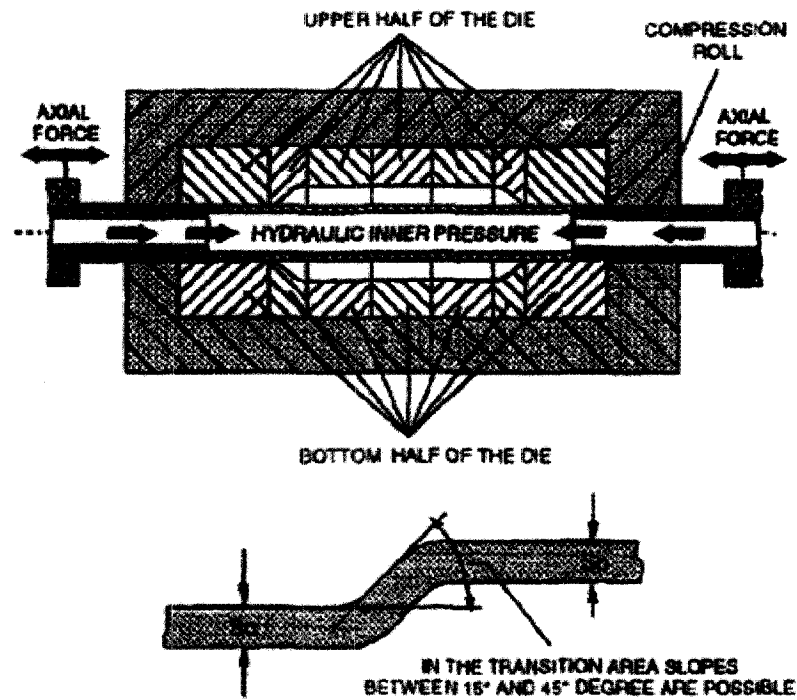


Figure 1.17: Hydraulic expansion in a flexible die. P. Amborn, S.K. Ghosh and I.K. Leadbetter (1997) [3]

The combination of hydraulic expansion and swaging technology is also possible depending on the final design requirements (see Fig. 1.18).

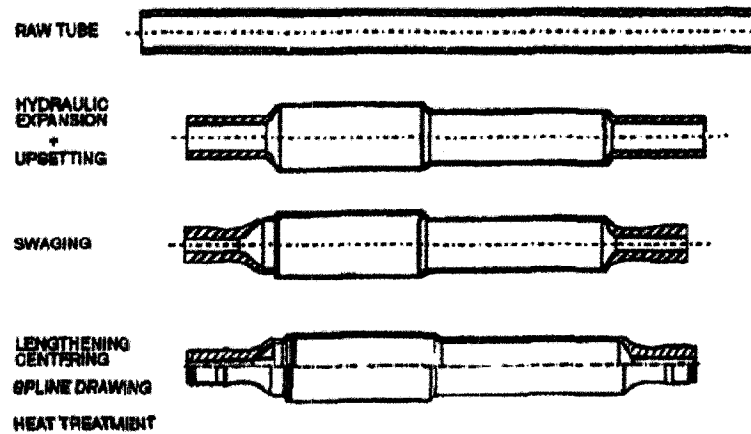


Figure 1.18: Combination of hydraulic expansion with rotary swaging. P. Amborn, S.K. Ghosh and I.K. Leadbetter (1997) [3]

Cold rolling of tubes could provide significant advantages in flexibility, cost effectiveness and freedom of design. However, trials to manufacture a standard monobloc tubular shaft were not successful (see Fig. 1.19). Further fundamental investigations are therefore needed to determine whether the technique offers any real opportunities.

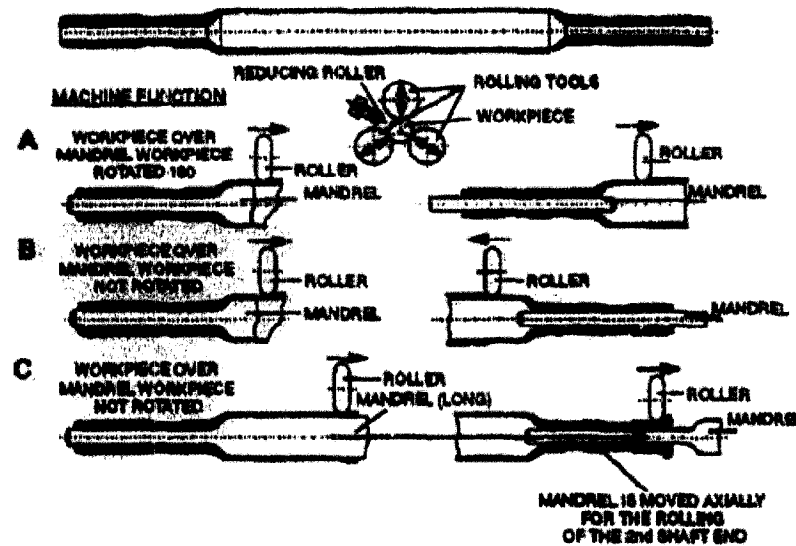


Figure 1.19: Universal copy roll technology. P. Amborn, S.K. Ghosh and I.K. Leadbetter (1997) [3]

1.2 SUPERALLOY MATERIALS FOR HIGH TEMPERATURES

In the paper by D.G. Backman and J.C. Williams (1992) [4], a review of advances for aircraft engine structural materials and processes is presented. New structural materials, notably composites and intermetallic materials are emerging, resulting in enhanced engine performance and reduced engine weight; thereby enabling the design of new aircraft systems.

The increase of engine performance has been paced by the development of improved materials and processing technologies for turbine disks and blades. Turbine disks and blades have traditionally been made with a high-strength, high-temperature class of nickel-, cobalt-, and iron-based alloys known as superalloys (see Table 1.1). Materials development and application research has focused on improving both the design and processing of these alloys.

Table 1.1: Nominal chemical compositions for several recent turbine disk and blade superalloy. Only major alloying elements have been included in the tabulation. D.G. Backman and J.C. Williams (1992) [4]

Alloy	Composition (percent by weight)										
	Co	Cr	Al	Ti	Nb	Mo	W	Hf	C	Fe	Ni
	<i>Blade superalloys</i>										
Mar-M 200 + Hf*	10.0	9.0	5.0	2.0	1.0		12.5	1.8	0.14		bal
Mar-M 247*	10.0	8.4	5.5	1.0		0.6	10.0	1.4	0.15		bal
Rene' 80 H†	9.5	14.0	3.0	4.8		4.0	4.0	0.75	0.08		bal
Rene' N4†	7.5	9.3	3.7	4.2	0.5	1.5	6.0	0.1			bal
	<i>Disk superalloys</i>										
Inconel 718‡		19.0	0.5	0.95	5.1	3.0			0.05	18.5	bal
MERL-76§	18.5	12.5	5.0	4.4	1.4	3.2		0.4	0.04		bal
Rene' 95†	8.0	13.0	3.5	2.5	3.5	3.5	3.5		0.05		bal
Rene' 88 DT†	13.0	16.0	2.1	3.7	0.7	4.0	4.0		0.05		bal

*Martin Marietta Corp. †General Electric Co. ‡International Nickel Co. §Pratt & Whitney.

Although the application of traditional metallurgical strategies, as typified by superalloy advances, has been the principal paradigm for development of modern turbine materials technology, future improvements for metallic materials are expected to be modest. Many

members of the materials developments community are looking toward intermetallic materials and composites to provide the next significant increase of materials performance.

Inconel 718 is a high-strength, corrosion and thermal resistant nickel-based alloy that plays an increasingly important part in the development and manufacture of jet aeroengines. M. Rahman, W.K.H. Seah and T.T. Teo (1997) [5] discuss the effect of cutting conditions on the machinability of Inconel 718. Due to the extreme toughness and work hardening of the alloy, the problem of machining Inconel 718 is one of ever-increasing magnitude. The flank wear of the inserts, workpiece surface roughness and cutting forces are used as performance indicators for tool life while machining is carried out using a CNC lathe.

Due to its extremely tough nature, the difficulty of machining Inconel 718 resolves itself into two basic problems: (1) the inability of the tool material to give long tool lives due to the work hardening and attrition properties of the alloy and (2) the metallurgical damage to the workpiece due to the very high cutting forces which also gives rise to work hardening, surface tearing and distortions in finally machined components due to induced stresses.

J. Albrecht (1999) [6] compared fatigue behaviour of titanium and nickel-based alloys. Titanium alloys are in competition with nickel-based alloys particularly in aerospace applications, where the lower density of titanium alloys is advantageous. For these applications fatigue strength is of primary advantage.

The lower density of titanium alloys is a general advantage; designers tend to relate the mechanical properties to density. Examples are shown in figure 1.23 and 1.24. The weight specific LCF data for IMI 834 and IN 718 are compared in figure 1.23, showing in this representation an advantage of the titanium alloy over the nickel-based material.

The fatigue crack propagation behaviour of the two alloys (long cracks) is compared in figure 1.24, where da/dN is plotted against the weight specific stress intensity amplitude, again showing an advantage of the titanium alloy, particularly at elevated temperatures.

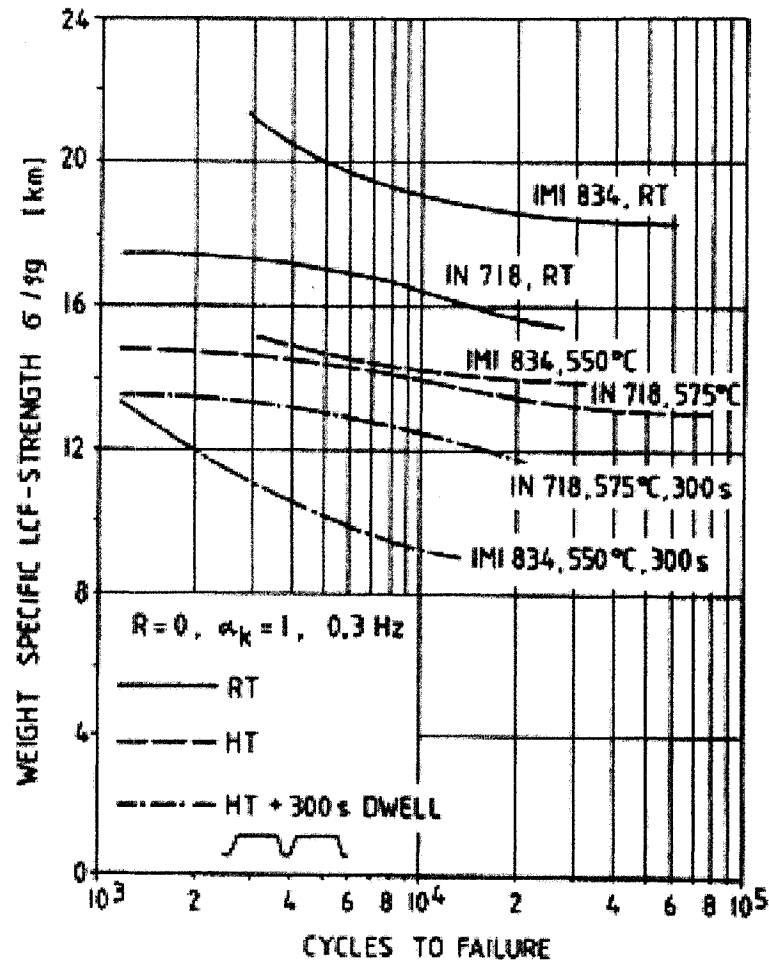


Figure 1.20: Weight-specific LCF comparison of IMI 834 and IN 718. J. Albrecht (1999) [6]

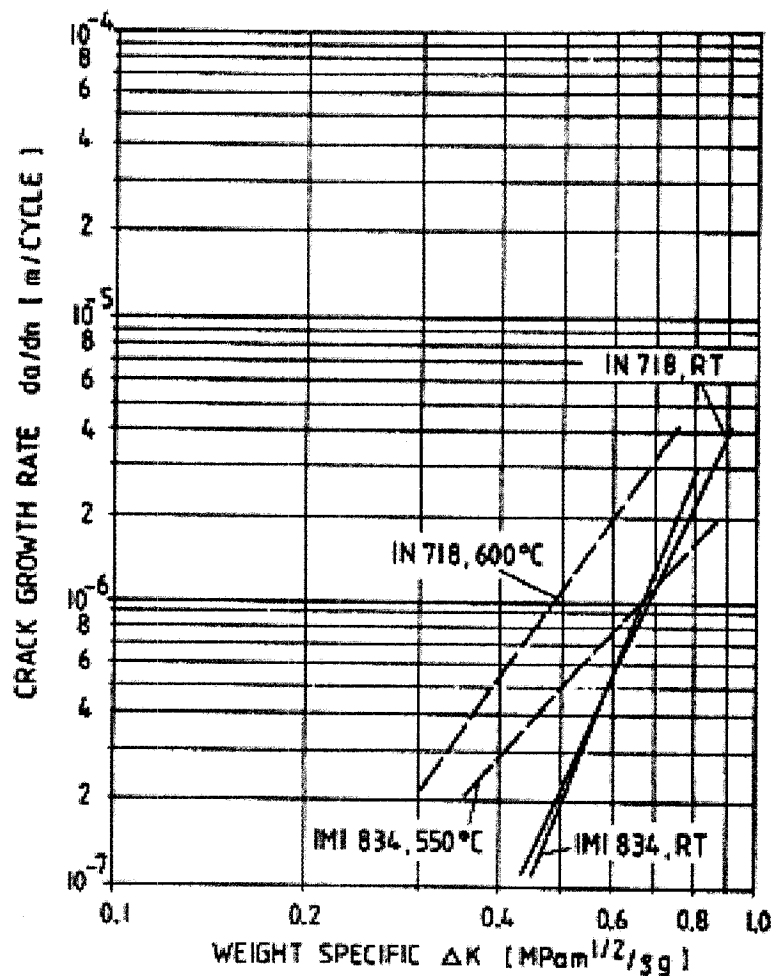


Figure 1.21: Weight-related macrocrack propagation, comparison of IMI 834 and IN 718. J. Albrecht (1999) [6]

The lower elastic modulus of titanium alloys, which may often be a disadvantage, is considered beneficial in a strain controlled LCF situation; with a given total strain amplitude, the plastic portion of this amplitude would be smaller in the lower modulus titanium alloy as compared to nickel alloys with the higher modulus.

Titanium and nickel-based alloys provide high temperature properties, corrosion resistance and high strength-to-weight ratio to ensure efficient fuel consumption for economic operation of flights and longer operational life. E.O. Ezugwu, J. Bonney and Y.

Yamane (2003) [7] made an overview of the machinability of aeroengine alloys. Advanced materials such as aeroengine alloys, structural ceramics and hardened steel provide a serious challenge for cutting tool materials during machining due to their unique combinations of properties such as high temperature strength, hardness and chemical wear resistance. Although these properties are desirable design requirements, they pose a greater challenge to manufacturing engineers due to the high temperatures and stresses generated during machining. The poor thermal conductivity of these alloys results in the concentration of high temperatures at the tool-workpiece interface.

Nickel-based alloys are the most widely used superalloy, accounting for about 50 wt.% of materials used in an aerospace engine, mainly in the gas turbine compartment (see Fig. 1.25). They provide higher strength to weight ratio compared to steel, which is denser. The use of nickel-based alloys in such aggressive environments is due to the fact that it maintains high resistance to corrosion, mechanical and thermal shock, creep and erosion at elevated temperatures. These properties are required for the efficient and effective service performance of the domains in which the alloy is used. In aeroengines these are specifically for the manufacture of turbine blades, which operate at higher pressure and temperature.

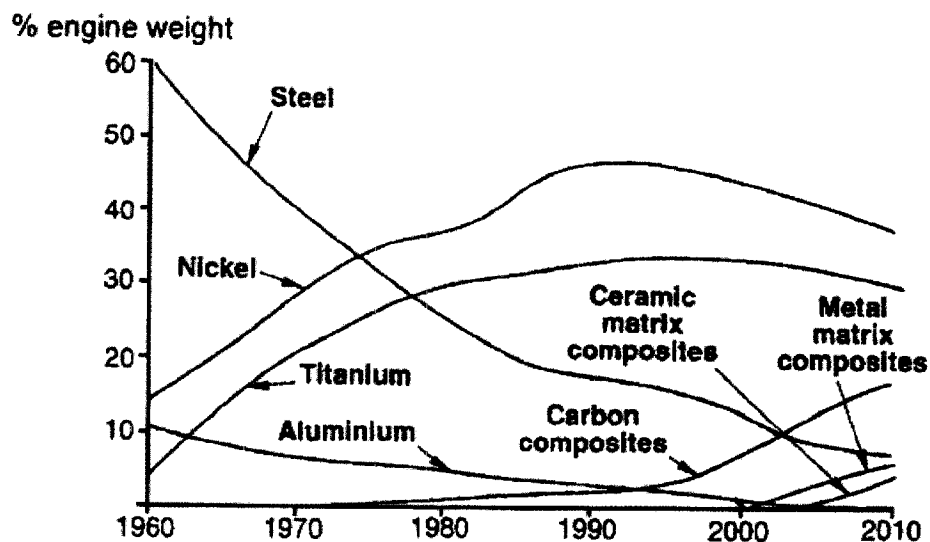


Figure 1.22: Evaluation of materials use in aerogas turbines. E.O. Ezugwu, J. Bonney and Y. Yamane (2003) [7]

Commercially available nickel-based alloys include Inconel, Nimonic, Rene, Udimet, and Pyromet. A comprehensive list of these alloys is given in Table 1.2. Inconel 718 is the most frequently used of the nickel-based alloys, accounting for 25 and 45% of the annual volume production for cast and wrought nickel-based alloys, respectively. It is therefore not surprising that a significant proportion of published information is on the machining of Inconel 718 in the last three decades.

Table 1.2: Commercially available nickel-based alloys. E.O. Ezugwu, J. Bonney and Y. Yamane (2003) [7]

Inconel (587, 597, 600, 601, 617, 625, 706, 718, X750, 901)
Nimonic (75, 80A, 90, 105, 115, 263, 942, PE 11, PE 16, PK 33, C-263)
Rene (41, 95)
Udimet (400, 500, 520, 630, 700, 710, 720)
Pyromet 860
Astroloy
M-252
Waspaloy
Unitemp AF2-IDA6
Cabot 214
Haynes 230

Titanium alloys, like nickel-based alloys, have very high strength-to-weight ratio making them very suitable for aircraft engines. The use of titanium alloys as engine component materials is due to their ability to maintain high strength at high operating temperatures of the engine. Titanium alloys exhibit exceptional resistance to corrosion, which provides savings on protective coating like paints that will otherwise be used in the case of steel. In aeroengines titanium alloys are used in both low and high-pressure compressors and for components subjected to high centrifugal loads such as disks and blades that have reduced flow diameters. Titanium alloys are used as well for components that operate under severe fatigue conditions.

Titanium alloys account for 30% of the total engine mass in commercial and 40% in military projects. This usage will increase if improved processing techniques are developed, eliminating defects that are detrimental to the efficient operation of the engine as a result of premature failure of components. One of these defects is the initiation of cracks by brittle inclusions in the alloy that can cause structural failures in the engine.

1.3 MANUFACTURING TECHNOLOGIES

This section makes a review of friction welding and flow-forming topics, which were suggested by PWC.

1.3.1 Assembling techniques

M. Soucail and Y. Bienvenu (1996) [8] explain the dissolution of the γ' phase in a nickel base superalloy at equilibrium and under rapid heating. A simple model had been derived which rests on a pseudo-binary thermodynamic equilibrium formalism and in which the kinetics are diffusion controlled. The method is particularly useful to predict the γ' structure of friction welds, which is crucial for the mechanical behavior of the weld and to adjust the friction welding parameters.

Y. Yamashita, T. Yoshida and K. Fujita (1998) [9] made an investigation on the application of friction welding of dissimilar metal joints for electric power plants. The effects of friction welding conditions upon impact and creep properties were considered for dissimilar metal friction welded joints.

M. Preuss, J.W.L. Pang, P.J. Withers and G.J. Baxter (2002) [10] paper describes a quantitative study of microstructure of nickel-based superalloy tubes joined by friction welding. Hardness profiles have been recorded to map the variation of strength across the weld line. M. Preuss, J.W.L. Pang, P.J. Withers and G.J. Baxter also wrote another paper (2002) [11], whereby steep micro structural gradients have been observed in nickel-based superalloy tube structures welded by friction welding and, the concomitant residual stresses have been mapped at depth using neutron diffraction.

L. D'Alvise, E. Massoni, S.J. Walløe (2002) [12] paper details how to do the finite element modeling of the friction welding process between dissimilar materials. The numerical multi-material model was proven to be numerically efficient in terms of multi-body contact and experimentally validated.

1.3.2 Cold forming techniques

The paper of M. Jahazi and G. Ebrahimi (2000) [13] studies the influences of flow forming parameters and the state of the microstructure on the quality and mechanical properties of a D6ac steel. The effects of feed rate, the shape of the contact line, the roller angle and the percentage reduction on the elimination of spinning defects such as a wave-like surface. Also, the influence of the preheat temperature, the holding time and the cooling rate on the microstructure and mechanical properties of the material were investigated.

The report of H. Näegel, H. Wörner and M. Hirschvogel (2000) [14] deals with the optimization of the process flow between bulk forming of parts and the subsequent machining processes of the forgings. The key aspect is to demonstrate the significance of

combining the forming and machining operations to be optimized by one supplier, and how it can be more effective than the alternative of simply delivering a formed part, which then has to subsequently be machined.

K.S. Lee and L. Lu (2001) [15] present studies conducted on the flow forming of cylindrical tubes using rolling mechanism. Theoretical analysis on the force of the flow forming was also carried out to study the influence of the different parameters.

Dynamic Machine Works (www.flowforming.com) are leaders in flow forming. After flow forming Inconel 718 for years, they conclude that flow forming offers the designer an opportunity to explore the very high tensile properties including grain refinement of Inconel 718 after a full solution heat treatment of the flow formed tubular parts. DMW also flow forms Ti-6Al-4V, which offers the designer of tubular parts to incorporate the higher strengths usually associated with a full solution and aging heat treatment at a superior level of tensile elongation.

1.4 LITERATURE REVIEW CONCLUSIONS

As mentioned in the introduction, PWC suggested the use of friction welding technique and the flow-forming technique as possibilities to manufacture this shaft. Following the literature review, it is possible to say that these techniques are recommended as explained in the papers of J.A. Miller and J.J. O'Connor (1980) [1] and P. Amborn, H. Frielingsdorf, S.K. Ghosh and K. Greulich (1995) [2] for the friction welding technique, and the paper of P. Amborn, S.K. Ghosh and I.K. Leadbetter (1997) [3] for the flow-forming technique of shafts.

With the friction welding technique, the opportunity of having a power shaft being a rigid one-piece construction that is manufactured using different steels, each selected for its location and function, is a very interesting option. For the flow-forming technique, the flexibility to adjust the diameter and wall thickness along the length of a power shaft represents a great advantage.

The PW307 power shaft is actually made with superalloy Inconel 718. In the literature review many papers support the use of superalloy Inconel 718 like D.G. Backman and J.C. Williams (1992) [4], M. Rahman, J. Albrecht (1999) [6] and E.O. Ezugwu, J. Bonney and Y. Yamane (2003) [7].

Nickel-based alloy maintains high resistance to corrosion, mechanical and thermal shock, creep and erosion at elevated temperatures, which is the case for the PW307 power shaft. These properties are required for the efficient and effective service performance of the domains in which the alloy is used. Nickel-based alloys provide higher strength to weight ratio compared to steel, which is denser.

CHAPTER 2. PROBLEM STATEMENT AND CONTEXT

The PW307 power shaft has a complex external profile and is hollow out in the centre using the gun drill technology. Presently, the shaft is manufactured starting from a bar of raw material in Inconel 718 and the problems are the following ones:

- **80% of raw material must be removed.**
- **The relationship of the concentricity between the internal diameters and the external diameter is very difficult to control.**
- **Inconel 718 is difficult to machine.**

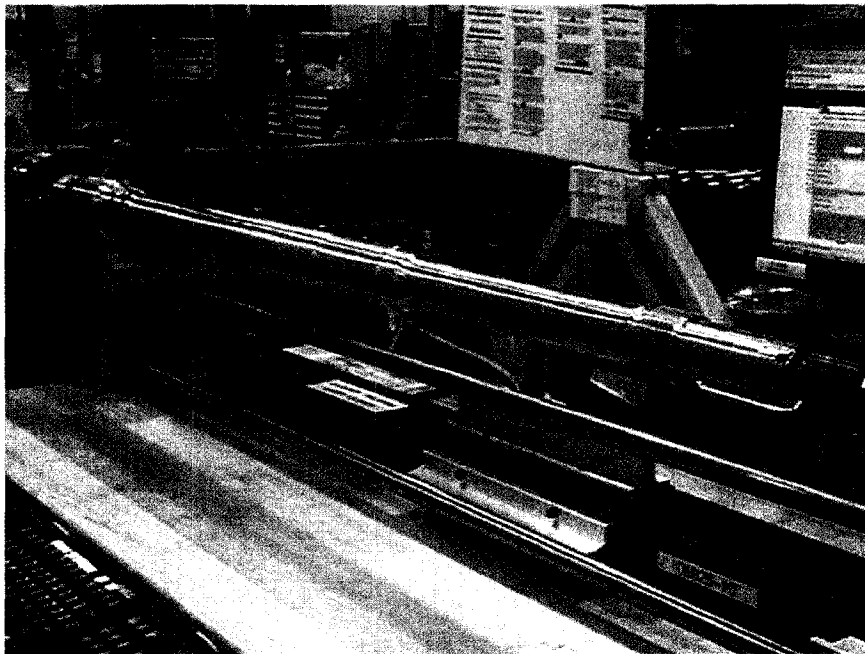


Figure 2.1: PW307 power shaft

Besides these technical problems, the cost of production of the shafts should be lowered in order for the company to stay competitive in the market.

2.1 OBJECTIVES

The main objective of this project is to solve the technical problems just stated for the shaft as well as having a cost reduction for the production of it. In order to achieve these goals, the approach being used is not only based on a change of the manufacturing technology but, also on the understanding and modifying of the actual design of the power shaft. It is essential to change and adapt the design to be able to use different manufacturing technologies that weren't possible to be used with the original design. Fundamentally, the design has to be integrated with the manufacturing to achieve the best performance and the lowest price. To do so, the objectives of the project are as follows:

- **Lower the machining time and material removal.**
- **Fix the concentricity problem between the inside and outside diameters.**
- **Overcome the difficulties of machining Inco718.**

Since the design of the shaft will be modified, another objective of this project is to make sure that the design of the shaft is optimized. The rule of the optimization consists in maximizing the use of the material in the shaft, in other words, avoiding over designed sections that would result in over weight without having better performances. Moreover, this optimization has to be implemented in a program that can execute it automatically on others PWC's shafts. Consequently, the following objectives are added:

- **Development of an optimization technique for the design of the power shaft.**
- **Development of a computer program performing the design optimization of the power shaft.**

Before starting the project, PWC suggested few manufacturing techniques to attempt to facilitate the machining of the power shaft. The potential techniques are the following ones:

- Friction-welding technique to manufacture a Bi-Material power shaft.
- Flow-forming technique.

2.2 MOTIVATION

Thanks to this master project, PWC will have the following benefits:

- **Cost reduction of the manufacturing of the power shaft.**
- **Weight reduction of the power shaft.**

These advantages will allow PWC to be an innovative leader with today manufacturing technologies used to manufacture power shafts for turbine engines.

CHAPTER 3. ACTUAL SHAFT

In this chapter, the actual configuration of the PW307 engine shaft is presented along with the manufacturing procedures and techniques that are used to produce it.

3.1 SHAFT DESIGN

The outside profile of a shaft is determined by the engine's components that are assembled on it and the available clearance between the shaft and the nearby components of the engine (See Fig. 3.1). However, the inside profile of the shaft depends on the stress and dynamic analyses as well as on the manufacturing technique used to hollow out the center of the power shaft.

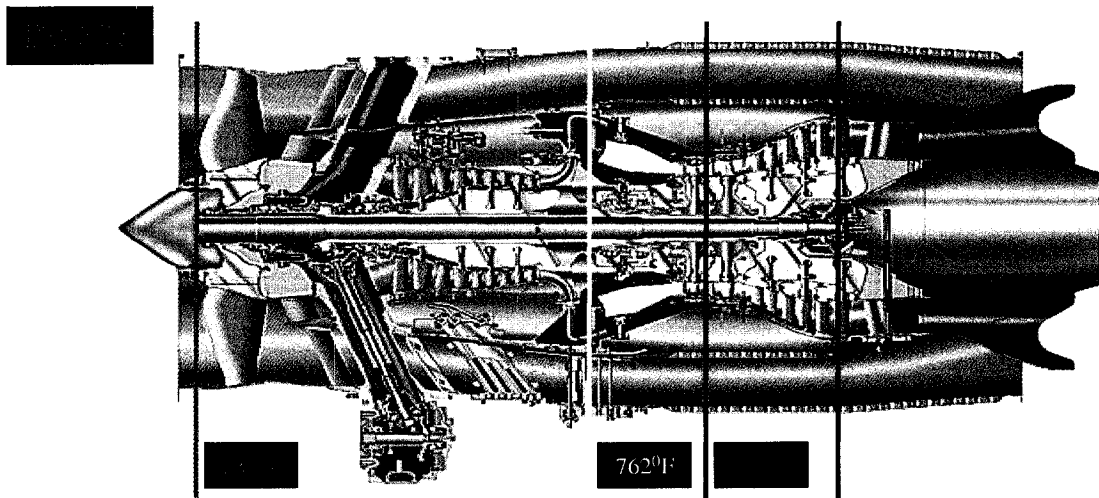


Figure 3.1: PW307 engine cross section with operational temperatures

3.1.1 P0889 Shaft Analysis Program

The stress analysis is performed using an in house PWC program specially conceived for this purpose. P0889 is a shaft strength analysis program written in FORTRAN 77 that is used to determine an effective stress and life of most PWC shafts. The program determines the life of the shaft undergoing simultaneous LCF-HCF (Low cycle fatigue & High cycle fatigue) loading and as well computes the Gyroscopic Precession life. It is

also capable of handling ultimate load analysis for blade-loss, bird-strike, and seizure torque cases, as well as limit analysis for medium bird-strikes. Basically, there are seven available types of analysis:

1. LCF-HCF Analysis
2. Gyroscopic Precession
3. Fan Blade-Loss (Ultimate Load Analysis)
4. Large Bird Strike (Ultimate Load Analysis)
5. Medium Bird Strike (Limit Load Analysis)
6. Turbine Blade-Loss (Ultimate Load Analysis)
7. Seizure Torque (Ultimate Load Analysis)

Since the shaft of the engine is rather complex with many different geometric features P0889 allows simultaneous:

1. External Fillet Feature
2. Section with Holes
3. External U-Cut
4. Standard Splines (N/A)
5. Switched-Back Splines (N/A)
6. External Axial Slot Feature
11. Fillet As Internal Feature
12. Section with Holes As Internal Feature
13. U-Cut As Internal Feature
0. Manual Section (N/A)

P0889 reads an input file and generates an output file of the same name `input_file_name.output`.

3.1.1.1 Input file

An example of input file, corresponding to the PW307 engine, is available in the appendix I at the end of this document. It is recommended to consult it as this section is being read.

Program control

The *first* line of the input file contains descriptive information about the engine that is being analyzed. The *second* line of the input file contains several flags (control parameters) that describe the type of analysis to be executed. It also includes information as to where the program should get its material information. P0889 is designed to read material data from the input file or to simply retrieve it from the PWC database. The *third* line will indicate the number of model sections.

Section geometry data

Following the above lines, every group of five continuous lines has specific information that describes each section. In the first line, the type of section is given with the section ID, the axial position on the shaft and the material type. In the second line, depending of the type of section, different dimensions define the size of the section. In the following figures, it is possible to see the typical values required to describe an external or internal fillet.

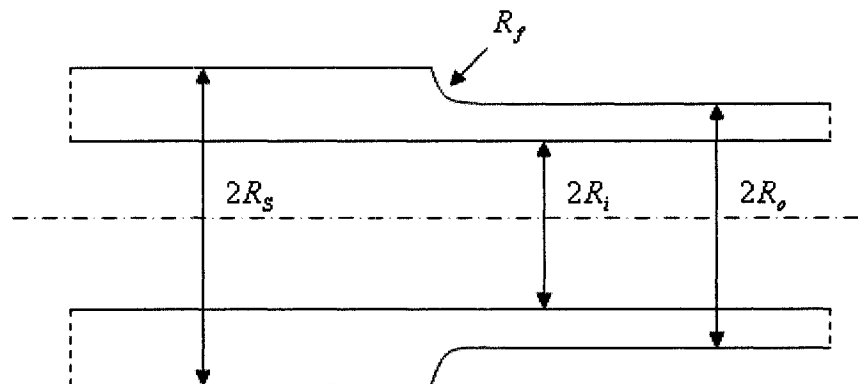


Figure 3.2: Feature dimension definition (external fillet) – PWC P0889 Shaft Analysis Program Engineering and Software Manual [16]

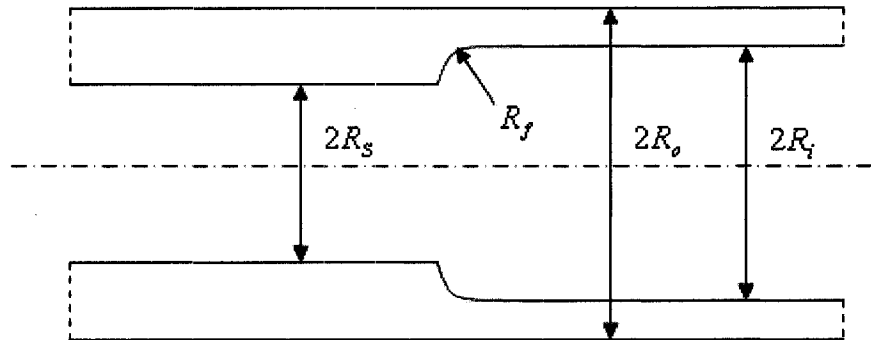


Figure 3.3: Feature dimension definition (internal fillet) - PWC P0889 Shaft Analysis Program Engineering and Software Manual [16]

The third line regarding the section data is for the stress of concentration values and the last two lines are for specific material data.

Section stress/forces data

After the groups of geometry section description, there is a line indicating the quantity of sets of loads, which also represent the number of analysis executed on the shaft by the program P0889. The following lines describe the load groups that act on each section for each type of analysis.

3.1.1.2 Output file

An example of output file, corresponding to the PW307 engine, is available in appendix I at the end of this document. It is recommended to look at it as this section is being read.

Structure

The output file is organized in tables. The tables within the file are identified as follows:

1. Section cross reference
2. Section physical description
3. Section material description

4. Analysis # 1 results
5. Analysis # 2 results
6. Analysis # 3 results
-
- n*. Analysis # *n* results
- n+1*. Design factor summary

The last table in the output file is a summary of all of the design factors calculated from the previous load sets. A summary of all the design factors included in the table is given below.

Table 3.1: Design Factors Summary

LOAD CASE	1	2	3	4	5	6	7	... <i>n</i>
SECT NUMB	LCF-HCF ANALYSIS	LCF-HCF ANALYSIS	GYROSCOPIC PRECESSION	COMPRESSOR BLADE-LOSS	COMPRESSOR BLADE-LOSS	MEDIUM BIRDSTRIKE	LARGE BIRDSTRIKE	
1								
2								
3								
...								
<i>n</i>								

Factors for PW307 engine shaft

In the case of the PW307 engine, seven analyses are executed for the shaft. The analyses are the same as the ones in the design factor summary table (Table 3.1).

The design factors are proportional to the life cycles. When the design factor is met, the life cycles correspond to the warranty life cycle. For an engine, a cycle represents a mission from the takeoff to the touchdown of an airplane. For PW307 engine, the warranty guarantees 20,000 life cycles.

In order to be acceptable, the design factors for each analysis should meet different target values.

For LCF-HCF (Low cycle fatigue & High cycle fatigue) Analysis:

The combined equivalent HCF elastic stress from the applied forces divided by the endurance strength of the shaft material is greater than **1.0**, the LCF-HCF analysis does not meet the target life.

For Gyroscopic Precession:

The combined equivalent gyroscopic HCF stress divided by the allowable HCF stress is above **1.0** than the analysis does not meet the target life.

For Ultimate Load Analysis:

The ultimate load factor, which is the effective plastic stress divided by the ultimate tensile strength, can be above 1.0, if it can be compared to experimental testing results. For PW307 engine shaft the required value is **1.34** for compressor blade-loss and **1.6** for large bird strike first 7 sections of the shaft.

For Limit Load Analysis:

The yield load factor, the ratio of the maximum elastic stress divided by the material yield strength, can be above 1.0 if it can be compared to experimental testing results. For PW307 engine shaft the required value is set to **1.7** for medium bird strike.

Table 3.2: Analysis values requirements for P0889 Shaft analysis program.

LCF-HCF ANALYSIS	GYROSCOPIC PRECESSION	COMPRESSOR BLADE-LOSS	MEDIUM BIRDSTRIKE	LARGE BIRDSTRIKE
<p><1.0 For all the sections of the shaft.</p>	<p><1.0 For all the sections of the shaft.</p>	<p><1.34 For all the sections of the shaft.</p>	<p><1.7 For the first 7 sections of the shaft.</p>	<p><1.6 For all the sections of the shaft.</p>

3.1.2 Dynamic analysis of the power shafts

When a new power shaft is designed, an important step for its final approval is the verification of critical speeds, steady state maneuver and unbalanced response, as well as transient rotor response under bird ingestion and blade loss scenarios. All these analyses are part of PWC best practices for rotordynamics. In order to validate the power shaft, P0571 computer program takes care of all of the mentioned analyses.

In general, before running the P0571 computer program, some data manipulation has to be done. Firstly, the 3D models of each components of the dynamical system are transformed in points with a function in CATIAV4 that was specifically created for this purpose. Afterwards, these points are treated in a special PWC computer program (NASBEAM) and a NASTRAN compatible file is created, which will be integrated in the input file that will be run in the P0571 computer program.

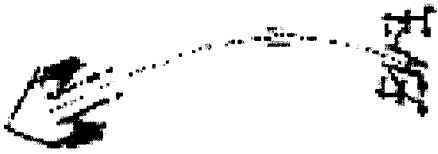
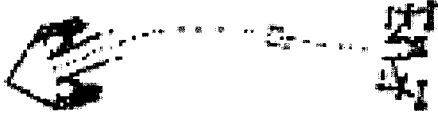
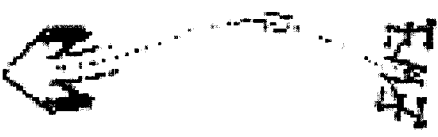
3.1.2.1 Procedure of P0571 Whirl speed analysis of coaxial shafts

The first part of this program utilizes shaft geometrical and material properties information to compute shaft element weights, inertias and flexibilities. The second part of the program utilizes these quantities to calculate the fundamental and overtone transverse natural frequencies of the undamped system of up to fifteen concentric, flexible, irregular, rotating and/or stationary shafts under dynamic loads and centrifugal

stiffening forces, for either a forward or backward precession. The effects of the radial and bending flexibility of the bearings and their supports are considered along with both the bending and shear flexibilities of the shafts. The variation in the relative speeds of the shafts during run-up is accommodated. Bearing with asymmetric stiffness can be specified.

Kinetic and strain energy distribution are calculated for each mode. The strain energy distribution is subdivided on the power shaft and on the two bearing supporting it. In table 3.3, the results of the computer program P0571 for the actual power shaft are shown. To have a shaft that is dynamically acceptable, the strain energy on the power shaft should not be over 50% of the total strain energy. The other important thing is that the third mode should happen at a speed of 120% of the redline speed of the engine (in our case 11,000 rpm). A printer plot of each mode is provided (see section 8 in annexes). For each case of bearing stiffness investigated, a summary of results is provided as long as the mathematical model contains no more than three coaxial shafts.

Table 3.3: PW307 power shaft critical speeds

PREDICTED MODE SHAPES AND WHIRLING SPEEDS				
Mode	Speed (% of redline speed 11000rpm)	% of strain energy distribution		
		Power shaft	Bearing No.1	Bearing No.2
1 st 	5052 (45.9%)	44.3 (<50%)	14.9	40.8
2 nd 	5918 (53.8%)	29.7 (<50%)	49.2	21.1
3 rd 	13414 (121.9%) (>120%)	80.4	10.4	9.2

3.1.2.2 Theory of P0571 Whirl speed analysis of coaxial shafts

The program uses the transfer matrix method to calculate the critical speeds of rotor-bearing system.

The rotor is represented by concentrated masses connected by massless shafts behaving according to the Euler bending and Timoshenko shear formulas. Bearings are modeled as springs acting on the shaft at the appropriate axial locations. The rotor cross section may vary in any prescribed manner provided circular symmetry is maintained. Any number of disks or symmetrical masses may be attached. The bearing support may have

symmetrical or asymmetrical stiffness. The gyroscopic effect associated with the moment of inertia of the disks on the rotor may be readily taken into account.

The rotor is modeled by specifying axial stations dividing the rotor into elements. For each rotor element, mass and inertias as well as bending and shear flexibilities are calculated. The mass and inertias are distributed at the two stations defining the element such that the center of gravity of the element is preserved. The shear and bending flexibilities of the element act between the two stations defining the element. There is no restriction on the values of the material properties. They can be changed at any point where it is required.

For more details on the P0571 computer program, the manual “IBM Program. Description of Computer Program UACL NO. P0571. Whirl Speed Analysis of Coaxial Shafts [17]” can be consulted.

3.2 SHAFT MANUFACTURING

As mentioned in chapter 2, the PW307 power shaft (Figure 3.4) has a complex external profile and is hollow out in the centre using the gun drill technology. To have a good image of the actual manufacturing process, an overview of the presently manufacturing operations of the power shaft will be done. The shaft manufacturing cost is presently estimated to be 10,000.00\$ CND.

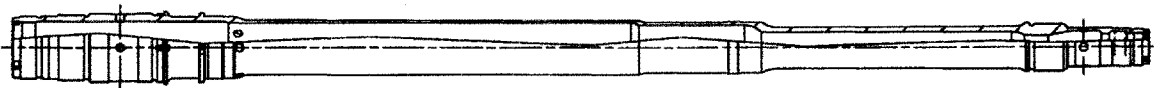


Figure 3.4: PW307 Power Shaft

3.2.1 Manufacturing operations summary

The power shaft is manufactured starting from a bar of raw material in Inconel 718. The first operations consist essentially in doing the roughing of the outside diameters on a

tour as well as pre-drilling the center of the bar on a gun drill machine (Figure 3.5). Afterwards, the outside diameters located in the middle section of the shaft are grinded before hollowing out the center of the shaft with the gun drill machine.

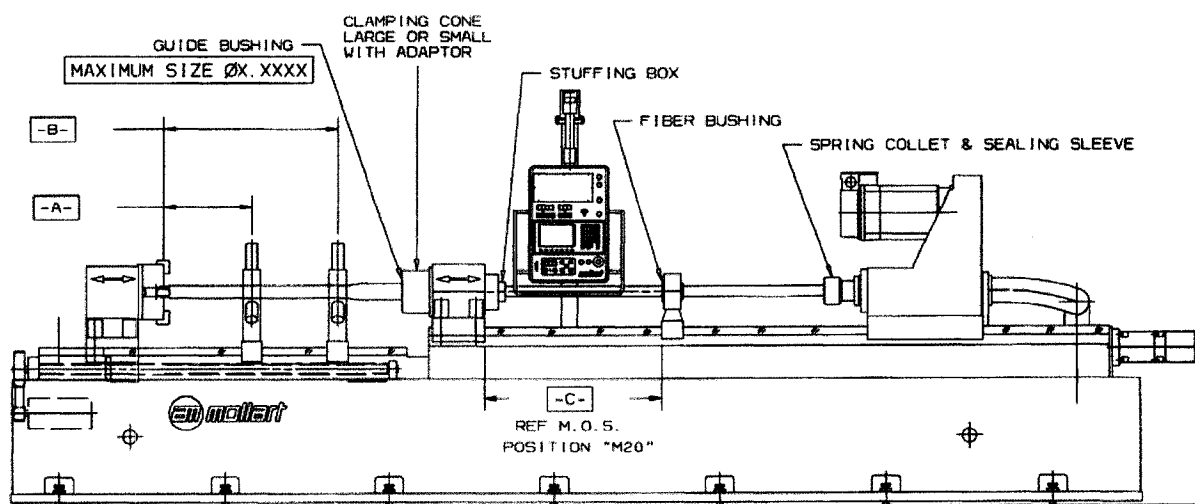


Figure 3.5: Mollart Gun Drill Machine

After the first pass to hollow out the center of the shaft, the center of the big end of the shaft is grinded so the centers of the shaft can be relocated using the SAUPAL backing ultrasonic inspection machine (Figure 3.6).

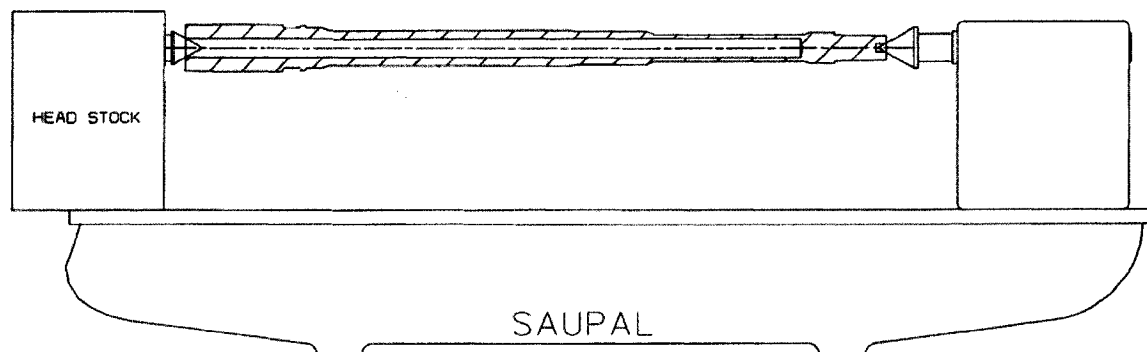


Figure 3.6: SAUPAL Ultrasonic Inspection Machine

At this point, the small end is turned and grinded for roughing and the inside diameters of the shaft are finished on the gun drill machine. Next, the center of the big end is grinded again so the centers of the shaft can be relocated once more. After that, the small end and big end of the shaft are turned and grinded for finish. Finally on both ends of the shaft there are some splines, which are done using a gear shaper (Figure 3.7).

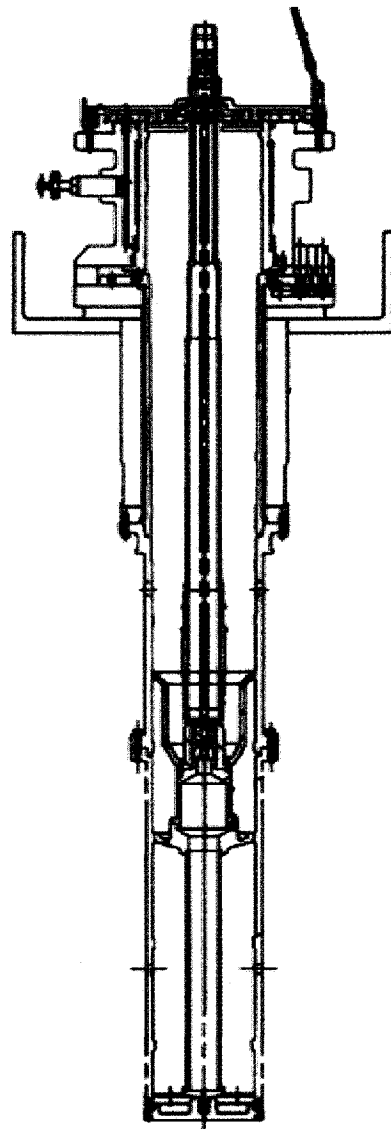


Figure 3.7: Fellows Gear Shaper

3.2.2 Manufacturing operations list

In details, the following list enumerates all the manufacturing operations required to make the actual PW307 power shaft at PWC. The manufacturing operations are as follows:

- | | |
|---------------------------------------|--|
| 1. Rough O/D & Identification | 25. Turn Finish B/End & Final Iden |
| 2. Pre-Hole 1.205 Dia | 26. Best Fit For Runout Improvemen |
| 3. Precipitation Harden Per Cpw2 | 27. Grind Big End |
| 4. Check Hardness | 28. Grind 2 Dia. Big End |
| 5. Spot Turn | 29. Grind Small End |
| 6. Spot Grind Prior Gun Drill | 30. Turn Thread Both Ends |
| 7. Deep Hole 1.460 Dia | 31. Drill & Mill Big End |
| 8. Grind Center Big End | 32. Drill & Mill Small End |
| 9. Spot Grind Prior Correction | 33. Deburr Slots Both Ends |
| 10. Relocate Centers | 34. Grind Spline Dia. Prior To Shaping |
| 11. Spot Grind | 35. Spline -L- |
| 12. Inspect Concentricity Saupal | 36. Spline -K- |
| 13. Turn Faces Small End | 37. Deburr All Over |
| 14. Spot Grind | 38. Power Wash |
| 15. Deep Hole 2.065 | 39. Detail Inspect |
| 16. 2.065 Dia Finish Rad 1.031 | 40. A.T.T.I. |
| 17. Deep Hole 2.275 Dia | 41. F.P.I. All Over Part |
| 18. Deep Hole 2.275 Dia Fini Rad .531 | 42. Power Wash |
| 19. Grind Center Big End | 43. P&P, Before Vendor |
| 20. Spot Grind Prior Correction | 44. Coat Per Cpw33-48 (Vendor) |
| 21. Relocate Center | 45. Inspect After Vendor (Incl. Lab Release) |
| 22. Spot Grind | 46. Grind Coating |
| 23. Inspect Concentricity Saupal | 47. Polish Coating |
| 24. Turn Finish Small End & Ident | 48. Alt Op. Coat Per Cpw33-48 Vendor |

49. Inspect After Vendor

50. Power Wash

51. Final Inspection

52. Preserve, Pack And Deliver

CHAPTER 4. SHAFT RE-ENGINEERING

In this chapter, the core of the project is presented and my personal contribution is enlightened. In the first part, the design aspect of the project is discussed after which, the manufacturing techniques that were retained are explained.

4.1 SHAFT DESIGN OPTIMIZATION

As mentioned in section 3.1 of this document, the outside profile of the shaft is determined by the engine's components that are assembled on it and the available clearance between the shaft and the nearby components of the engine. The inside profile of the shaft depends on the stress and dynamic analyses as well as on the manufacturing technique used to hollow out the center of the power shaft. In section 3.2 of this document, it is shown that the manufacturing technique to hollow out the center of the power shaft is done using the *Mollart Gun Drill* machine. This technique does not allow a complex inside profile, it only allows steps and the more the cutter goes deeper in the shaft's material the more it is hard to control the concentricity accuracy.

4.1.1 Optimization technique

To keep things simple, the outside of the power shaft is kept as it is. It would be too long for the purpose of this project to start verifying the possibility of modifying the outside profile of the shaft because of too many unknowns. Another reason is that, it would be more difficult to get it accepted within PWC. Therefore, the focus of the optimization of the shaft is to work on the inside profile of the shaft, which is the most difficult to manufacture.

In the section 3.1.1.2 of this document the output file of the P0889 Shaft analysis program is explained and the different requirements for each analysis are given. For each section of the shaft, the results of each analysis should meet the required values for the shaft to be accepted. In Figure 4.1 it is possible to see the different sections of the power shaft, where each represents a concentration of stress.

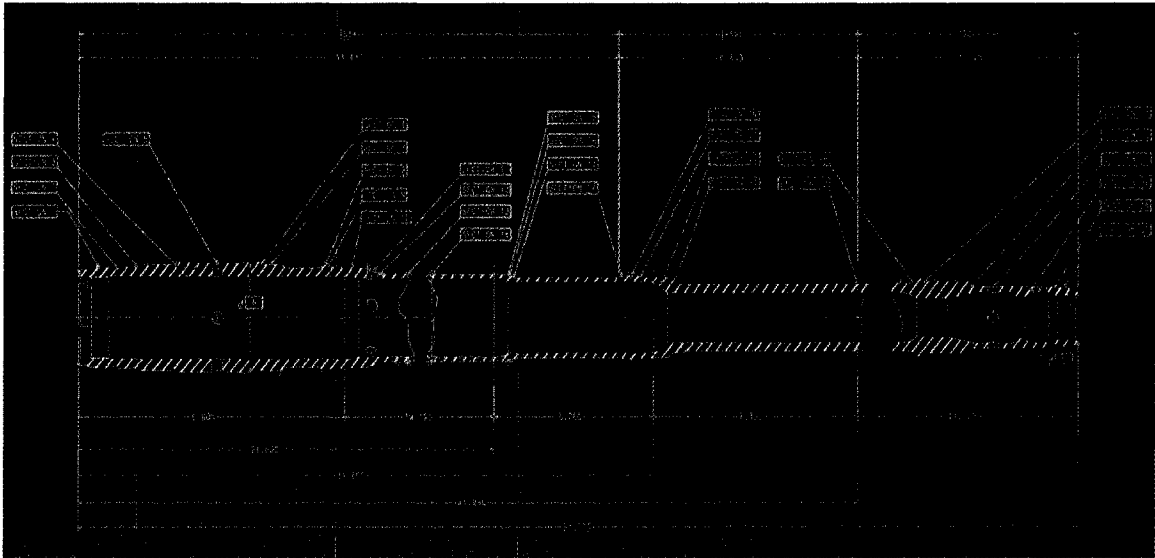


Figure 4.1: PW307 power shaft stress concentration sections

Starting with the LCF-HCF (Low cycle fatigue & High cycle fatigue) Analysis, the combined equivalent HCF elastic stress from the applied forces divided by the endurance strength of the shaft material for a section to be acceptable should not be greater than 1.0 to meet the target life.

In the following graph it can be seen the Equivalent/Allowable stress results for the LCF-HCF Analysis for our original power shaft. The graph was built with the data of the table 4 in appendix II. For the graph in Figure 4.2 the EQUIV/ALLOW (Equivalent/Allowable) column was used, on the other hand for Figure 4.3 the MAXIMUM LCF-LIFE column was used.

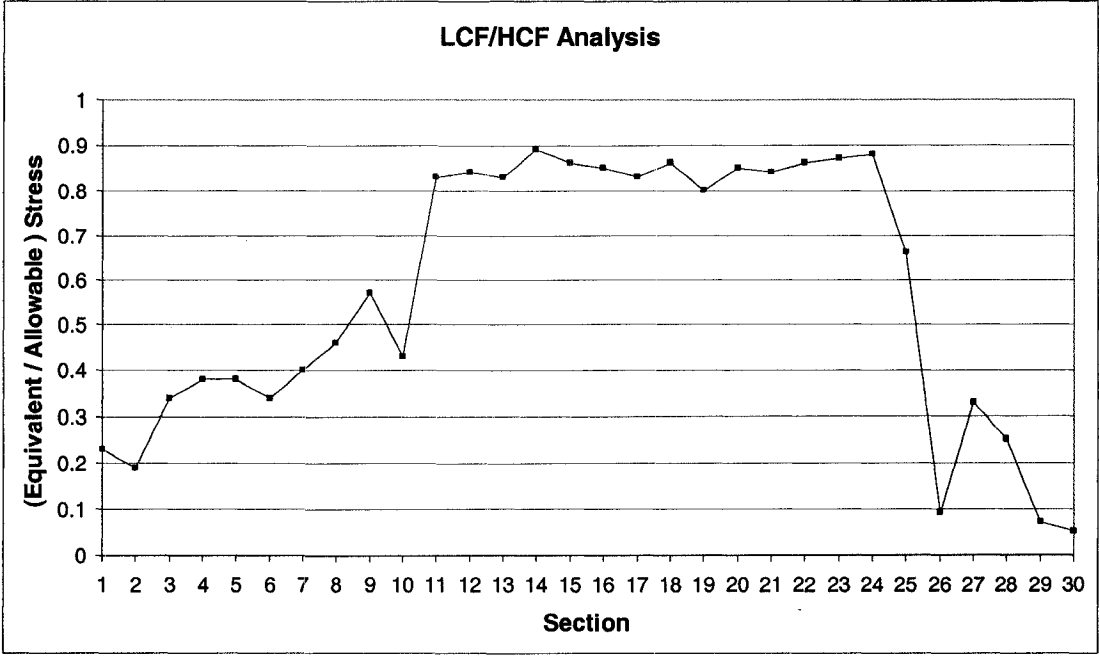


Figure 4.2: Results of LCF/HCF Analysis for PW307 actual power shaft (Equiv/Allow)

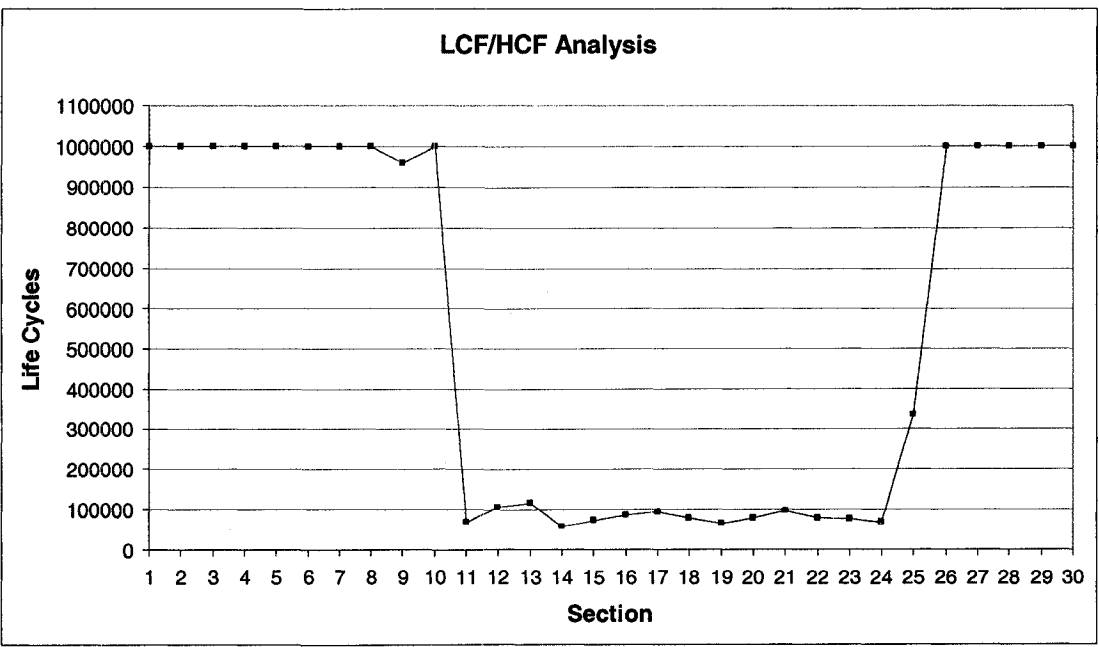


Figure 4.3: Results of LCF/HCF Analysis for PW307 actual power shaft (Life Cycles)

In Figure 4.2 it is possible to notice that all the sections have a value lower than 1.0 and therefore are all acceptable. However, values that are very far from the value of 1.0 have as meaning an over design for that particular section being too strong. That is true for the sections between 1 and 10 as well as between 25 and 30.

That can also be supported by the graph in Figure 4.3, if the values for life cycles are observed for the section just mentioned; it is possible to see the link because these results are of 1,000,000 cycle life which is the same thing as saying that these sections have an infinite life and therefore are over designed. The power shaft for the PW307 engine is guaranteed for 20,000 cycles. Between Figure 4.2 and Figure 4.3 it is also possible to notice the correlation among the value of Equiv/Allow being proportional inverse to the life of the section. As the value of Equiv/Allow approaches 1.0, the life approaches 20,000 cycles. In the other hand, the more the value of Equiv/Allow approaches 0 the more the life approaches 1,000,000 cycles.

The optimizing technique is based on the increase of the section inside diameter value so that when the LCF/HCF Analysis is performed, the Equiv/Allow value for that section will be close to the value of 1.0. As explained in section 3.1 of this document, each section has a geometrical description in the input file used to run the P0889 computer program for shaft analysis. From appendix I, section 16 is taken as an example and from Table 4.1 it is possible to see the value of the inside diameter which is 2.2800”.

Table 4.1: Geometrical description of section 16 for the actual power shaft.

Outside diameter	Type of section	Section ID Label	Section axial position on shaft	Material (4 = Inconel 718)
2.4800	1. ShdIDRf 16	13.761	4.	0.0000
0.000	2.2800	0.5000	2.0600	0.0000
534.4	0.000	0.000		0.0000
534.4				0.297
		Inside diameter	Fillet radius	Shoulder radius
				Material density
				Poisson rate
Outside temperature	Inside temperature			

On the other hand, once the inside diameter value is increased the geometrical description of section 16 would be like in Table 4.2. This information is also available in appendix III. It can be noticed that the inside diameter value was increased to 2.2950”.

Table 4.2: Optimized geometrical description of section 16 (Inside diameter is increased to 2.2950”).

Outside diameter	Type of section	Section ID Label	Section axial position on shaft	Material (4 = Inconel 718)			
2.4800	1. ShdIDRf 16	13.761	4.	0.0000	0.0000	0.0000	
0.000	2.2950	0.5000	2.0600				
534.4	0.000	0.000					
534.4							
	Inside diameter	Fillet radius	Shoulder radius			0.297	0.290
	Inside temperature					Material density	Poisson rate
	Outside temperature						

What is very important to retain here is the value resulting from the LCF-HCF Analysis after the modification to the inside diameter was made. The appendix II represents all the results that were generated from P0889 computer program for the actual power shaft and in appendix IV we can see the table 4 which are the results of the LCF-HCF Analysis for the optimized section. Going back to table 4 in appendix II and looking at the line of section 16, the results for Equiv/Allow and life cycles are 0.85 and 83948. Observing appendix IV, which includes results for LCF-HCF Analysis for sections that have been optimized, more precisely on the line of section 16 it is possible to see that the results for Equiv/Allow and life cycles became 0.91 and 46902.

It is possible to notice with these results that an optimized section remains acceptable compared to the requirements of the analysis and that weight is saved, since the inside diameter is increased. The same exercise was repeated for each section of the power shaft by modifying manually the input file and re-running every time the P0889 computer

program for shaft analysis. The result of the LCF/HCF Analysis of this optimization that is in appendix IV is plotted in Figure 4.4.

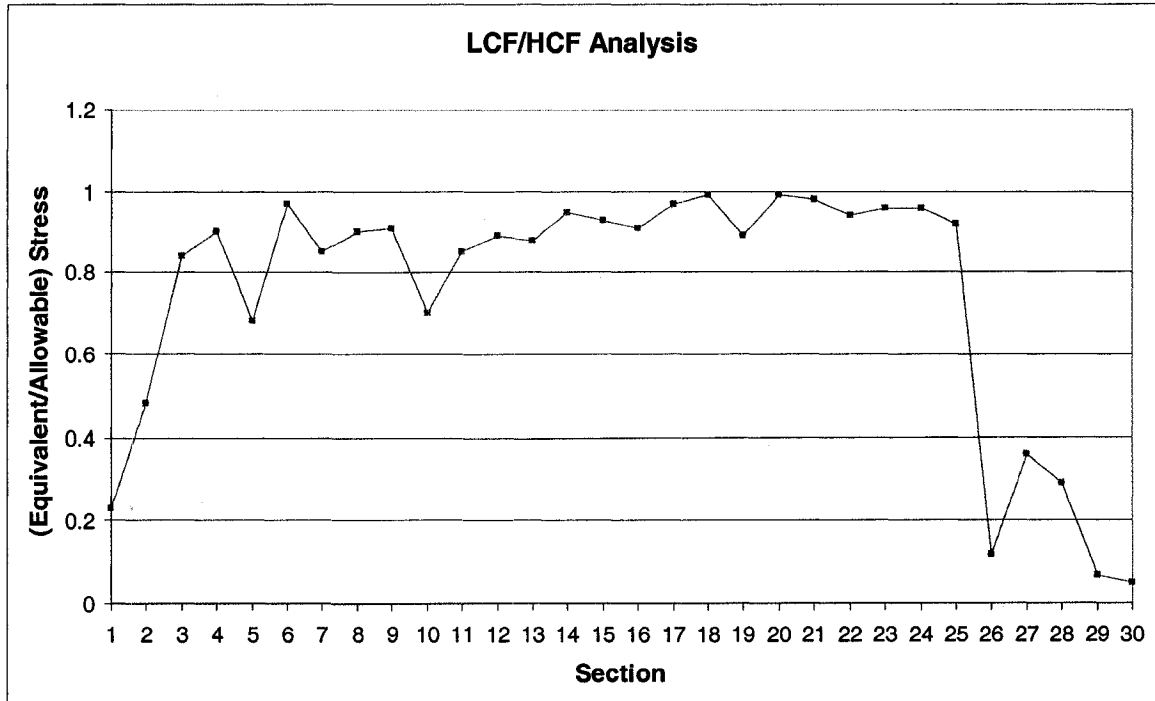


Figure 4.4: Results of LCF/HCF Analysis for PW307 optimized power shaft (Equiv/Allow)

It is possible to see that the values of Equiv/Allow are pretty close to the value of 1.0 for almost all the sections of the power shaft. If the life cycles are analyzed, it is possible to notice in Figure 4.5 that most of the section's life cycles are close to 20,000 cycles.

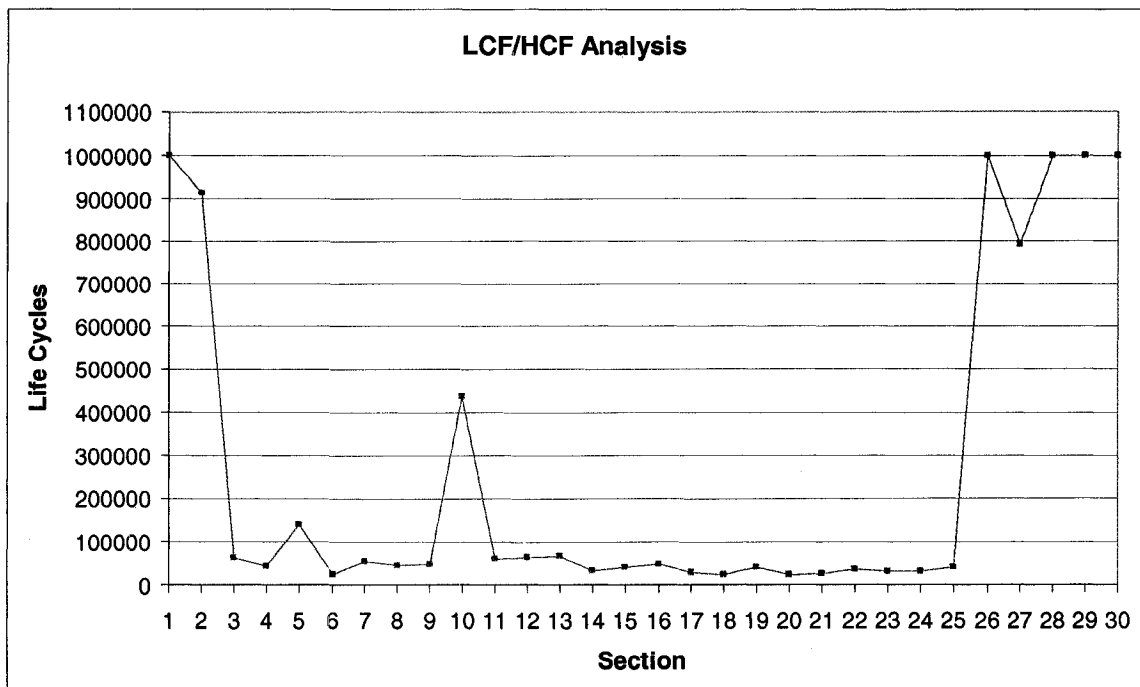


Figure 4.5: Results of LCF/HCF Analysis for PW307 actual power shaft (Life Cycles)

In Figure 4.6 and 4.7 it is possible to see the effect of this optimization for each section compared to the old or actual one.

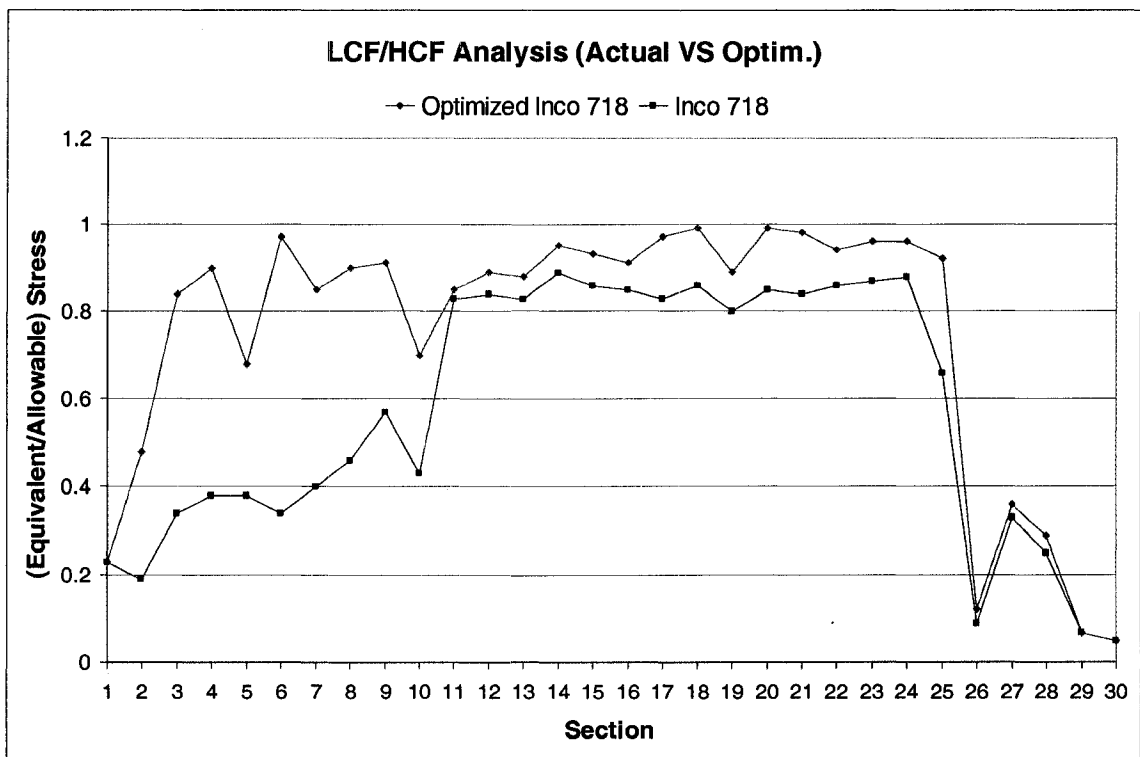


Figure 4.6: Results of LCF/HCF Analysis for Actual VS Optimized (Equiv/Allow)

In Figure 4.6 between section 1 and 10, the value of Equiv/Allow changed drastically and for the rest of the sections it raised considerably. The proportionally inverse situation happened for the life cycles in Figure 4.7 where the life cycle lowered drastically between section 1 and 10 and lowered considerably for the rest of the sections.

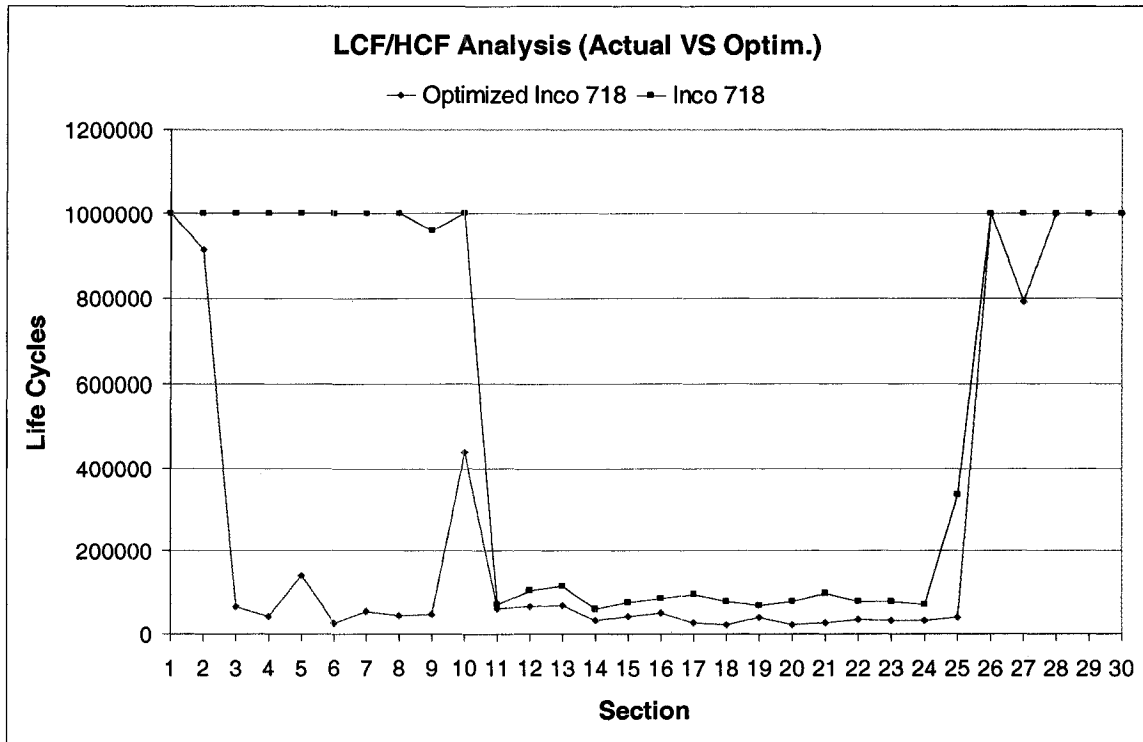


Figure 4.7: Results of LCF/HCF Analysis for Actual VS optimized (Life Cycles)

If the increase of the inside diameter values of each section are translated in weight, it is possible to see the influence of the optimization on the PW307 shaft that counts 30 sections and is 53.125" long. In Figure 4.8 it is possible to notice the weight difference at each section that was optimized as well as the total weight saving of 5.472 lb.

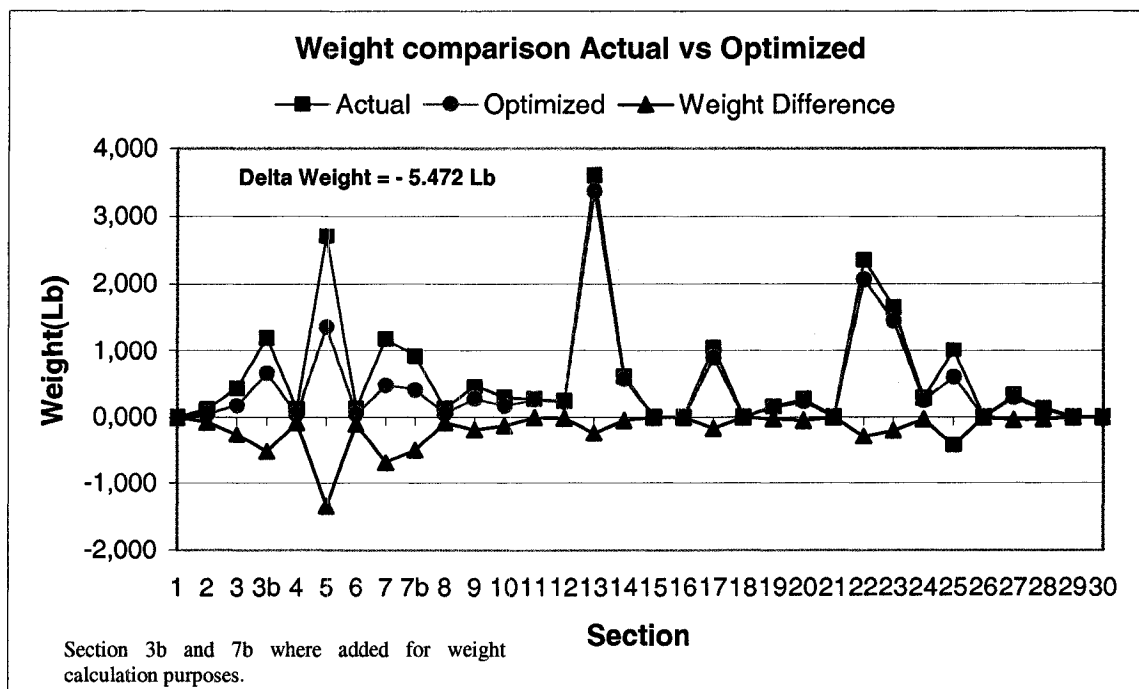
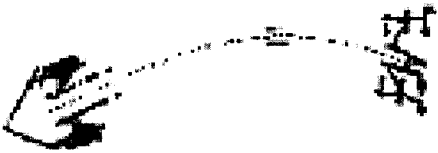
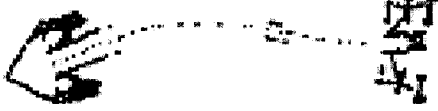



Figure 4.8: Optimization weight savings per section for PW307 power shaft.

As mentioned in section 3.1.2, an important step for a new design's final approval is the verification of critical speeds, steady state maneuver and unbalanced response, as well as transient rotor response under bird ingestion and blade loss scenarios. In table 4.3 the results of the dynamical analysis of the computer program P0571 shows that the third mode happens at 124.5% of the redline speed, which is more than the required 120% of the redline speed and, the power shaft supports less than 50% of the strain energy distribution for the first two modes, which makes the optimized shaft design approvable.

Table 4.3: PW307 optimized power shaft critical speeds

PREDICTED MODE SHAPES AND WHIRLING SPEEDS FOR OPTIMIZED DESIGN OF THE POWER SHAFT				
Mode	Speed (% of redline speed 11000rpm)	% of strain energy distribution		
		Power shaft	Bearing No.1	Bearing No.2
1 st 	5070 (46.1%)	38.3 (<50%)	12.4	48.3
2 nd 	6085 (55.3%)	20.0 (<50%)	66.8	12.8
3 rd 	13691 (124.5%) (>120%)	88.6	4.1	5.7

Coming back to section 3.1.1.2 of this document, in the case of the PW307 engine seven analyses are executed for the shaft. This means, it's not because our values for the LCF-HCF Analysis are respected for each section that the other analysis are good. Following discussion with experts in shaft stress analysis of PWC, it was suggested that if the values were good for the LCF-HCF Analysis, chances that the other analysis weren't good was very small and that maybe just a few sections would have needed to be retouched. By retouch meaning that the inside diameter would have to be lowered to respect the requirements of other analysis. Basically, this was also the reason why the optimization principle is based on the LCF-HCF analysis. Once this optimization would work for this

analysis, it would be easy to adjust it and make each section respect the requirements of all the analysis.

Since the optimization of section based on the values of LCF-HCF analysis was manual and very long, it was decided to reduce it with computer programming. The P0889 computer program for shaft analysis is written in FORTRAN77 and it was resolute to write the optimization program in FORTRAN77 as well to be able to loop on the original P0889 computer program without modifying it. This would permit an easier acceptance of the optimization computer program because the code of the P0889 computer program would not need to be re checked.

4.1.2 Development of P0889opt Automated Shaft Analysis Program

A computer program was developed for the optimization to be repeatable and in order to make the shaft optimization simple and fast.

4.1.2.1 Purpose

P0889opt is a shaft strength analysis program that has been written in FORTRAN 77 that is used to determine an effective stress and life of most PWC shafts. The program is based on the already existing P0889 program, which determines the life of the shaft undergoing simultaneous LCF-HCF loading and as well computes the Gyroscopic Precession life. It is also capable of handling ultimate load analysis for blade-loss, bird-strike, and seizure torque cases, as well as limit analysis for medium bird-strikes. *The role of P0889opt is to make sure that the effective stress and life of the shaft meets the warranty requirements of the corresponding engine.* This way, P0889opt makes sure that the material of the shaft is used to the maximum of its capacity over the entire shaft length.

4.1.2.2 Description

To understand the purpose and functionality of the program P0889opt, a previous lecture of “P0889 - Shaft Analysis Program, Engineering and Software Manual” is strongly recommended.

When P0889opt is run, the program loops on P0889 and it analyze every time the equivalent stress and life of each section of the shaft. Subsequently, P0889opt modifies the inner radius for each section in order to converge towards targeted dimensions, which will make the equivalent stress and lifetime correspond to the engine’s warranty lifetime and equivalent stress.

4.1.2.3 Required inputs

P0889opt reads an input file and generates an output file of the same name input_file_name.output. The input file is an ASCII text file that can be edited with any text editor. The input file structure is exactly the same as the one required for the P0889 computer program. If a new input file has to be created, the user should consult the section 3.1.1.1 Input File and appendix I for an example.

4.1.2.4 P0889opt Overview

As mentioned in section 3.1.1 of this document, P0889 is a P&WC controlled in-house program used to analyse shafts in turbofan, turboprop and turbo shaft engines. There are seven types of stress analysis currently available.

1. LCF-HCF Analysis
2. Gyroscopic Precession
3. Fan Blade-Loss (Ultimate Load Analysis)
4. Large Bird Strike (Ultimate Load Analysis)
5. Medium Bird Strike (Limit Load Analysis)
6. Turbine Blade-Loss (Ultimate Load Analysis)
7. Seizure Torque (Ultimate Load Analysis)

Details concerning each of these types of analysis are included in P0889 - Shaft Analysis Program, Engineering and Software Manual [16].

In order to be successful, each analysis should meet different requirements. The original requirements stated in table 3.2 were modified in P0889opt. Instead of having a number as a target, P0889opt has an interval, which allows the computer program to converge faster. For safety purpose, a security factor was also added.

For LCF-HCF Analysis:

The combined equivalent HCF elastic stress from the applied forces divided by the endurance strength of the shaft material is greater than 1.0 than the LCF-HCF analysis does not meet the target life. *For P0889opt the required value is set between 0.95 and 0.99.*

For Gyroscopic Precession:

The combined equivalent gyroscopic HCF stress divided by the allowable HCF stress is above 1.0 than the analysis does not meet the target life. *For P0889opt the required value is set between 0.95 and 0.99.*

For Ultimate Load Analysis:

The ultimate load factor, which is the effective plastic stress divided by the ultimate tensile strength, can be above 1.0, if it can be compared to experimental testing results. *For P0889opt the required value is set between 1.29 and 1.33 for compressor blade-loss and between 1.55 and 1.59 for large bird strike first 7 sections of the shaft.*

For Limit Load Analysis:

The yield load factor, the ratio of the maximum elastic stress divided by the material yield strength, can be above 1.0 if it can be compared to experimental testing results. For *P0889opt* the required value is set between 1.65 and 1.69.

4.1.2.5 Principals of P0889opt computer program

P0889opt will be explained by detailing the different phases of the operations that the program executes during its use. The phases of P0889opt are the following:

1. Reading of inputs
2. Storing of starting inside diameters
3. Optimization of sections for each analysis
4. Selection of minimum inside diameter
5. Manufacturing constraints application
6. Results output

In this section the phases will be explained textually, while in chapter 5 it will be possible to consult the algorithm structure of each phase.

4.1.2.6 Reading of inputs

When P0889opt is executed, it prompts the number of steps existing in the inside of the shaft, at which section of the shaft each of the steps starts and at which section they end. In the following page, a drawing of a typical shaft is illustrated showing how to establish the prompted inputs.

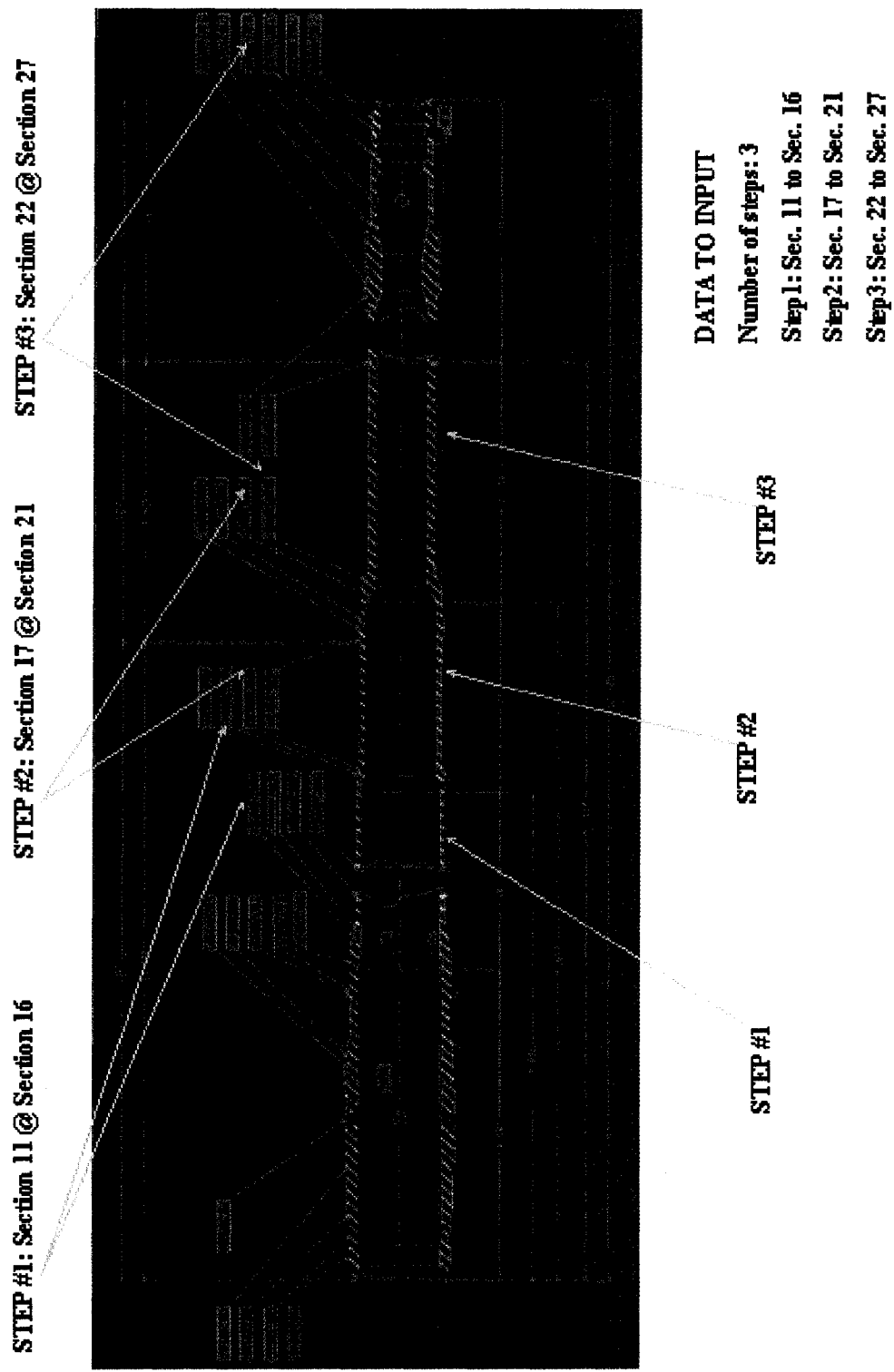


Figure 4.9: PW307 Actual power shaft with data prompted when running P0889 Shaft analysis program

4.1.2.7 Storing of starting inside diameters

Since in the following section it will be question of optimization of each analysis, it is important to retain the dimensions of the starting inside diameter present in the input file. These inside diameters need to be recovered and available for whichever analysis, when it has to be optimized.

4.1.2.8 Optimization of sections for each analysis

The optimization of sections is done for each type of stress analysis executed by the P0889 program. When P0889opt reaches the optimization phase of operations, it makes sure that each section of the shaft meets very closely the requirements of each the stress analysis avoiding that the shaft is over designed and it stores the optimum inside diameter of each analysis in a table.

To simplify the description of the optimization phase of the program, the phase will be divided in three sub phases. The corresponding sub phases are the following ones:

1. Optimization of one section;
2. Repetition of the optimization for all the sections;
3. Repetition of point 1 and 2 for each type of the stress analysis.

P0889opt reads the inside diameter of the first section in the shaft and adds an increment (for example an increment of 0.010”) to it. Afterwards, the program calls the P0889 program and when results are back, it verifies the requirement of the current analysis that is being optimized and the wall thickness dimension.

If the resulting value is smaller than the required value tolerance, another increment is added to the inside diameter and P0889 is called again.

If the resulting value is greater than the required value tolerance and the wall thickness is greater than 0.060", which is a manufacturing constraint, the increment is split in two and once its added to the inside diameter and P0889 is called again.

If the wall thickness is smaller than 0.060", the last inside diameter previously to the increment, that made the wall thickness smaller than 0.060", is kept as the good one, even if the resulting value is lower than the required value tolerance.

Finally, when the resulting value is within the required value tolerance and that the wall thickness is greater than 0.060", P0889opt passes onto the next section and starts the same optimization procedure all over again. Furthermore, when all the section are optimized, P0889opt passes onto the next stress analysis and the same optimization procedure is done for all the sections but with different required value tolerance corresponding to the current stress analysis.

4.1.2.9 Selection of inside diameter

After optimization is completed, P0889opt returns optimized inside diameters for each section in the shaft for each type of stress analysis that was done. At this point, for each section the minimum of the optimized inside diameters is retained.

4.1.2.10 Manufacturing constraints application

Once P0889opt selected the entire minimums optimized inside diameters for each section, it may happen that a shaft with those dimensions cannot be manufactured with any manufacturing technique.

Presently, the available manufacturing technique is the gun drill. Therefore, P0889opt applies manufacturing constraints that take into account the gun drill technique requirements. When the gun drill technique is used to manufacture a shaft, this one will have different steps in the inside diameter.

In section 4.1.2.6, it was specified that the user had to enter the number of steps in the inside diameter of the shaft and at which section the steps start and at which section they end. With this data, P0889opt selects the minimum optimized diameter of the sections that are within the step, which means that for each step there will be a constrained optimized inside diameter.

4.1.2.11 Output file of P0889opt

The output file of P0889 Automated Shaft Analysis Program is similar to the one of the P0889 Shaft Analysis Program. The only difference, the data entered from the user when P0889opt is run is located at the beginning of the output file. An example of the output file of P0889opt is available in appendix IX.

4.2 NEW MANUFACTURING TECHNOLOGIES

As mentioned in the introduction, PWC suggested the use of friction welding technique and the flow-forming technique as possibility to manufacture this shaft. Following the bibliographic review it is possible to say that these techniques are recommended as explained in the papers of J.A. Miller and J.J. O'Connor (1980) [1] and P. Amborn, H. Frielingsdorf, S.K. Ghosh and K. Greulich (1995) [2] for the friction welding technique, and the paper of P. Amborn, S.K. Ghosh and I.K. Leadbetter (1997) [3] for flow-forming technique of shafts.

4.1.1 Friction welded shaft

Firstly, the friction welding process is explained and a little review is done on the different materials that can be used with this technique. Subsequently, some power shaft configurations are proposed with stress analyses to support them. Finally, the tests that are being done to prove the feasibility of this process for the PW307 power shaft are presented.

4.2.1.1 Friction welding process

The Friction Welding process, is defined in the American Welding Society Abstract, Recommended Practices for Friction Welding (<http://www.nctfrictionwelding.com>):

"In the direct drive variation of friction welding, one of the workpieces is attached to a motor driven unit, while the other is restrained from rotation (Figure 4.10). The motor driven workpiece is rotated at a predetermined constant speed. The workpieces to be welded are moved together, and then a friction welding force is applied. Heat is generated as the faying surfaces (weld interface) rub together. This continues for a predetermined time, or until a preset amount of upset takes place. The rotational driving force is discontinued, and the rotating workpiece is stopped by the application of a braking force. The friction welding force (forge force) is maintained or increased for a predetermined time after rotation ceases (Figure 4.11)."

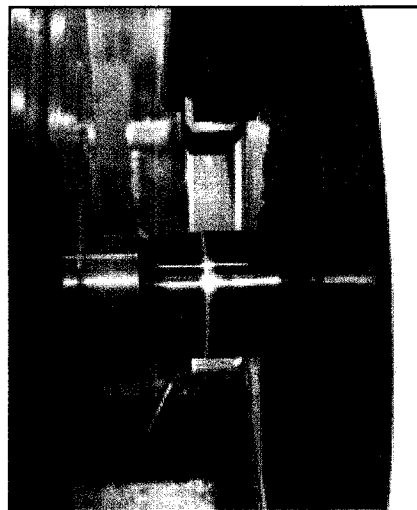


Figure 4.10: Phase 1 - Low temp interface heat cycle by spinning one component against another stationary component.

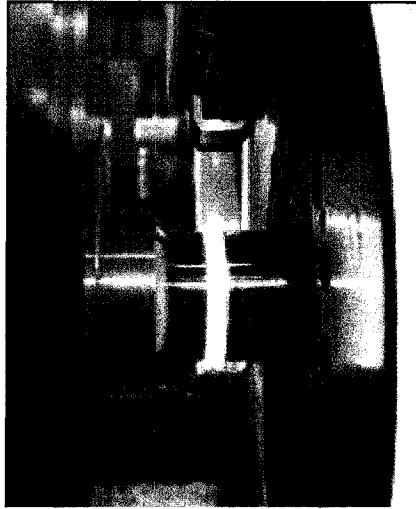


Figure 4.11: Phase 2 - Solid forging cycle showing displaced plastic state material when final axial forging force is applied

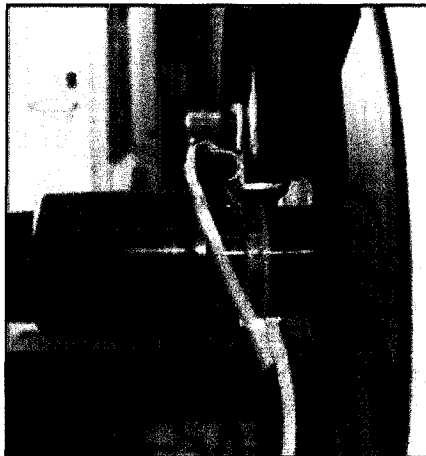


Figure 4.12: Phase 3 - Plastic state flashing is removed easily, even for hardenable materials that would otherwise require grinding

Friction welding is a low temperature, solid state welding process producing repeatable, CNC controlled high quality weld joints. Interface temperature is raised to a plastic state level through friction by spinning one part against another, and then applying a forging force to bond the weldment.

By producing a full cross-sectional surface forging, the process yields a very high

strength, low stress weld with no porosity, and, in most cases, eliminates the need for costly pre-machining. Joint strength is equal to parent material strength. Another principal advantage of friction welding is that it allows for the joining of dissimilar materials such as steel to stainless steel, aluminum to steel or copper, and a host of other combinations using various materials that are not weldable through traditional methods.

Unlike other methods, the process is low temperature (plastic state versus liquified metal as per traditional welding) and has a very small heat-affected zone. Material micro-structure and most material properties are maintained as well. Only solid, internal material exists across the interface with no third alloy added. Many material combinations that are not consider weldable can be joined by this process, all without the use of fillers, or field gases. Also, it is possible to remove the flash (the plastic state material displaced during forging) while it is still soft and pliant during the process cycle even when hardenable materials are used, thus eliminating costly grinding (Figure 4.12).

4.2.1.2 Materials

The PW307 power shaft is actually made out of superalloy Inconel 718. In the bibliographic review, many papers support the use of superalloy Inconel 718 like D.G. Backman and J.C. Williams (1992) [4], M. Rahman, J. Albrecht (1999) [6] and E.O. Ezugwu, J. Bonney and Y. Yamane (2003) [7]. The paper of W.K.H. Seah and T.T. Teo (1997) [5] discussed the problem of machining Inconel 718 due to the extreme toughness and work hardening of the alloy. PWC had the possibility to experience this difficulty of machining Inconel 718 when making this power shaft and this is one of the reasons of this project.

Consulting the graph of ultimate tensile strength versus temperature in appendix VII, it is possible to see that Inconel 718 (AMS5662) can be used approximately up to 1100F°. If we go back to Figure 3.1 it can be noticed that the maximum temperature of operation is situated in the hot section of the engine and is 928F°. Analyzing the temperatures of

operation, it can be found that only the section at 928F° of the power shaft really needs the superalloy Inconel 718 which means in numbers 21% or 11.125” out of the 53.125”.

After this analysis, it can be suggested that only the section with high temperature would use Inconel 718 and for the rest of the power shaft steel alloy could be used. This can be technically possible with the use of inertia welding which allows dissimilar materials to be joints as mentioned in section 4.2.1.1. Since at PWC the materials that are used should be selected from their characterized material database, CPW245 (0.9Cr – 0.5Mo – 0.3V – 0.40 to 0.50C) and HCM3 (3.25Cr – 0.55Mo – 0.55Mn – 0.20V – 0.20Ni – 0.22Si – 0.39C – Fe balance) are the steel alloys that could be used to make the rest of the power shaft.

4.2.1.3 Power shaft configurations and stress analysis for friction welding

In order to verify the possibility of making a power shaft using dissimilar materials a shaft stress analysis would confirm it from the stress point of view. The following configurations of multi material power shaft have been proposed:

- CPW245 & Inconel 718;
- HCM3 & Inconel 718;
- CPW245 & HCM3 & Inconel 718.

Some analysis were made using the P0889 shaft analysis computer program using a modified input file having the material type change in the section geometry data (see section 3.1.1.1). Since the input file was being modified, the inside diameter were also modified to optimize the shaft as explained in section 4.1.1. In future work, the P0889opt Automated Shaft Analysis Program can be used to do this kind of exercise.

CPW245 & Inconel 718 multi material power shaft

The first configuration consists in using CPW245 over the sections having temperatures going from 534F° to 762F° and Inconel 718 over the section of 928F°. CPW245 is

serviceable to about 825F°, above which diminishing strength and creep disqualify the alloy. In Figure 4.13 the model 3D of the multi material power shaft in CPW245 and Inconel 718 is presented.

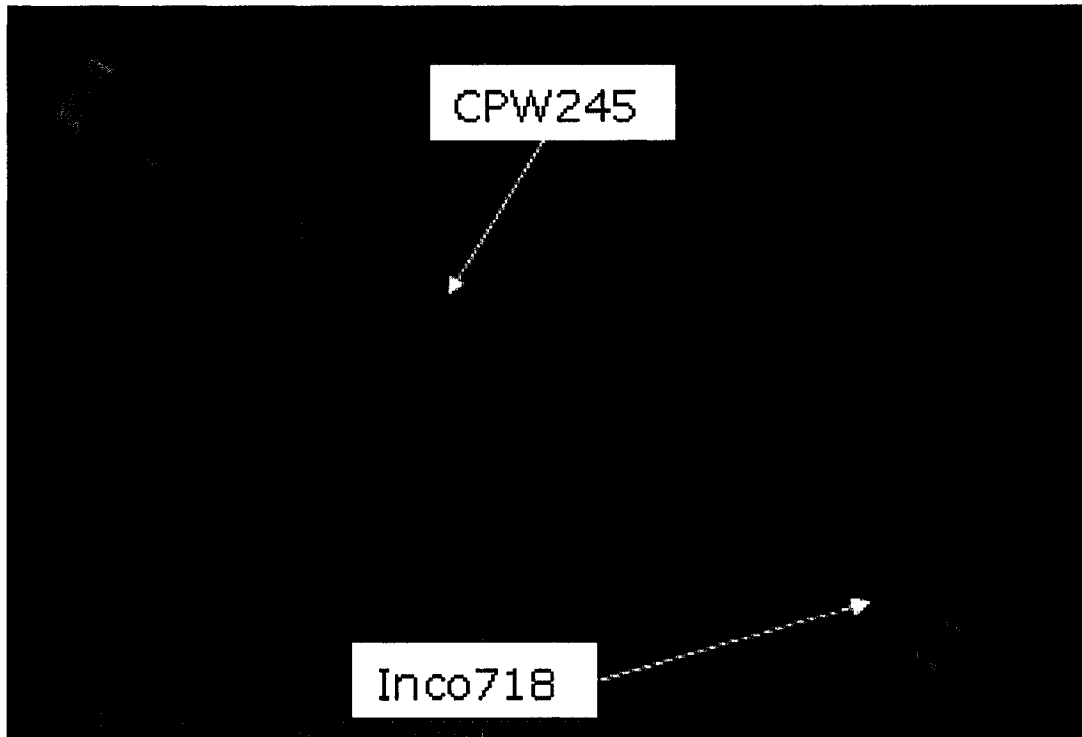


Figure 4.13: Multi material power shaft - CPW245 & Inconel 718

The shaft analysis had to be done twice in order to consider the interface (section 23) of the weld. Since it is known that the characteristics of the material at the interface is equal to parent material strength, the section 23 was analyzed once using Inconel 718 as material type and once using CPW245. In the case that the section would pass both analyses it is possible to state that the weld should pass as well. Figure 4.14 presents results of HCF-LCF analysis for the multi material power shaft in CPW245 and Inconel 718 and it can be seen that all the Equiv/Allow values are below 1.0 and at that section 23 as well respects the value of 1.0 for both types of materials.

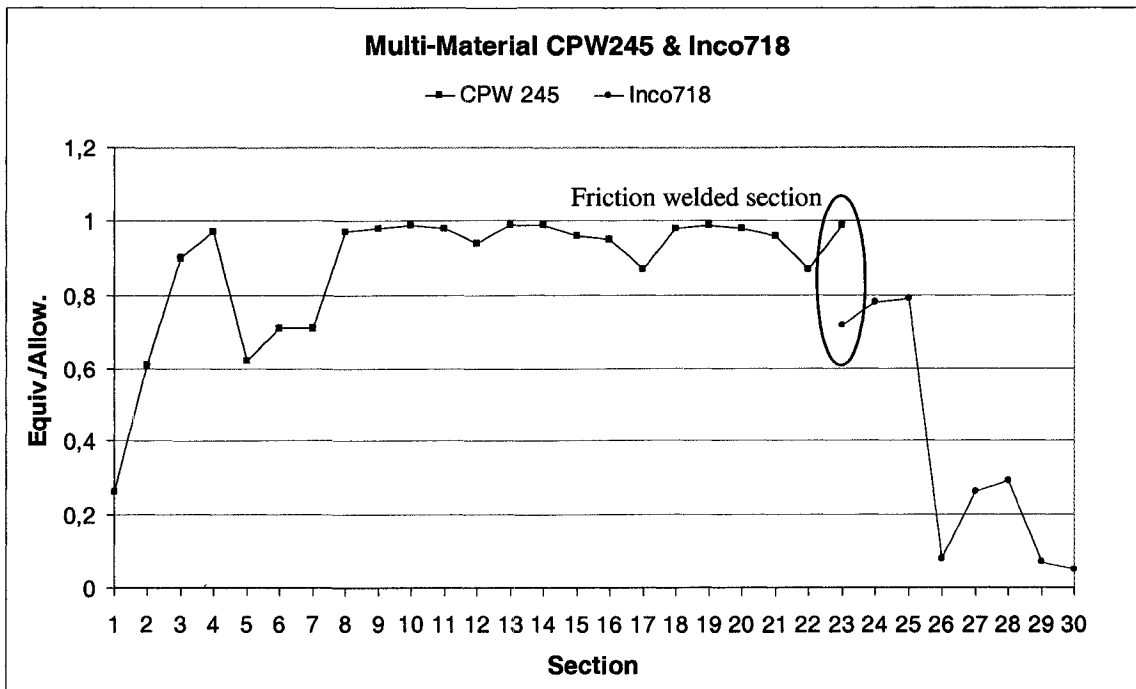


Figure 4.14: Results of LCF/HCF Analysis for PW307 multi material power shaft (Equiv/Allow) - CPW245&Inconel 718

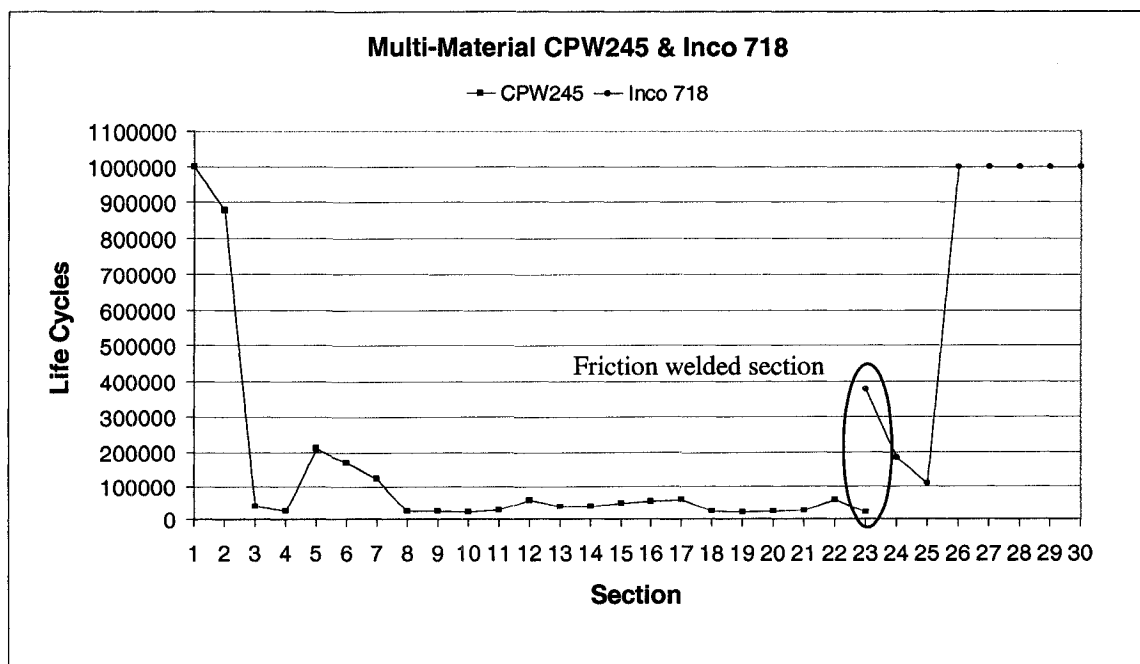


Figure 4.15: Results of LCF/HCF Analysis for PW307 multi material power shaft (Life Cycles) - CPW245&Inconel 718

In Figure 4.15 thanks to the optimization, the life cycles for all sections are very close to the 20000 cycles warranty of the PW307 engine. The weight saving per section due to the optimization is presented in Figure 4.16.

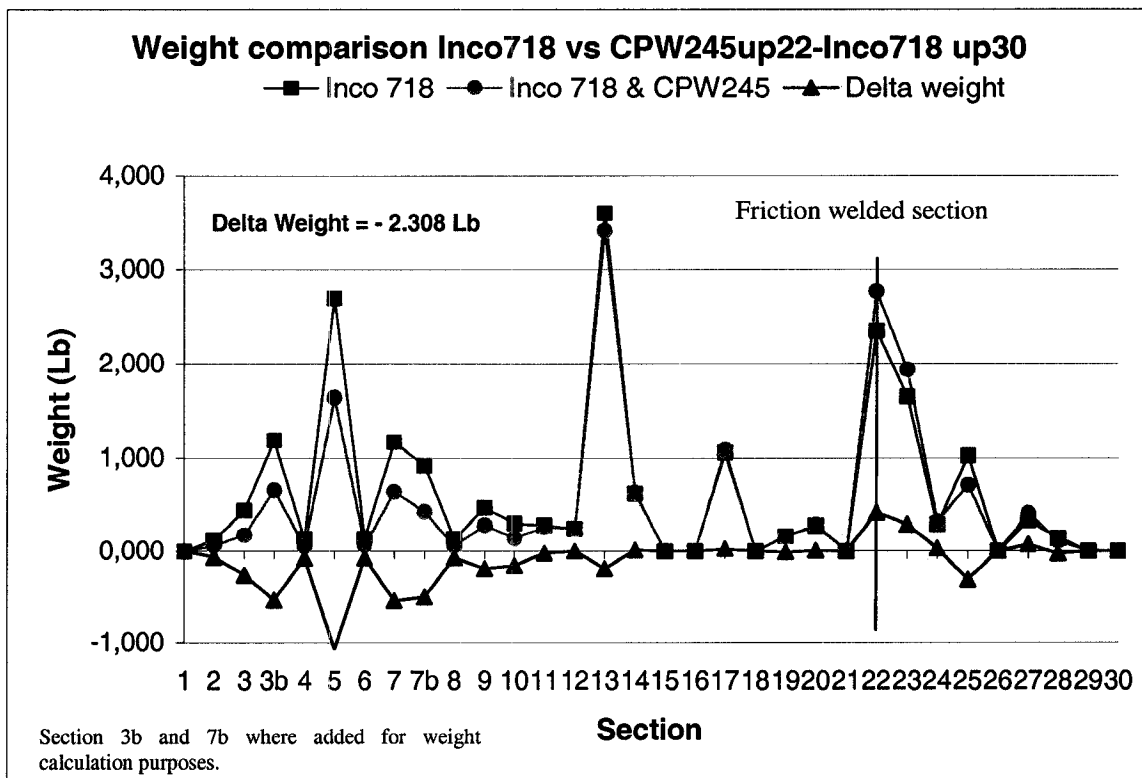

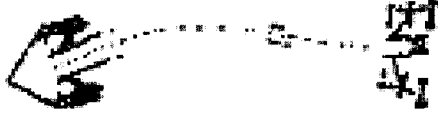



Figure 4.16: Optimization weight savings per section for PW307 multi material (CPW245&Inconel 718) power shaft.

In table 4.4 the results of the dynamical analysis of the computer program P0571 shows that the third mode happens at 123.1% of the redline speed, which is more than the required 120% of the redline speed and, the power shaft supports less than 50% of the strain energy distribution for the first two modes, which makes the CPW245 & Inconel 718 multi material shaft design approvable.

Table 4.4: CPW245 & Inconel 718 multi material power shaft critical speeds

PREDICTED MODE SHAPES AND WHIRLING SPEEDS FOR CPW245 & INCONEL 718 MULTI MATERIAL DESIGN OF THE POWER SHAFT				
Mode	Speed (% of redline speed 11000rpm)	% of strain energy distribution		
		Power shaft	Bearing No.1	Bearing No.2
1 st 	5137 (46.7%)	38.2 (<50%)	15.7	45.1
2 nd 	6097 (55.4%)	19.8 (<50%)	63.2	16.5
3 rd 	13544 (123.1%) (>120%)	87.2	5.0	6.2

Finally, by using friction welding and this configuration with two different types of materials to make the power shaft, it is possible to save 3957\$ of machining due to the machinability B of CPW245 compared to D of Inconel 718. The application of the optimization technique also allowed some weight saving on the power shaft of 2.308lb.

HCM3 & Inconel 718 multi material power shaft

This configuration is composed of HCM3 over the sections having temperatures going from 534F° to 762F° and Inconel 718 over the section of 928F°. HCM3 is serviceable to

about 850F° which is similar to the CPW245. In Figure 4.17 the model 3D of the multi material power shaft in HCM3 and Inconel 718 is shown.

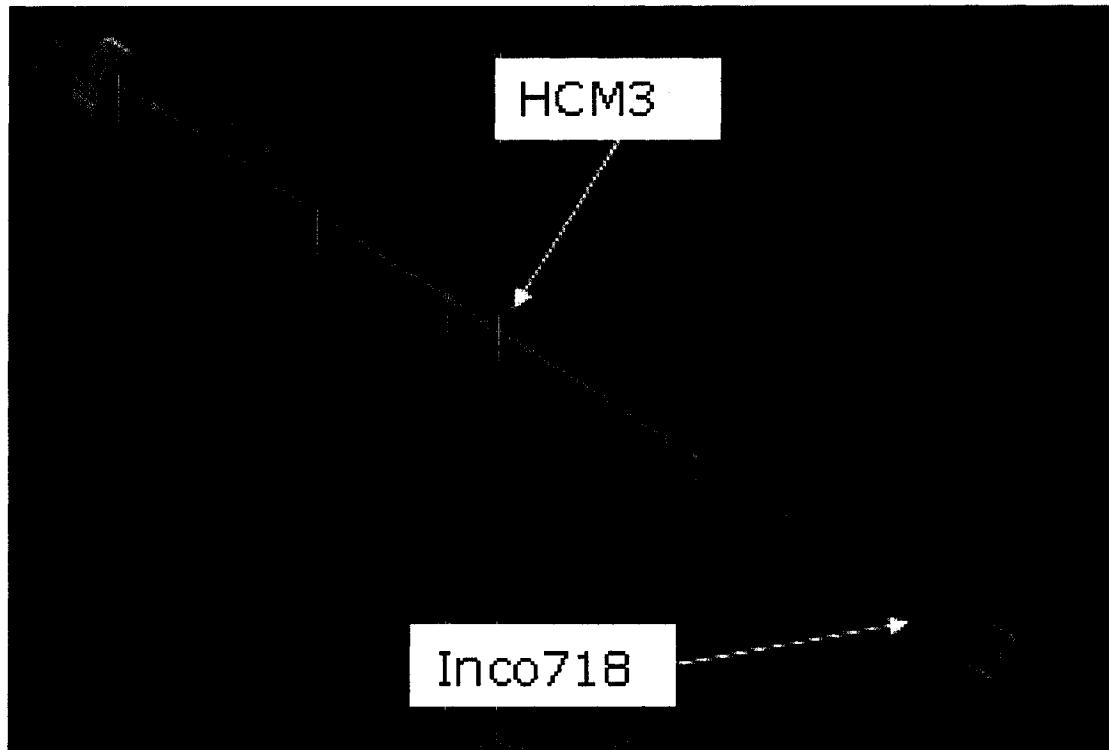


Figure 4.17: Multi material power shaft - HCM3 & Inconel 718

Even for this configuration the shaft analysis had to be done twice in order to consider the interface (section 23) of the weld. Figure 4.18 presents results of HCF-LCF analysis for the multi material power shaft in CPW245 and Inconel 718 and it can be seen that all the Equiv/Allow values are below 1.0 and at that section 23 as well respects the value of 1.0 for both types of materials.

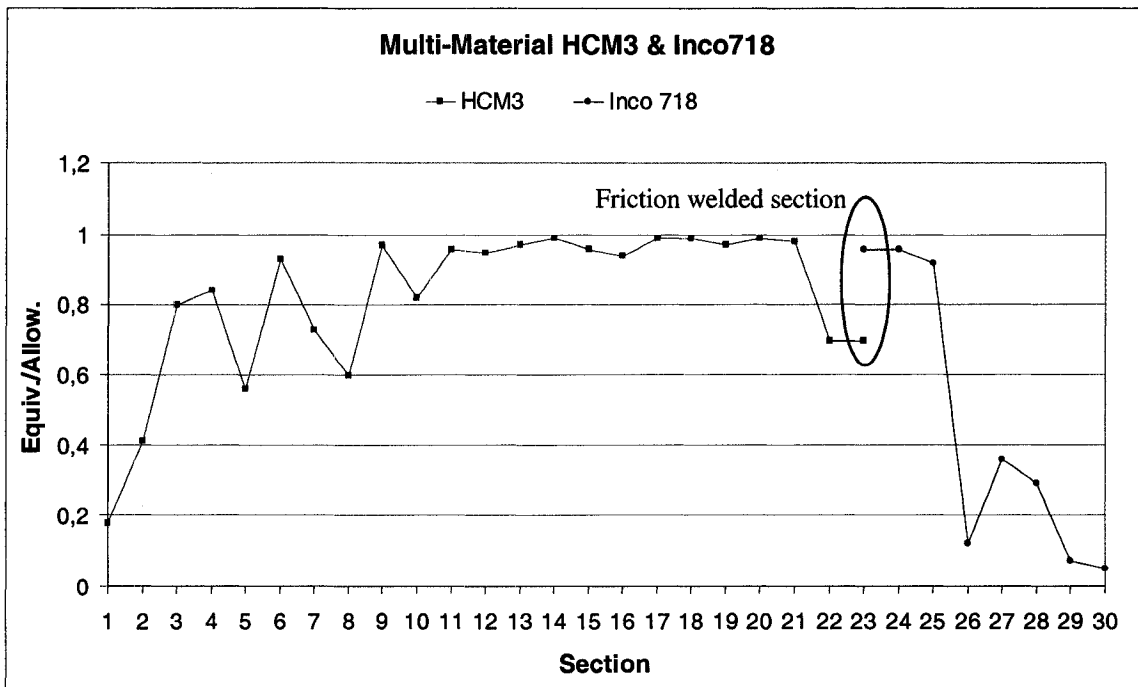


Figure 4.18: Results of LCF/HCF Analysis for PW307 multi material power shaft (Equiv/Allow) - HCM3&Inconel 718

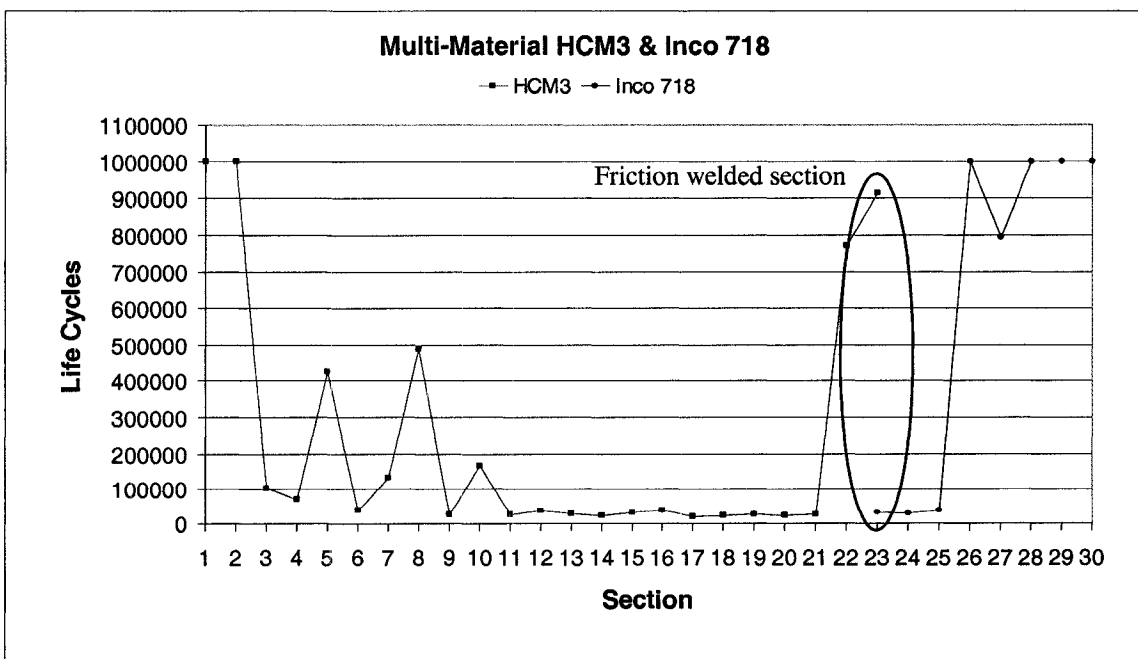


Figure 4.19: Results of LCF/HCF Analysis for PW307 multi material power shaft (Life Cycles) - HCM3&Inconel 718

In Figure 4.19 thanks to the optimization, the life cycles for all sections are very close to the 20000 cycles warranty of the PW307 engine. The weight saving per section due to the optimization is presented in Figure 4.20.

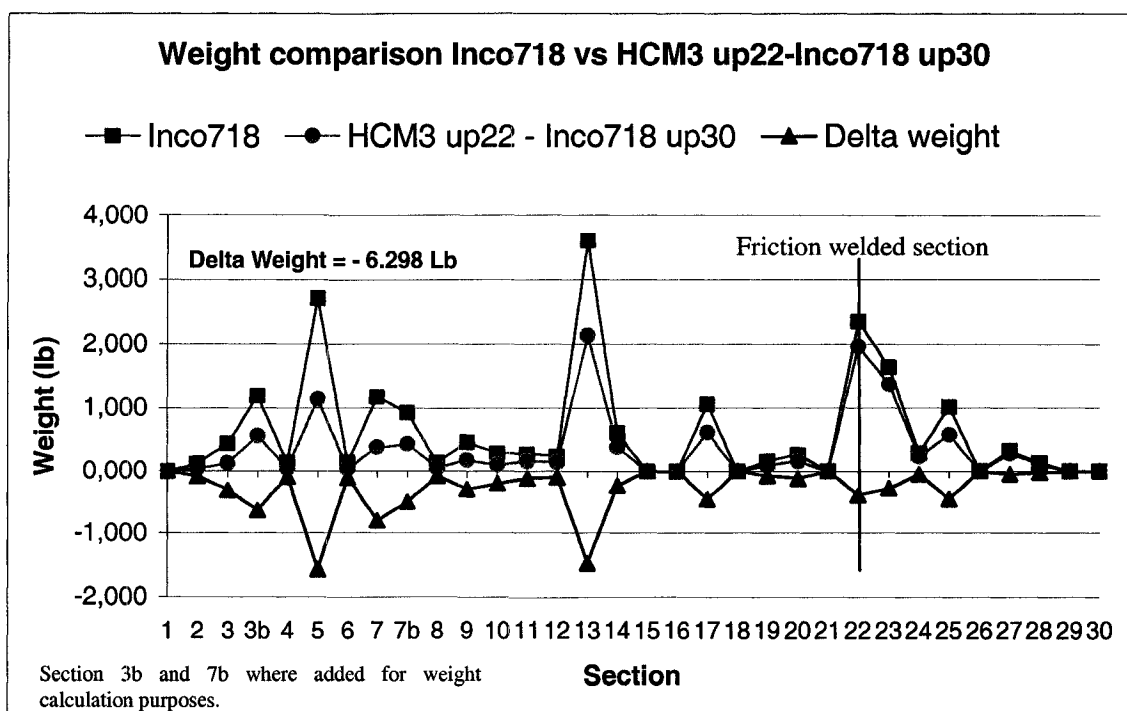
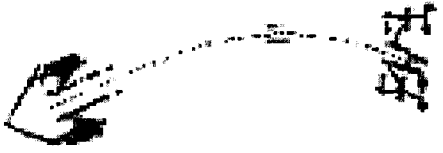
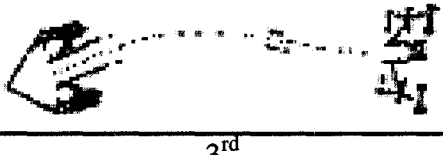
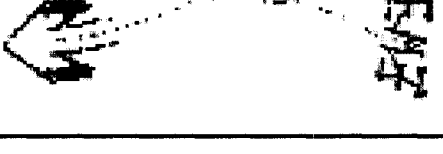


Figure 4.20: Optimization weight savings per section for PW307 multi material (HCM3&Inconel 718) power shaft.

In table 4.5 the results of the dynamical analysis of the computer program P0571 shows that the third mode happens at 135.5% of the redline speed, which is more than the required 120% of the redline speed and, the power shaft supports less than 50% of the strain energy distribution for the first two modes, which makes the HCM3 & Inconel 718 multi material shaft design approvable.

Table 4.5: HCM3 & Inconel 718 multi material power shaft critical speeds

PREDICTED MODE SHAPES AND WHIRLING SPEEDS FOR HCM3 & INCONEL 718 MULTI MATERIAL DESIGN OF THE POWER SHAFT				
Mode	Speed (% of redline speed 11000rpm)	% of strain energy distribution		
		Power shaft	Bearing No.1	Bearing No.2
1 st 	4998 (45.4%)	38.0 (<50%)	9.6	51.4
2 nd 	6081 (55.3%)	19.7 (<50%)	70.3	9.7
3 rd 	14907 (135.5%) (>120%)	90.1	3.5	4.6

In conclusion, with the HCM3 and Inconel 718 multi-material configuration for the power shaft, it is possible to save only 830\$ of machining due to the machinability C of HCM3 compared to D of Inconel 718. The application of the optimization technique allowed a weight saving on the power shaft of 6.298lb.

CPW245, HCM3 & Inconel 718 multi material power shaft

After studying both CPW245 with Inconel 718 and HCM3 with Inconel 718 configurations, another pattern was analyzed. If there is a possibility to make a power shaft out of two materials thanks to friction welding, why not consider the option of making the power shaft out of three materials. Therefore, three versions of CPW245 with

HCM3 and Inconel 718 were analyzed. Referring to Figure 4.1 for the numbering of the sections of the shaft, the first version of the three materials power shaft consists in CPW245 material type from the left end up to section 9, HCM3 up to section 22 and the rest of the shaft in Inconel 718. The second version is similar, going with CPW245 from the left end up to section 14, HCM3 up to section 22 and the rest of the shaft in Inconel 718. Finally, the third version starting with CPW245 from the left end up to section 19, HCM3 up to 22 and Inconel 718 for the rest of the shaft.

In Figure 4.21 the configuration of the first version of the three materials power shaft is shown. The same shaft analysis that were done like in the case of the preceding two material power shaft.

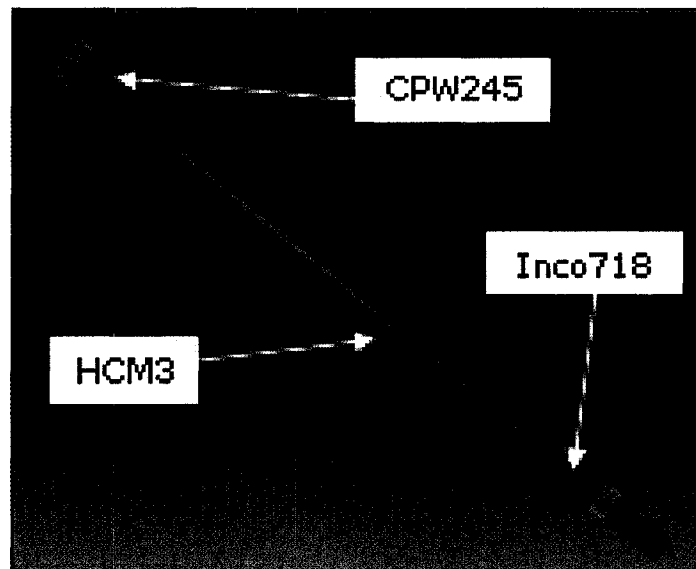


Figure 4.21: Multi material power shaft – CPW245 up to section 9, HCM3 up to section 22 and Inconel 718 to the end

For this configuration the shaft analysis had to be done four times in order to consider the two interfaces (section 9 & 22) of the welds. Figure 4.22 presents results of HCF-LCF analysis for the multi material power shaft and it can be seen that all the Equiv/Allow

values are below 1.0 and at sections 9 and 22 as well the value of 1.0 is respected for both types of materials.

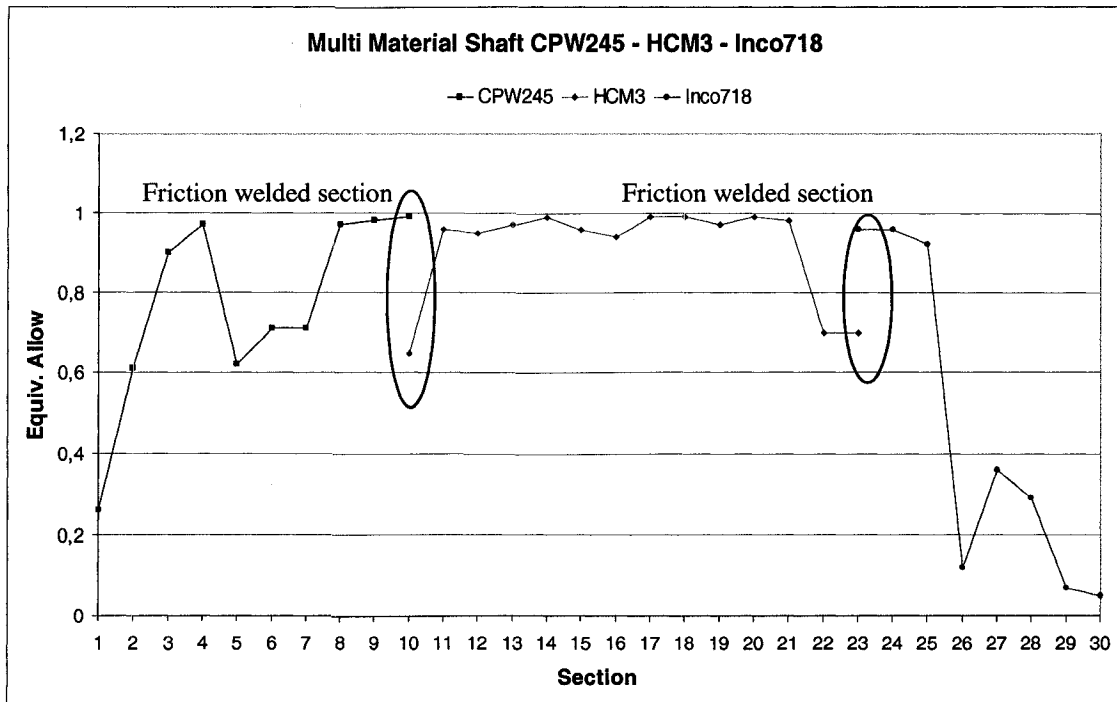


Figure 4.22: Results of LCF/HCF Analysis for PW307 multi material power shaft (Equiv/Allow) - CPW245 up to section 9, HCM3 up to section 22 and Inconel 718 to the end

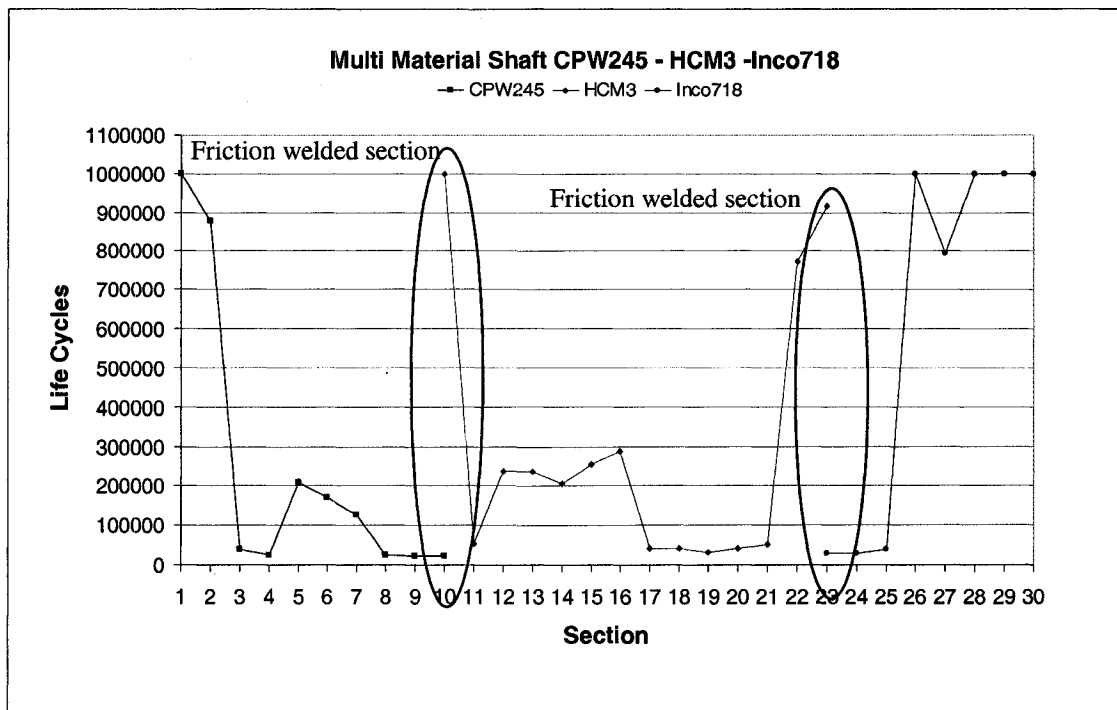


Figure 4.23: Results of LCF/HCF Analysis for PW307 multi material power shaft (Life Cycles) - CPW245 up to section 9, HCM3 up to section 22 and Inconel 718 to the end

In Figure 4.23, the life cycles for all sections, besides for the interfaces, are very close to the 20000 cycles warranty of the PW307 engine. The dynamical analysis of the computer program P0571 proved that the third mode happens at 133% of the redline speed, and that the power shaft supports less than 50% of the strain energy distribution for the first two modes, making this configuration acceptable.

Finally, with the first version of CPW245 with HCM3 and Inconel 718 configuration, it is possible to save 1481\$ for machining and a weight saving of 4.813lb.

In Figure 4.24 the configuration of the second version of the three materials power shaft is shown. The same shaft analyses were done on this version of power shaft.

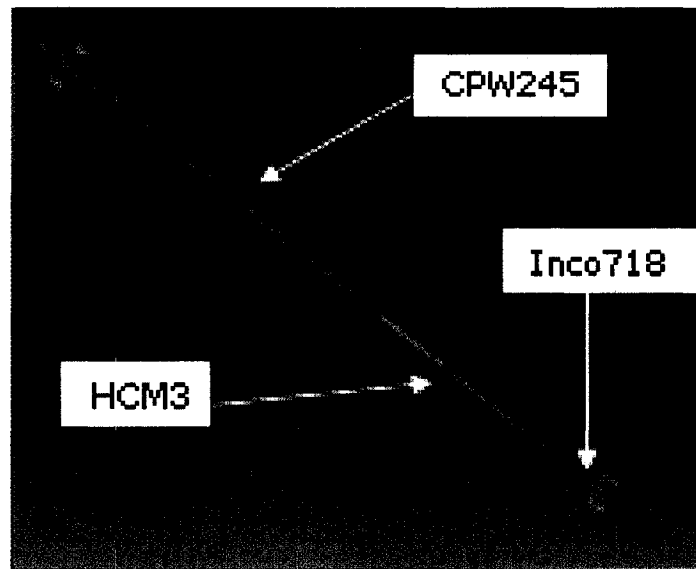


Figure 4.24: Multi material power shaft – CPW245 up to section 14, HCM3 up to section 22 and Inconel 718 to the end

For this configuration the shaft analysis had also to be done four times in order to consider the two interfaces (section 14 & 22) of the welds. Figure 4.25 presents results of HCF-LCF analysis for the multi material power shaft and it can be seen that all the Equiv/Allow values are below 1.0 and at sections 14 and 22 as well the value of 1.0 is respected for both types of materials.

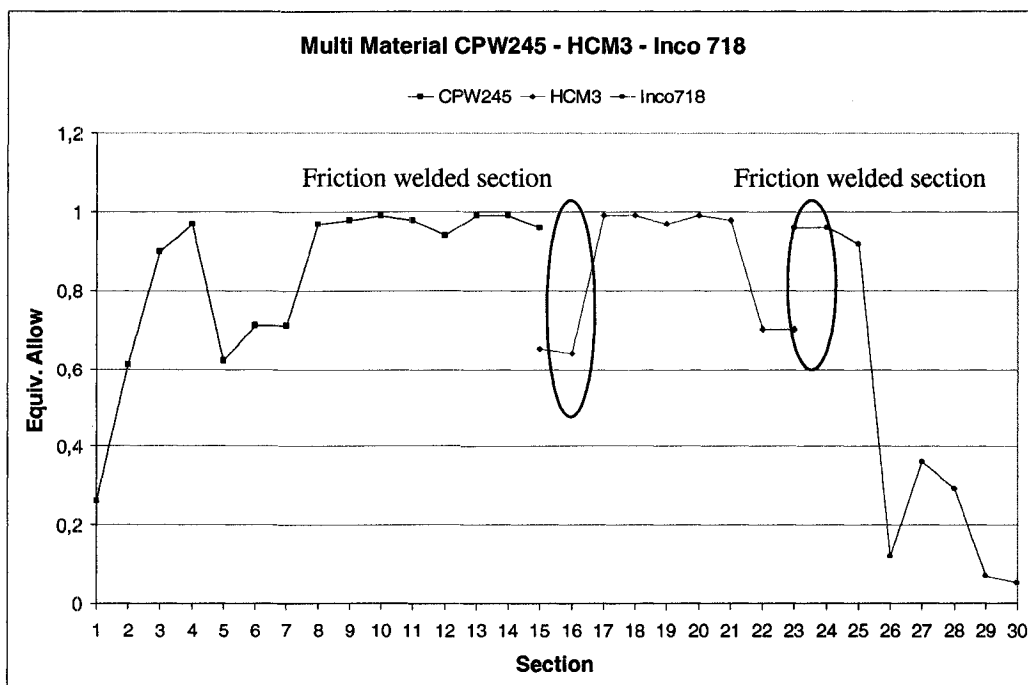


Figure 4.25: Results of LCF/HCF Analysis for PW307 multi material power shaft (Equiv/Allow) - CPW245 up to section 14, HCM3 up to section 22 and Inconel 718 to the end

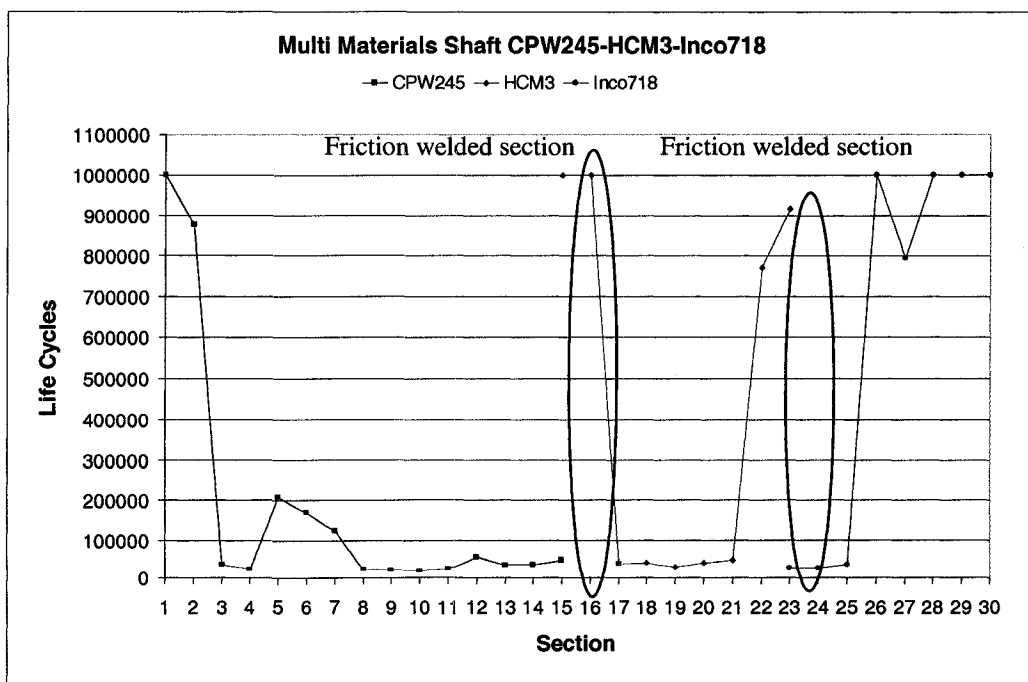


Figure 4.26: Results of LCF/HCF Analysis for PW307 multi material power shaft (Life Cycles) - CPW245 up to section 14, HCM3 up to section 22 and Inconel 718 to the end

In Figure 4.26, the life cycles for all sections, besides for the interfaces, are very close to 20000 cycles. The dynamical analysis proved that the third mode happens at 128% of the redline speed, and that the power shaft supports less than 50% of the strain energy distribution for the first two modes, making this configuration acceptable.

Finally, with the second version of CPW245 with HCM3 and Inconel 718 configuration, it is possible to save 2985\$ for machining and a weight saving of 3.700lb.

In Figure 4.27 the configuration of the third version of the three materials power shaft is shown. The same shaft analyses were done as well on this version of power shaft.

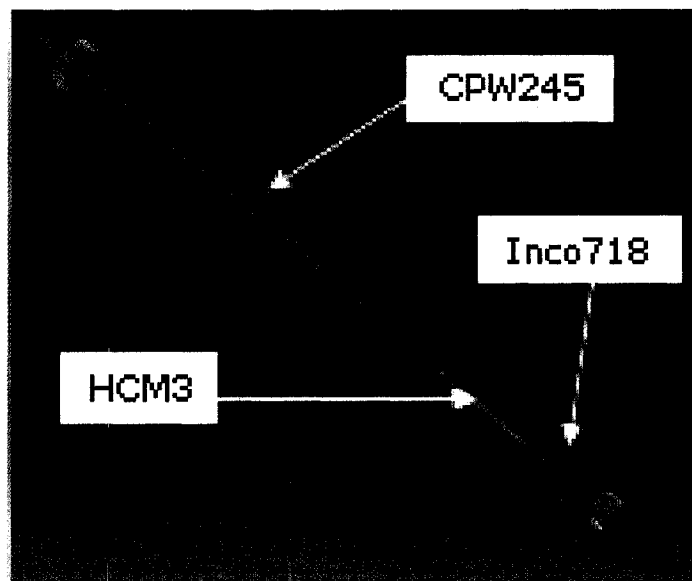


Figure 4.27: Multi material power shaft – CPW245 up to section 19, HCM3 up to section 22 and Inconel 718 to the end

For this configuration the shaft analysis had also to be done four times in order to consider the two interfaces (section 19 & 22) of the welds. Figure 4.28 presents results of HCF-LCF analysis for the multi material power shaft and it can be seen that all the Equiv/Allow values are below 1.0 and at sections 19 and 22 as well the value of 1.0 is respected for both types of materials.

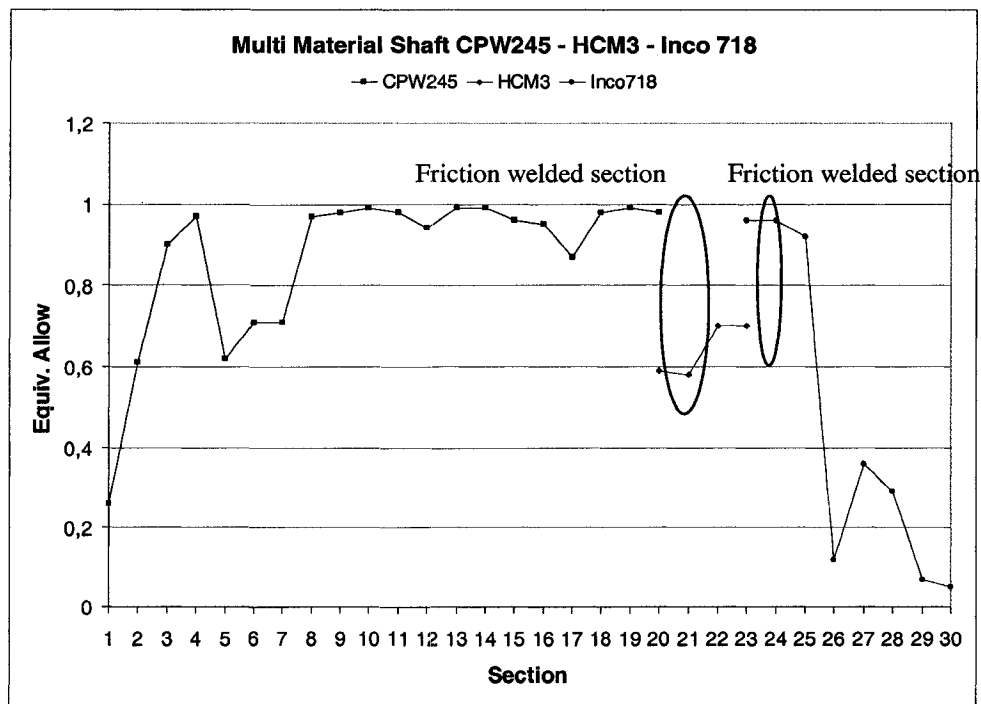


Figure 4.28: Results of LCF/HCF Analysis for PW307 multi material power shaft (Equiv/Allow) - CPW245 up to section 19, HCM3 up to section 22 and Inconel 718 to the end

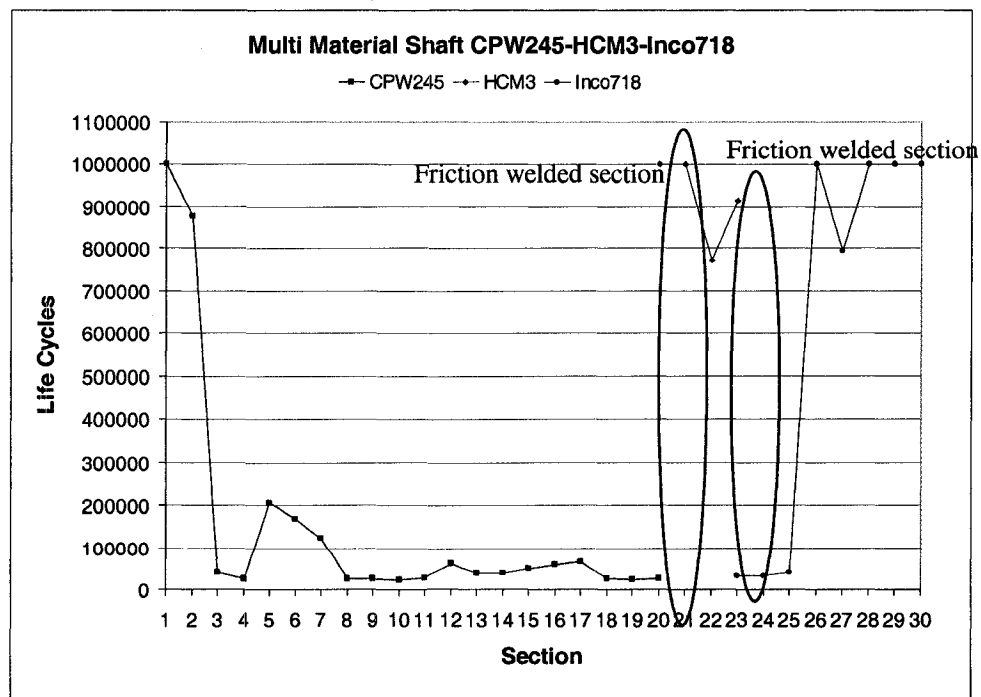


Figure 4.29: Results of LCF/HCF Analysis for PW307 multi material power shaft (Life Cycles) - CPW245 up to section 19, HCM3 up to section 22 and Inconel 718 to the end

In Figure 4.29, the life cycles for all sections, besides for the interfaces, are very close to the 20000 cycles. The dynamical analysis proved that the third mode happens at 125% of the redline speed, and that the power shaft supports less than 50% of the strain energy distribution for the first two modes, making this configuration acceptable.

Finally, with the third version of CPW245 with HCM3 and Inconel 718 configuration, it is possible to save 3360\$ for machining and a weight saving of 3.114lb.

Multi material power shaft configurations summary

Examining the different configurations, some have great machining cost savings and others have outstanding weight saving. The different configurations that were analyzed are the following:

1. Optimized Inconel 718 power shaft (seen in section 4.1.1).
2. Multi-material power shaft - CPW245 & Inconel 718.
3. Multi-material power shaft - HCM3 & Inconel 718.
4. Multi-material power shaft - CPW245 up to section 9, HCM3 up to section 22 & Inconel 718 to the end.
5. Multi-material power shaft - CPW245 up to section 14, HCM3 up to section 22 & Inconel 718 to the end.
6. Multi-material power shaft - CPW245 up to section 19, HCM3 up to section 22 & Inconel 718 to the end.

In Table 4.6 a summary of all the configurations is shown with the respective machining cost savings and weight savings.

Table 4.6: Power shaft configurations with machining cost savings and weight savings

1	Optimized Inconel718 Δ weight = -5.472lb Δ cost = 0\$	4	CPW245 (09) & HCM3 (22) & Inconel718 Δ weight = -4.813lb Δ cost = 1481\$
2	CPW245 & Inconel718 Δ weight = -2.308lb Δ cost = 3957\$	5	CPW245 (14) & HCM3 (22) & Inconel718 Δ weight = -3.700lb Δ cost = 2985\$
3	HCM3 & Inconel718 Δ weight = -6.298lb Δ cost = 830\$	6	CPW245 (20) & HCM3 (22) & Inconel718 Δ weight = -3.114lb Δ cost = 3360\$

The CPW245 with Inconel 718 configuration represents the best machining cost savings of 3957\$ (almost 40% cost reduction) and the HCM3 with Inconel 718 configuration corresponds to the greatest weight saving of 6.298lb. The cost of friction welding for one section is 100\$ US.

4.2.1.4 Tests

To verify the feasibility of friction welding, some tests were undertaken with Edison Welding Institute (EWI), a research center in United States of America. Out of all multi material configurations, the CPW245 & Inconel 718 configuration was retain for the tests since PWC has extensive properties data on both materials. In the case of HCM3, PWC is still in the process of characterizing the material even if it already entered the company.

For the tests, 20 pairs of CPW245 and Inconel 718 test pieces were sent. The configuration of the tests pieces is shown in Figure 4.30 and Figure 4.31. In Figure 4.32 and 4.33 the actual test pieces are shown.

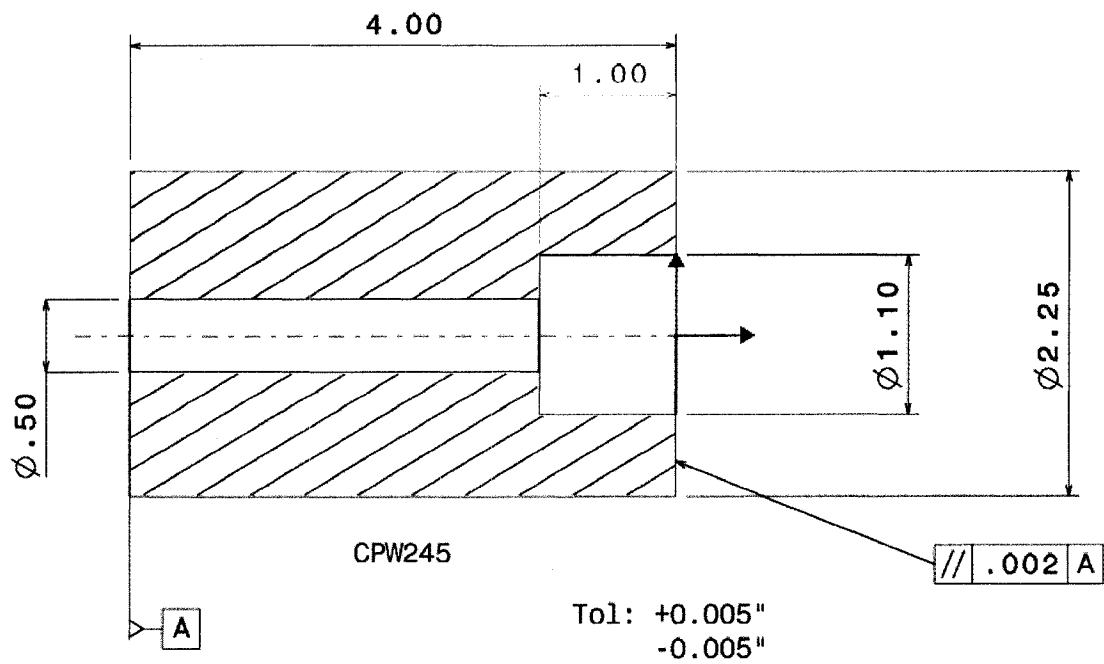


Figure 4.30: CPW245 test piece configuration for friction welding

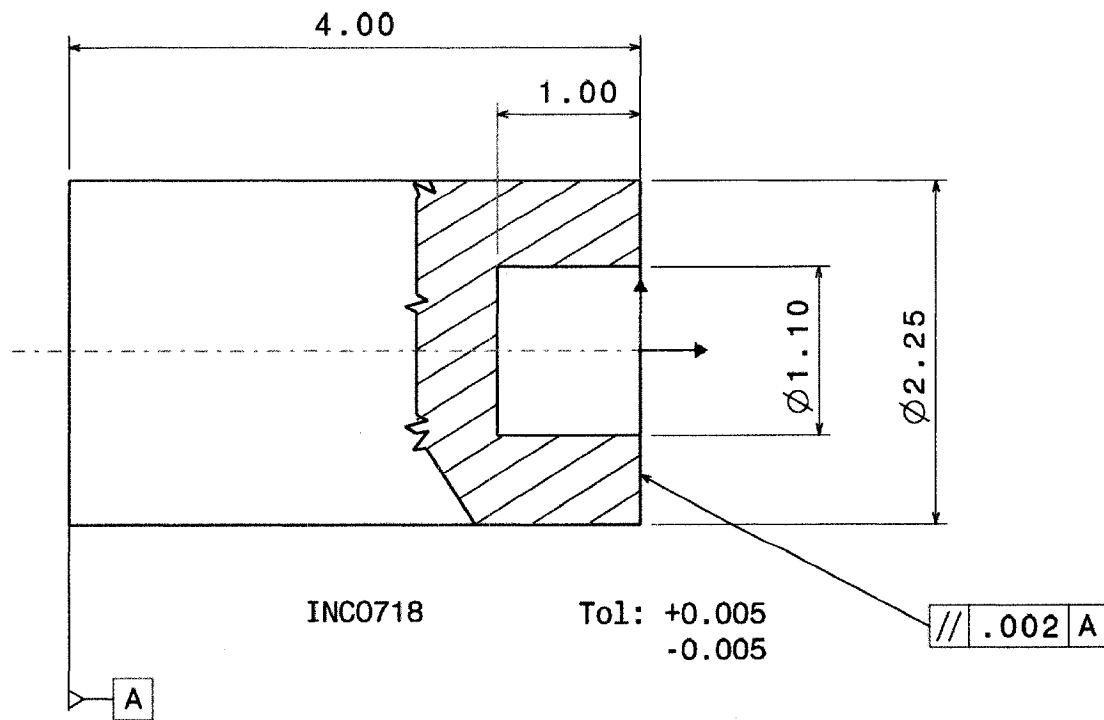


Figure 4.31: Inconel 718 test piece configuration for friction welding

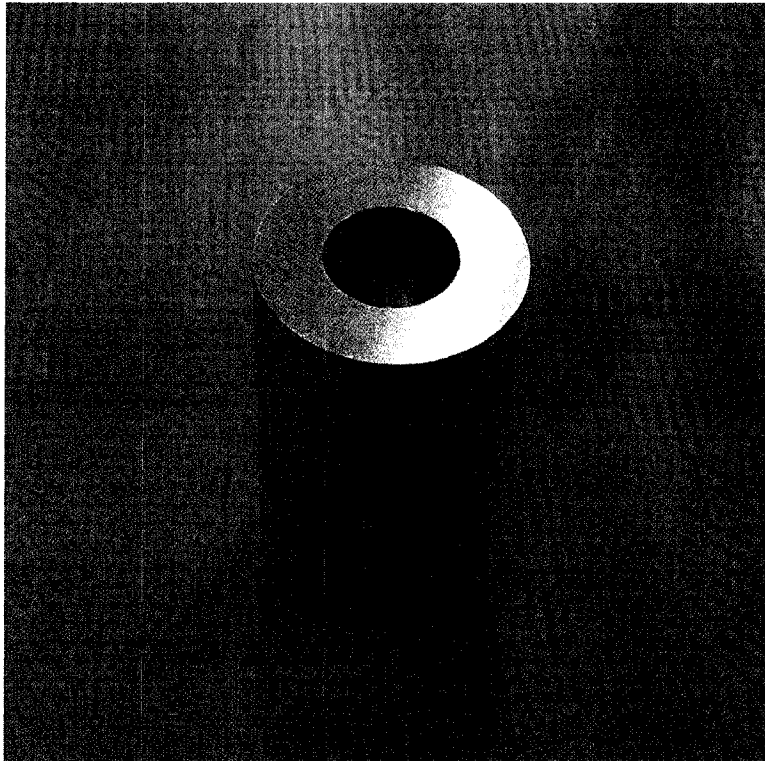


Figure 4.32: CPW245 Test piece for friction welding

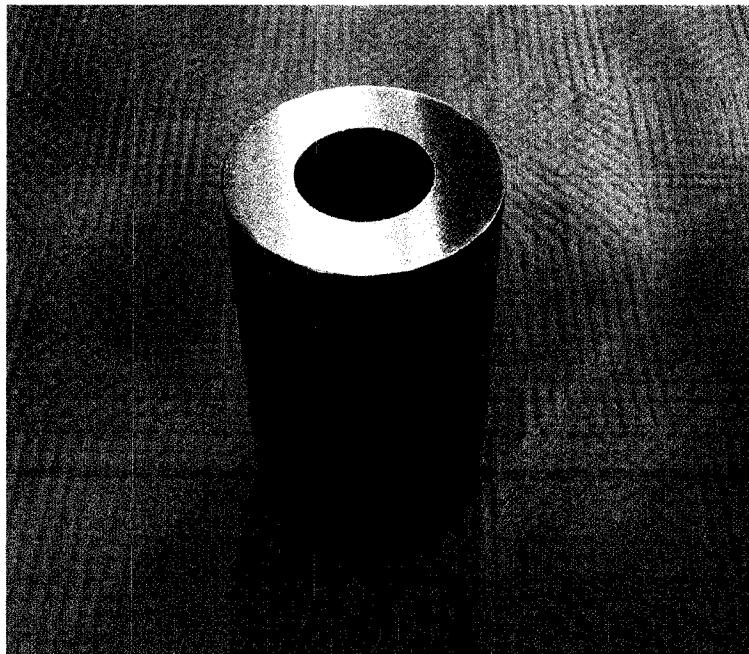


Figure 4.33: Inconel 718 Test piece for friction welding

In order to control the parameters of friction welding, EWI started with two welds (IW1 and IW2) and the first one can be seen in Figure 4.34, and 4.35. Between the two welds, one was made with a slightly higher RPM than the other (1000 versus 760). There was a small alignment issue with the second weld, but metallurgically it looks the same as the first one (Figure 4.36 and 4.37). Following this test, CPW245 and Inconel 718 test pieces have respectively a total loss of 0.525-in. and 0.400-in on their length.

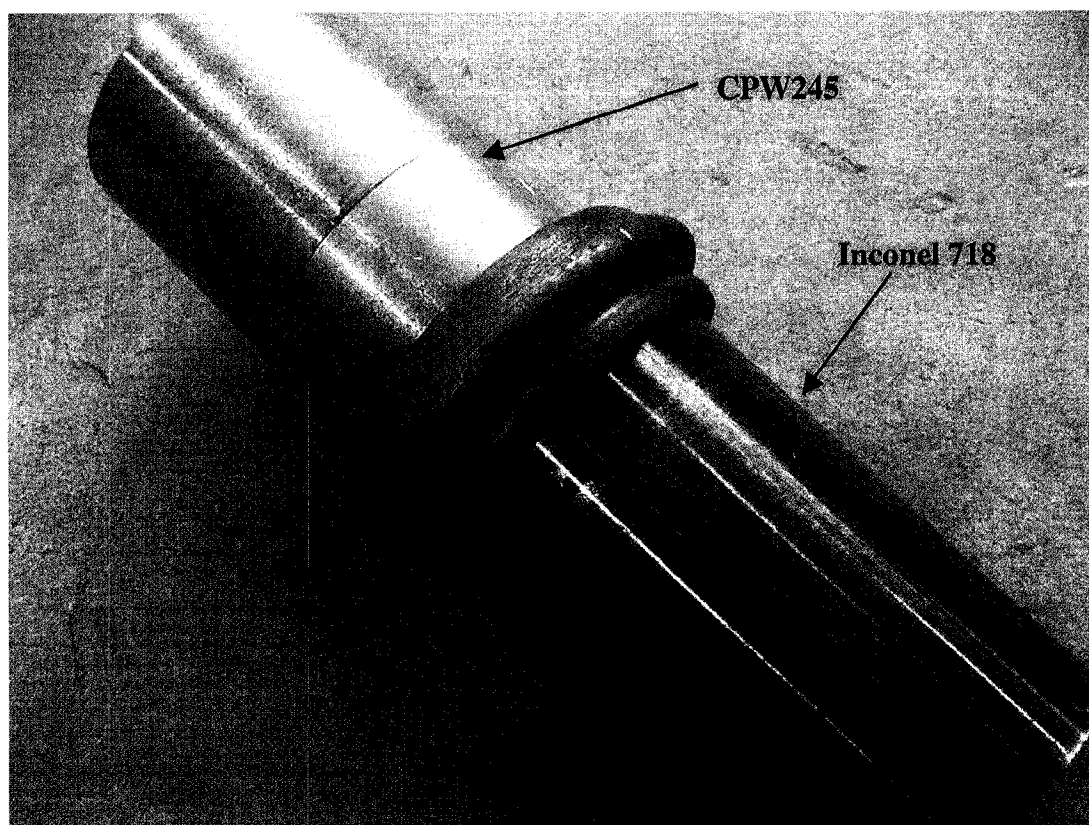


Figure 4.34: IW1 - First test pieces pair being friction welded

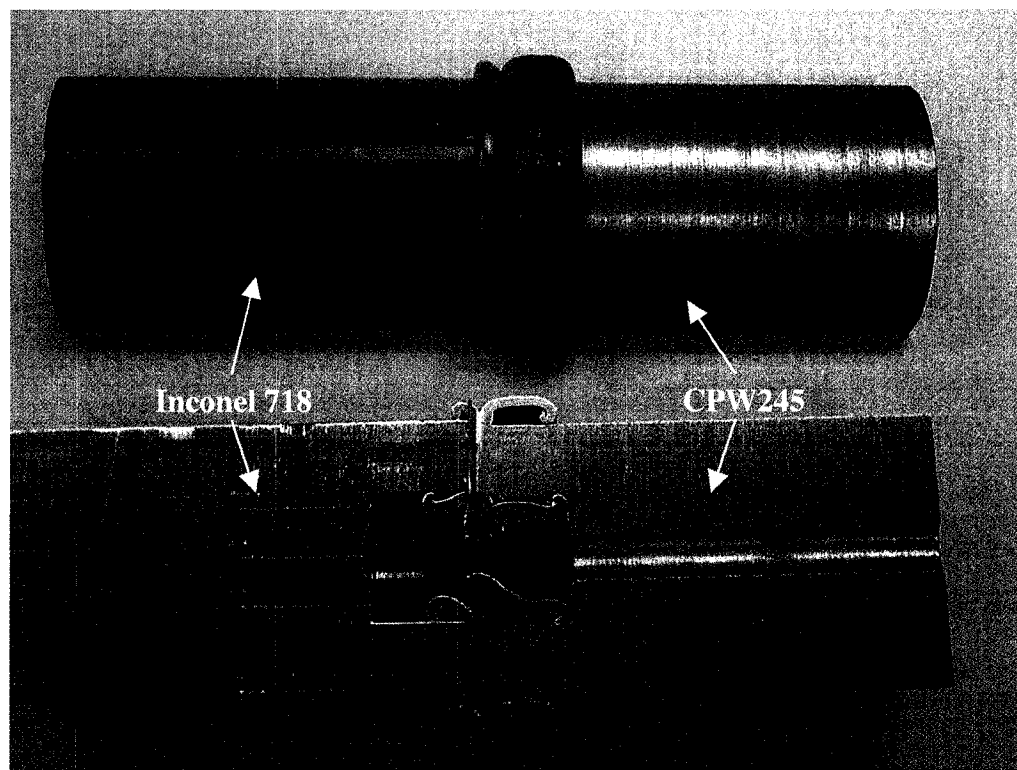


Figure 4.35: IW1 - First test pieces pair being friction welded (section cut)

Afterwards, two bend sections from each of the two welds were done using a three-point bend with a 3/4-in radius. The test pieces were prescribed with 1-in. gauge marks and remeasured to get a strain value when a crack starts. For the first weld (higher RPM), the calculated percent strain from the two bend samples was 3.3 and 4.2%. For the second weld (lower speed) the values were 5.8% and 1.2%. The 1.2% value appears to be related to the misalignment of the tube wall, which was then fixed. Analyzing the failure mode, EWI concluded that the fractures were on the Inconel 718 side of the bondline and that they may be due to the gamma prime constituents going back into solution very near the bondline. EWI is still not sure what effect the 1100°F for 2 hours post-weld heat-treat will have on the final microstructure.

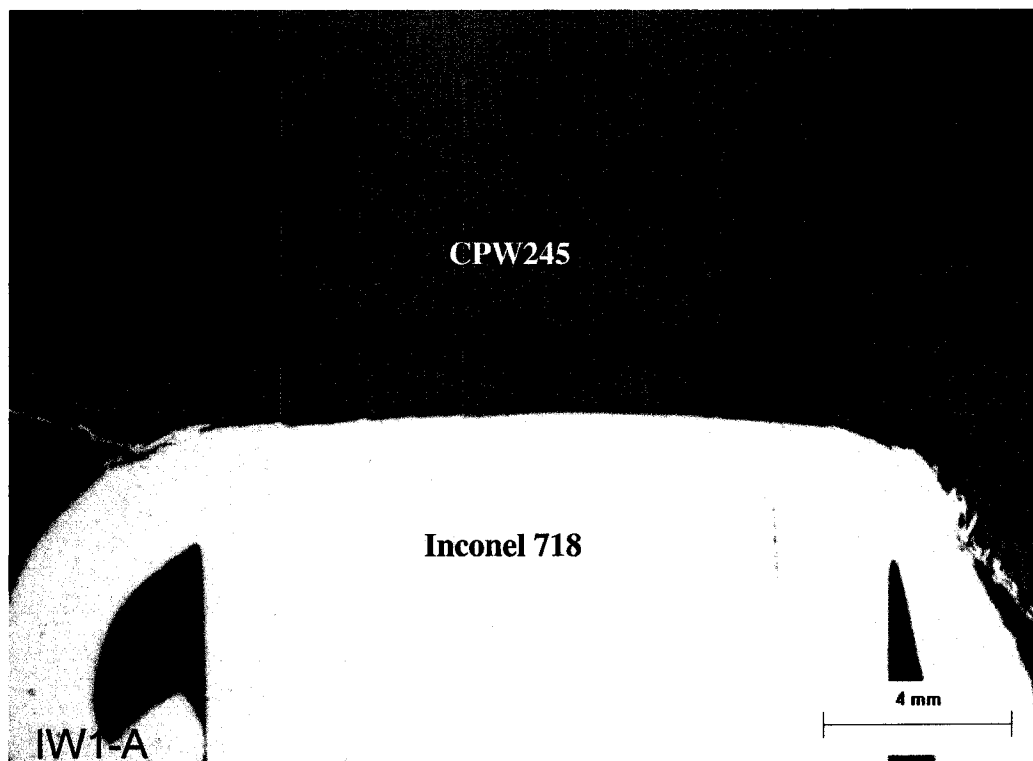


Figure 4.36: IW1 - Met section of first friction weld

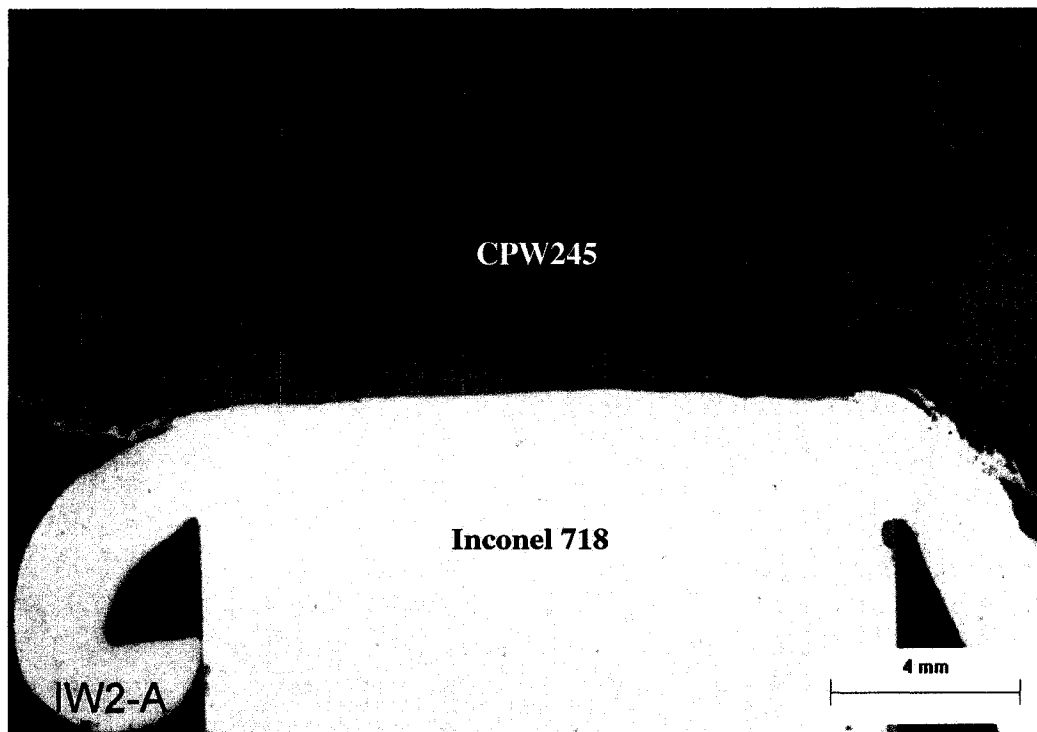


Figure 4.37: IW2 - Met section of second friction weld

Two tensile tests were done for each weld. From Figure 4.38 to 4.41, the interface and profiles of the welds are shown.

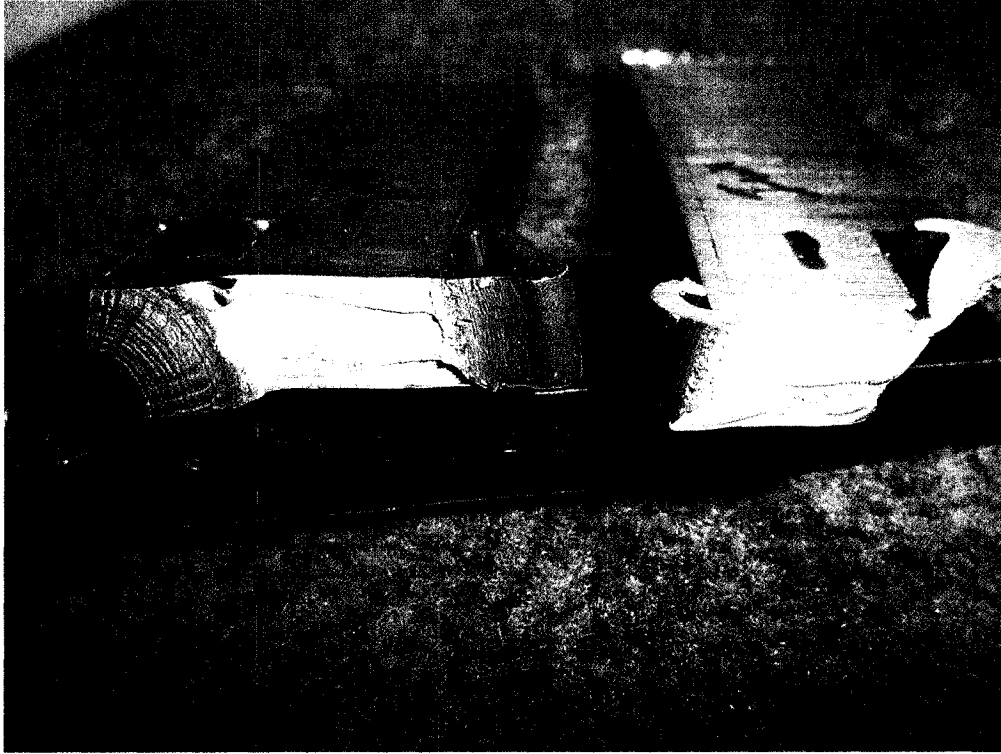


Figure 4.38: IW1 - Interface of the weld after tensile test

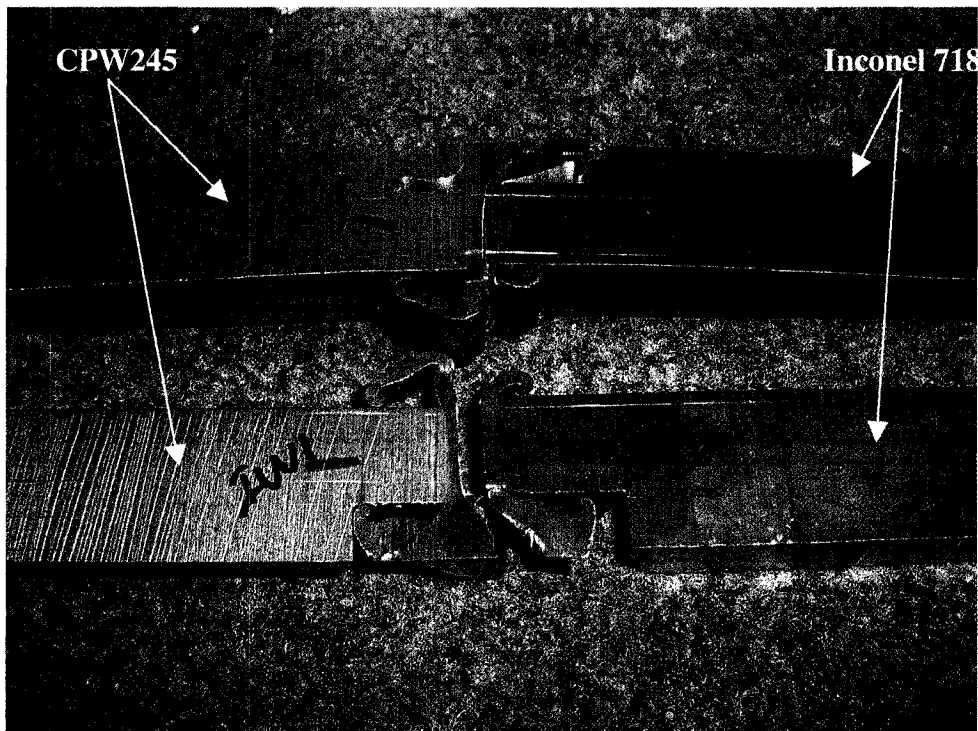


Figure 4.39: IW1 - Profile of the weld after tensile test

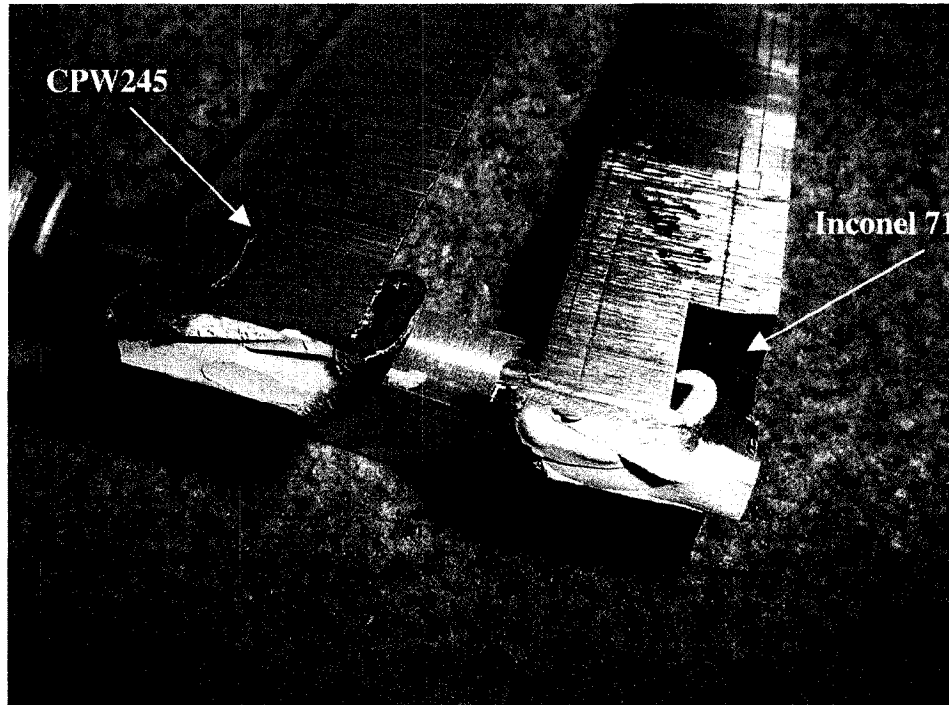


Figure 4.40: IW2 - Interface of the weld after tensile test

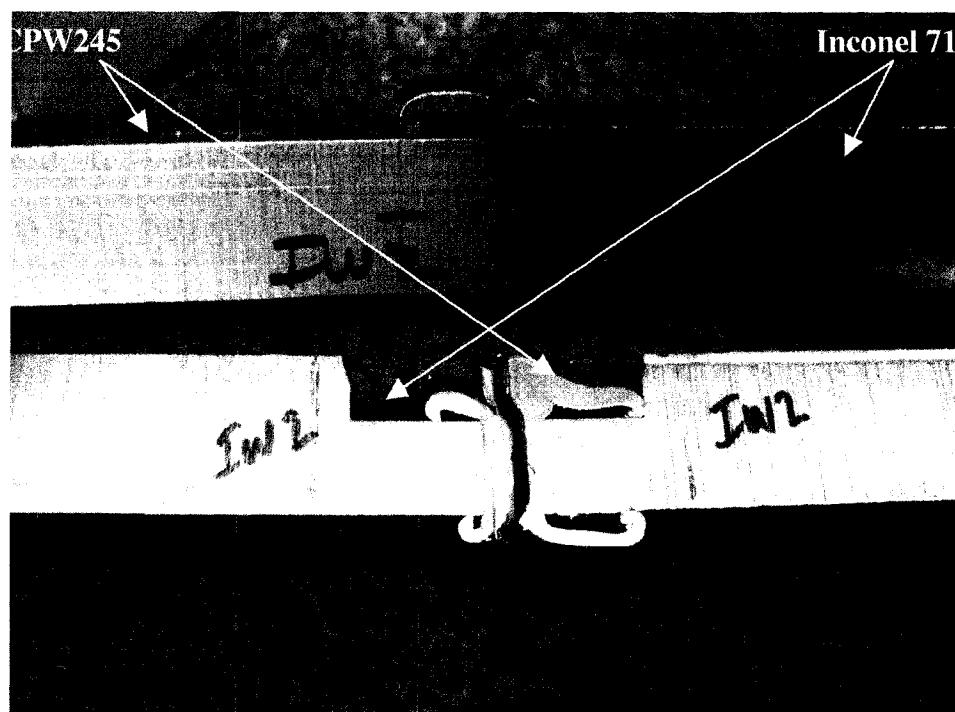


Figure 4.41: IW2 - Profile of the weld after tensile test

Finally, four welds were made and stress relieved for 2 hours @ 1100°F. First, a Vickers hardness profile was obtained (Figure 4.42) as well as tensile tests (Figure 4.43). Fractures for all four of them were all well away from the bondline (Figure 4.44). One of the welds was etched for the steel side, Inconel 718 was not attacked (Figure 4.45).

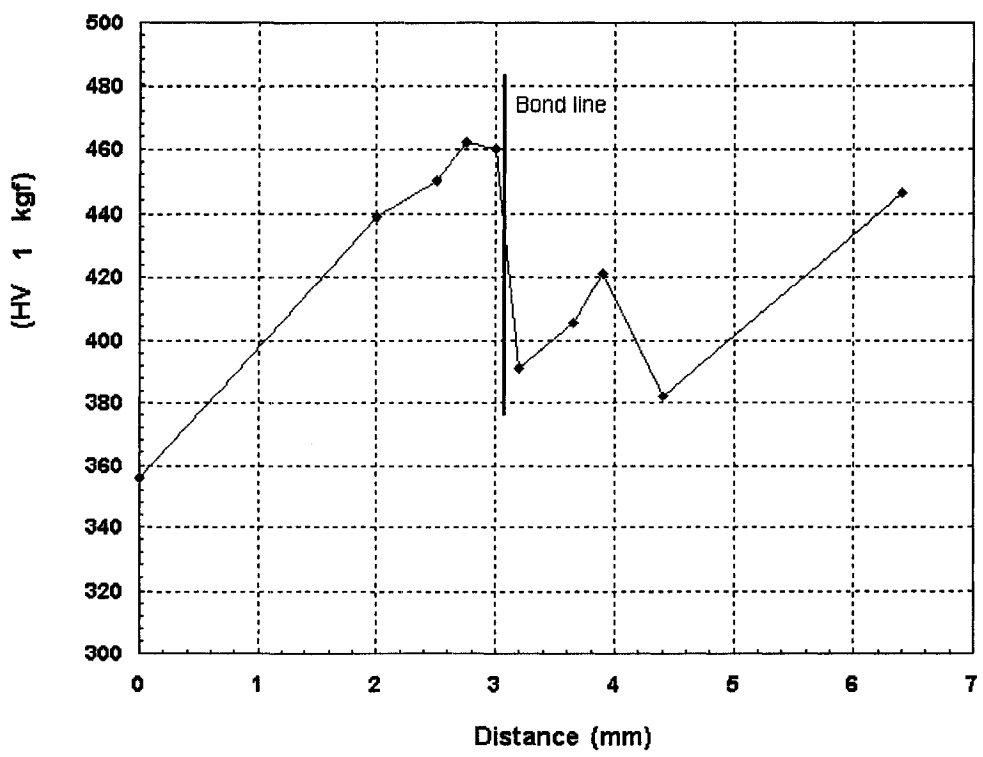


Figure 4.42: Vickers hardness test on sample 4-1 - stress relieved for 2 hours

Specimen Orientation:		Transverse section from a welded tube.									
Specimen Type:		Round									
Nominal Gage Length:		25.4 mm					1 in.				
Test Rate:		1.27 mm/min					0.05 in./min				
Specimen Identification	Specimen Diameter		Test Temperature		Ultimate Strength		0.2% Yield Strength		Elongation (%)	Reduction of Area (%)	Failure Location
	(mm)	(in)	(°C)	(°F)	(MPa)	(ksi)	(MPa)	(ksi)			
4-1	8.27	0.247	22	72	1168.3	168.4	984.8	142.8	11.2	60.1	Base

Figure 4.43: Tension test results for sample 4-1

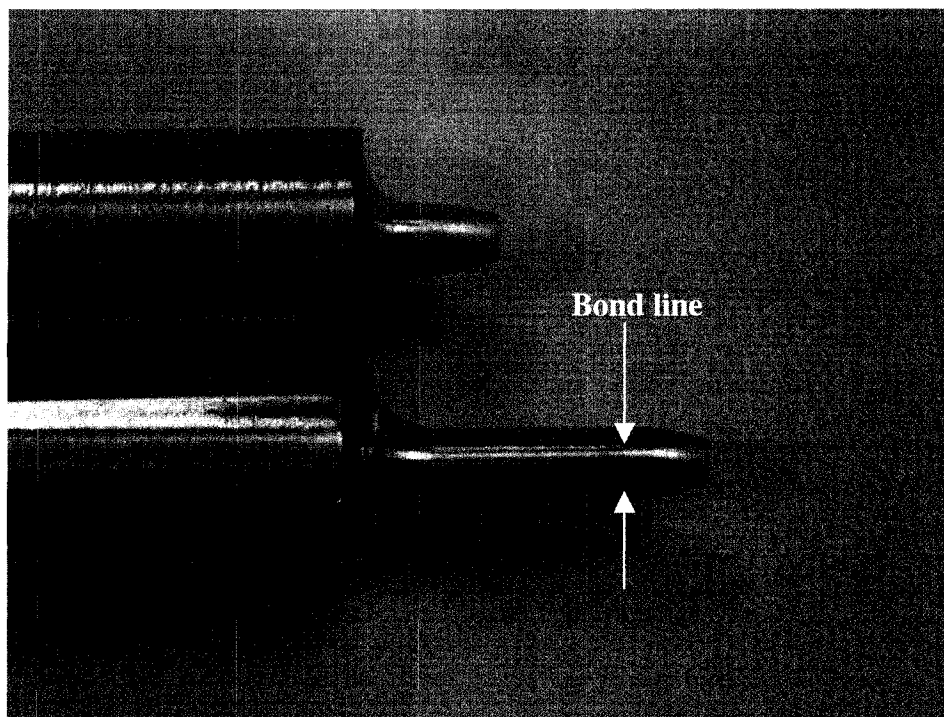


Figure 4.44: Tensile test on sample 4-1 - stress relieve for 2 hours

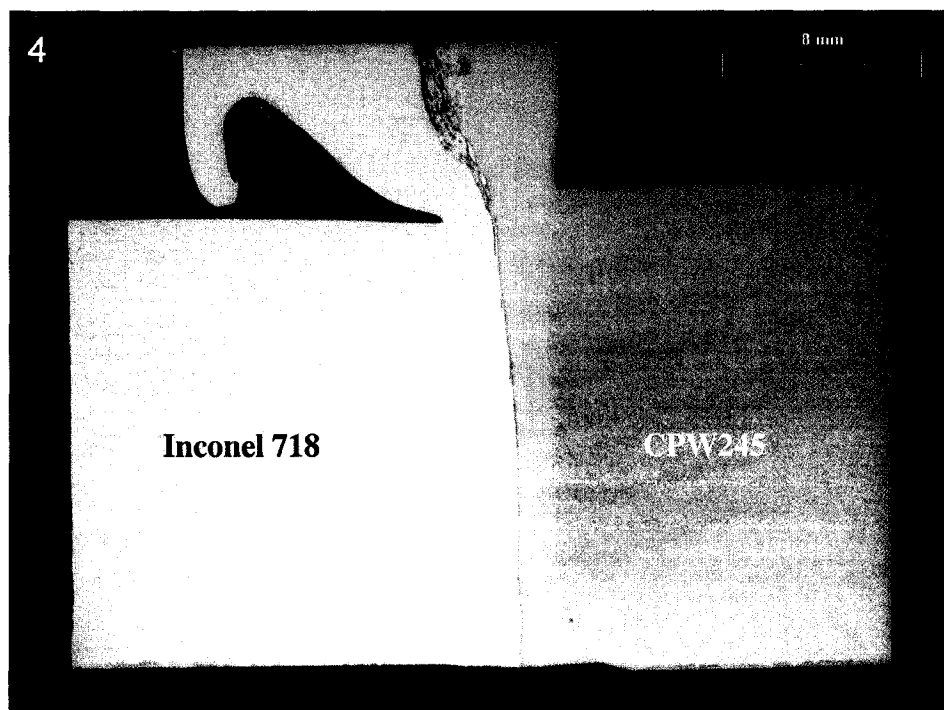


Figure 4.45: Etched sample 4-1 - stress relieved for 2 hours

As future development, the next step of the test is to make 10 welds with the 2 hours stress relief to finally define all the parameters of friction welding before welding a prototype.

4.1.2 Flow-formed shaft

Firstly, the flow forming process is explained with the different existing techniques. Subsequently, the accuracy of the process, the advantages and disadvantages as well as the cost effectiveness, are presented. Finally, a contract proposal for tests is being discussed with “Dynamic Machine Works” in order to make flow formed PW307 power shafts.

4.2.2.1 Flow-forming process

In www.flowforming.com, it is detailed that flow forming is performed by the application of uniform compression to the outside diameter of a cylindrical component using a combination of axial and radial forces from three CNC controlled rollers (Figure 4.46) located 120 degrees apart around the circumference of the workpiece. Each of the three rollers has a specific geometry to support its particular role in the forming process. The position of the rollers is staggered axially and radially in relation to each other (Figure 4.47). The metal is compressed and plasticized above its yield strength and made to flow in the axial direction onto a mandrel. The workpiece, the rollers and the inner mandrel (Figure 4.49) are all rotating.

The starting blank, generally referred to as "preform", can be flow-formed in either the solution annealed or hardened condition. Preforms can be made by hot or cold extrusion, forged, deep drawn, spun or machined from solids. If the finished component requires close tolerances, the preforms will be machined prior to being flow-formed for dimensional accuracy.

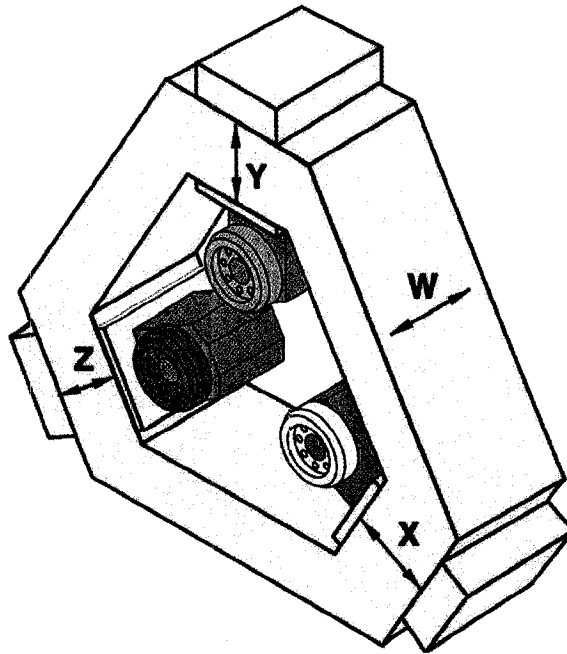
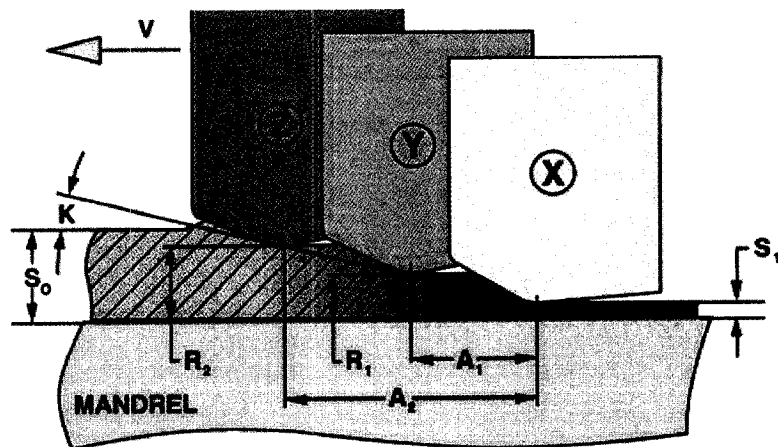


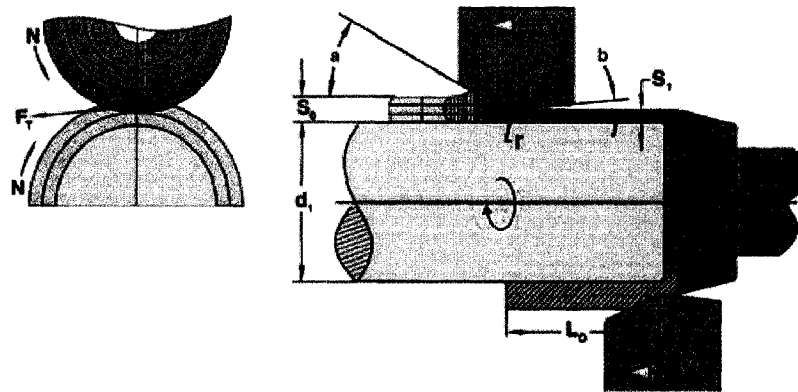
Figure 4.46: Longitudinal carriage with roller housing



(Rollers shown on the same plane for clarity)

R1	R2	Radial roller offset	S0	Starting wall thickness
A1	A2	Axial roller offset	S1	Finished wall thickness
K		Preform lead angle	v	Direction of feed

Figure 4.47: Position of the rollers



FR: Radial force
 FA: Axial force
 FT: Tangential force

S0: Starting wall thickness
 S1: Finished wall thickness
 L0: Starting length
 D1: Inside diameter

a: leading angle
 b: Trailing angle

r: Nose radius

N: Direction of rotation
 V: Feed

Figure 4.48: Mandrel

4.2.2.2 Methods of flow-forming

For flow-forming, two types of techniques can be used. One technique is the forward flow-forming and the other is the reverse flow-forming.

Forward flow forming

Forward flow forming is employed when the component to be flow formed has one closed or semi closed end, such as a cylinder. Clamped by the hydraulic force of the tailstock, the bottom of the preform rests against and rotates with the mandrel. As rollers are fed in a right to left direction, the flow formed material moves in the same direction (Figure 4.49).

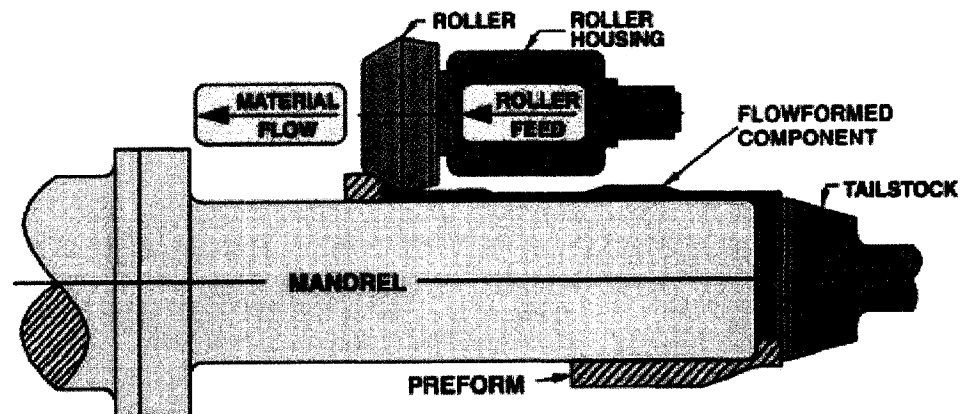


Figure 4.49: Forward flow forming

Reverse flow-forming

Reverse flow-forming is utilized for a component, which has two open ends, such as a tube. The preform is placed onto the mandrel and pushed to the end against a drive ring, which has a series of protruding splines on its face. Rotational motion to the workpiece is received when the axial thrust of the rollers push the preform against the drive ring. As in forward flow-forming, the longitudinal feed moves right to left. In this case however, the flow-formed metal moves in the opposite direction of the rollers (Figure 4.50).

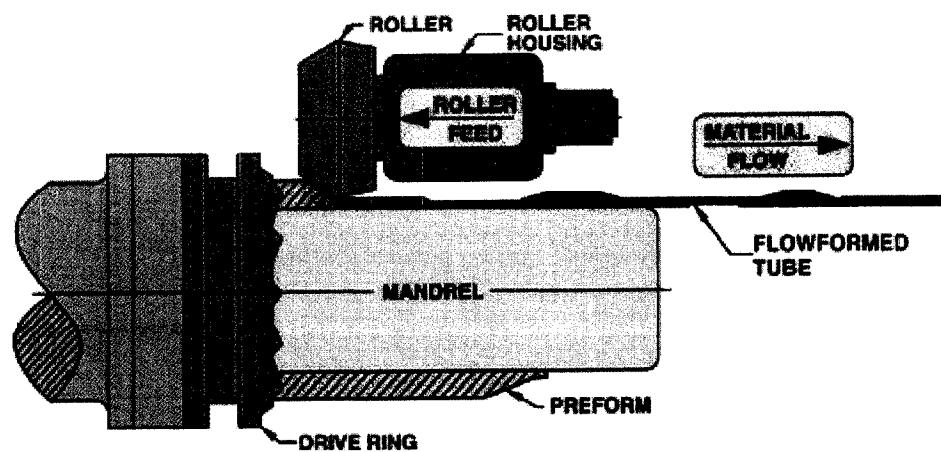


Figure 4.50: Reverse flow forming

4.2.2.3 Flow forming accuracy

In Figure 4.51, the geometrical tolerances are given in function of the inside diameter dimensions and wall thickness.

SIZE RANGE OF FINISHED COMPONENT					
INSIDE DIAMETER	inch	.866--3.94	3.94--9.84	9.84--15.75	15.75--24.50
	mm	22--100	100--250	250--400	400--622
WALL THICKNESS	inch	.006--.200	.010--.250	.015--.350	.020--.600
	mm	0.15--5.0	0.25--6.35	0.40--9.0	0.50--15.25
TOLERANCES*					
Inside Diameter ^{***}	inch	+/- .002	+/- .003	+/- .004	+/- .005
	mm	+/- 0.05	+/- 0.075	+/- 0.10	+/- 0.125
Wall Thickness	inch	+/- .001	+/- .0015	+/- .002	+/- .003
	mm	+/- 0.025	+/- 0.04	+/- 0.05	+/- 0.075
Ovality (max.)	inch	.003	.005	.008	.010
	mm	0.075	0.125	0.20	0.25
Concentricity (max.)	inch	.001	.002	.0025	.003
	mm	0.025	0.050	0.065	0.075
Straightness (max.)	inch	.001/ft	.0015/ft	.002/ft	.003/ft
	mm	0.08/1000	0.125/1000	0.17/1000	0.25/1000
Internal Surface Finish	μ inch	8	8	8	8
	μm	0.2	0.2	0.2	0.2
External Surface Finish	μ inch	16	24 ^{**}	32 ^{**}	32 ^{**}
	μm	0.4	0.6 ^{**}	0.8 ^{**}	0.8 ^{**}

Material Dependent

Or less if other dimensional tolerances can be relaxed

It is preferable to control inside diameter and wall thickness than outside diameter and wall thickness

Figure 4.51: Flow forming accuracy

4.2.2.4 Advantages and disadvantages

The flow-forming technique has the following advantages and disadvantages.

Advantages

- High dimensional accuracy
- Precise/stable/thin cross sections
- Seamless construction to net shapes
- Tapered walls and/or components

- Complex geometries
- Exceptional surface finishes
- Uniform, directional grain structure
- Improved tensile/hoop strength & hardness
- Refined grain size
- Ability to form pre-hardened metals
- Integral flange on one or both ends

Disadvantages

- Unwanted residual stresses
- Suitable for cylindrical parts only
- Limited on the complexity of the external and internal profile

4.2.2.5 Cost Effectiveness

- Exceptional reduction rates up to 90% of wall thickness reduced in one pass.
- High production rates from seconds to a few minutes.
- Repeatable accuracy part to part --- lot to lot.
- Chip less production.
- Superior internal surface finishes as low as 8 micro inch.
- Low labor cost employing one operator and one machine.
- Economical tooling cost of one mandrel.

4.2.2.6 Tests

To validate the possibility of flow forming the power shaft, a contract proposal was requested from “Dynamic Machine Works”, which is a company specialized in flow forming and is located in the United States of America. The company has been successfully flow forming Inconel 718 for many years.

Dynamic Machine Works tests on Inconel 718

After flow forming, shafts with a wall-thickness of 0.098" were given a standard solution heat treatment (at a temperature of 1750° F) and a two-step precipitation or aging heat treatment. Flat-type tensile specimens having the curvature of the tube were prepared from a representative piece. The results from these tests are given in Table 4.7.

Table 4.7: Properties of flow formed Inconel 718 after solution & aging heat treatment

Spec. #	Yield Stress, ksi	Ultimate Tensile Stress, ksi	Elongation, %	Hardness, Rockwell C
9-1	192.0	222.0	20.6	48
9-2	192.0	221.0	21.0	48
9-3	185.0	219.0	20.8	48
9-4	188.0	221.0	20.2	48
Average	189.2	220.8	20.8	48

A typical microstructure of Inconel 718 is shown in Figure 4.52. The specimen was etched in Kallings' (non-water containing) etching solution by immersion for 5 minutes. The grain sizes range from ASTM 5.5 – 6.

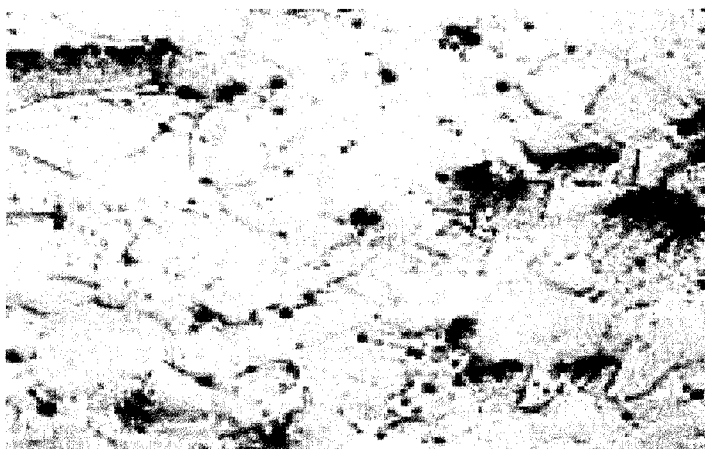


Figure 4.52: Preform 100X etched

The microstructure of flow formed Inconel 718 after a full heat treatment is shown in Figures 4.53 and 4.54. The specimen was electrolytically etched in a solution of 50% hydrochloric acid, 50% water plus a few drops of hydrogen peroxide for 30 seconds at 6 volts. The grain sizes range from ASTM 11 -12.

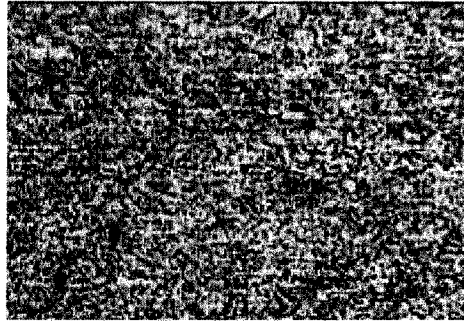


Figure 4.53: Flow formed 100X etched

The directionality imparted by the flow forming process is shown in Figure 4.54 at a magnification of 700X.

The etching procedure delineates the secondary phases but the grain boundaries of the matrix are not visible. However, based on prior experience, the very high density of the secondary phases indicates an extremely fine grain structure as would be expected from solution heat treating a heavily cold-worked structure at 1750°F during the full heat treatment.

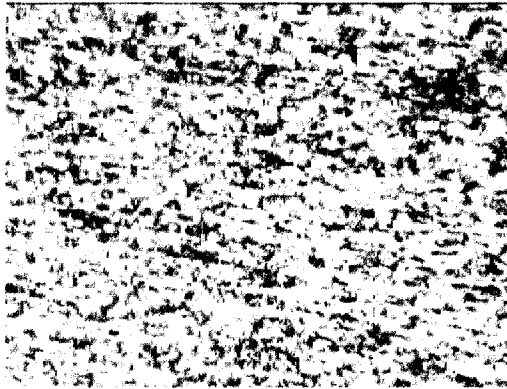


Figure 4.54: Flow formed 700X etched

It is noteworthy that microstructural examination of specimens from this and other parts reveals no evidence of internal cracking, galling or tearing of the metal from the flow forming process. Typical surface finishes R_t are 8 micro inch on the internal surface and 16 on the external surface.

The flow forming process offers an opportunity to explore the very high tensile properties including grain refinement of Inconel 718 after a full solution heat treatment of the flow formed tubular parts.

In Figure 4.55 it is possible to see an example of the final flow formed part in Inconel 718 with the preform, and in Figure 4.56 the micro inch finish of the inside diameter is shown.

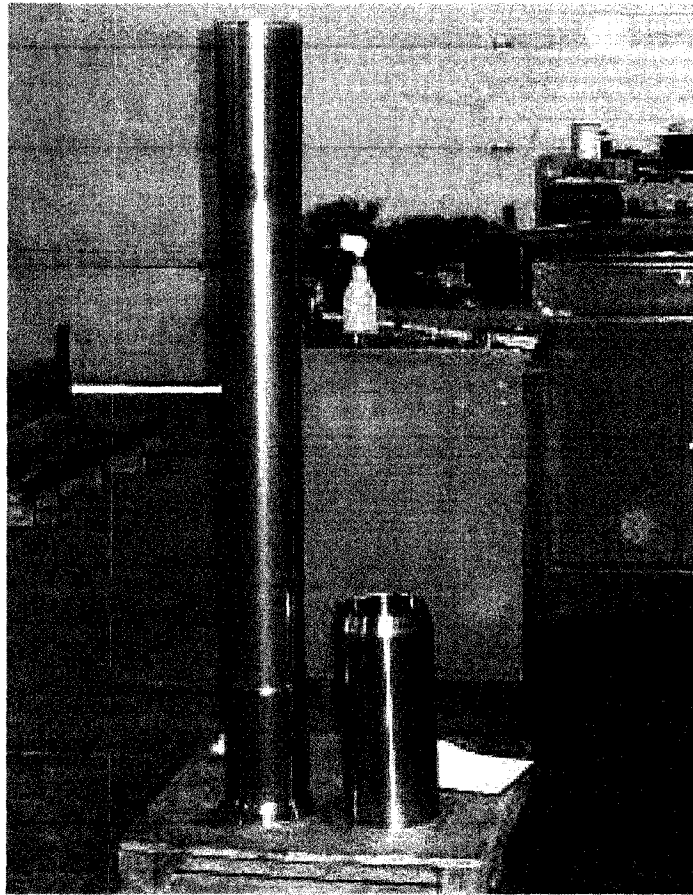


Figure 4.55: Flow formed Inconel 718. Preform on the right.



Figure 4.56: Flow formed Inconel 718 micro inch finish in the ID

“Dynamic Machine Works” Contract Proposal

After discussing with “Dynamic Machine Works”, they accepted to make a contract proposal for the PW307 power shaft. Since the first contract proposal, many revisions have been done in order to make sure that the dimensioning was perfectly respected. Although, some modifications were done in the inside diameter where there are steps because of material flow issues.

The drawings of the last version of the final flow formed part with the mandrel and drift pin that were proposed by “Dynamic Machine Works” are available in appendix X.

CONCLUSION

A successful optimization technique for the design of the power shaft was conceived. This technique allows an optimal distribution of the material in the shaft respecting the requirements of the different stress analyses. This optimization consent to insure, that the weight of the shaft is the smallest achievable one. A computer program performing the design optimization of the power shaft was developed in order to facilitate the optimization operation.

It is possible to make a power shaft made of different materials, using the friction welding technique. The stress and dynamic analytic analyses confirms the feasibility of friction welding a multi material power shaft. The CPW245 and Inconel 718 configuration represents the best machining cost savings of 3957\$ (almost 40% cost saving) and is the safest option, since PWC has good knowledge on these materials. Also, some friction welding tests have confirmed in tensile stress that the sample breaks in the weaker material side but never at the weld bondline.

The advantages of having a multi material shaft are the following:

1. Slight change in the manufacturing process.
2. No machinery investment if friction welding is sub-contracted.
3. CPW245 material being gun drilled has a better machinability than Inconel 718.
4. Gun drilling CPW245 creates less problems of concentricity between the inside and outside diameters compared to Inconel 718 gun drilling.
5. Machining time is lowered.
6. No more difficulties in the machining of Inconel 718, since the portion of the shaft in Inconel 718 is only long 11.125”.

After reviewing the work done by Dynamics Machine Works on the flow forming of Inco718, a contract proposal was worked out with them in order to make the power shaft. The central stepped section of the shaft as well as all the inside diameters would be finished by flow forming and only both ends would have to be turned and milled. A flow formed power shaft prototype will eventually confirm a new option and would be a great innovation in the aeronautic industry.

The advantages of flow forming a power shaft are the following:

1. Material removal is inexistent.
2. Machining time goes down drastically.
3. The concentricity problems between the inside and outside diameters disappear.
4. The interior finish of the shaft is the same as the one of the mandrel used to flow form and it is easy to control.

Thanks to the computer program performing the design optimization, weight reduction of the power shaft is achievable. Using friction welding or the flow forming technique, great cost reduction of the manufacturing of the power shaft is attainable.

Future work

For the future, it is very important to:

1. Finish the tests for friction welding as well as for flow forming.
2. Manufacture the first prototypes for each solution.
3. Rig test the power shafts for each solution.
4. Test power shafts in PW307 turbofan engine for each solution.
5. Do a business case to implement the optimum solution in the production line.

REFERENCES

- [1] Miller, J.A., O'Connor, J.J. (1980). Inertia and electron beam welded turbine engine power shaft. *AWS 61st Annual Meeting held in Los Angeles, California, during April 14-18, 1980.*
- [2] P. Amborn, H. Frielingsdorf, S.K. Ghosh and K. Greulich (1995). From Metal Cutting to Metal Forming Modern Side-Shafts for Passenger Cars: Manufacturing Aspects. *Journal of Materials Processing Technology*, 48, 3-12.
- [3] P. Amborn, S.K. Ghosh and I.K. Leadbetter (1997). Modern Side-Shafts for Passenger Cars: Manufacturing Processes II – Monobloc Tubed Shaft. *Journal of Materials Processing Technology*, 63, 225-232.
- [4] D.G. Backman and J.C. Williams (1992). Advanced Materials for Aircraft Engine Applications. *Science*, 255, 5048, 1082-1087.
- [5] M. Rahman, W.K.H. Seah and T.T. Teo (1997). The Machinability of Inconel 718. *Journal of Materials Processing Technology*, 63, 199-204.
- [6] J. Albrecht (1999). Comparing behavior of titanium and nickel-based alloys. *Materials Science and Engineering*, A263, 176-186.
- [7] E.O. Ezugwu, J. Bonney and Y. Yamane (2003). An overview of the machinability of aeroengine alloys. *Journal of Materials Processing Technology*, 134, 233-253.
- [8] M. Soucail and Y. Bienvenu (1996). Dissolution of the γ' phase in a nickel base superalloy at equilibrium and under rapid heating. *Materials Science and Engineering*, A220, 215-222.

- [9] Y. Yamashita, T. Yoshida and K. Fujita (1998). Investigation of application of friction welding to dissimilar metal joints for electric power plants. *Welding International*, 12, (4), 266-271.
- [10] M. Preuss, J.W.L. Pang, P.J. Withers and G.J. Baxter (2002). Inertia Welding Nickel-based Superalloy: Part I. Metallurgical Characterization. *Metallurgical and Materials Transactions*, 33A, 3215-3225.
- [11] M. Preuss, J.W.L. Pang, P.J. Withers and G.J. Baxter (2002). Inertia Welding Nickel-based Superalloy: Part II. Residual Stress Characterization. *Metallurgical and Materials Transactions*, 33A, 3227-3234.
- [12] L. D'Alvise, E. Massoni, S.J. Walløe (2002). Finite element modelling of the inertia friction welding process between dissimilar materials. *Journal of Materials Processing Technology*, 125-126, 387-391.
- [13] M. Jahazi and G. Ebrahimi (2000). The influence of flow-forming parameters and microstructure on the quality of a D6ac steel. *Journal of Materials Processing Technology*, 103, 362-366.
- [14] H. Nägele, H. Wörner and M. Hirschvogel (2000). Automotive parts produced by optimizing the process flow forming – machining. *Journal of Materials Processing Technology*, 98, 171-175.
- [15] K.S. Lee and L. Lu (2001). A study on the flow forming of cylindrical tubes. *Journal of Materials Processing Technology*, 113, 739-742.

- [16] Unknown (2002). P0889 Shaft Analysis Program Engineering and Software Manual. PWC internal publication. This document is based on “Wharram, G.E. December 19,1995. Shaft Stress and Life Analysis Methodology for Program P0889. C.E.F.# S-4925, S-4926.” .
- [17] Unknown (1989). IBM Program. Description of Computer Program UACL NO. P0571. Whirl Speed Analysis of Coaxial Shafts. PWC internal publication.

APPENDIX I

Input file for P0889 Shaft analysis program (Actual Power Shaft)

PW307A	HOTD/Fn-REV	LP Shaftv2:1_t3az	24K LCF	21/06/02				
1.	0.	0.	1.	1.				
30.								
3.Thread	1	-14.273	4.					
2.7887	2.3750	0.0094	2.8700	0.0000	0.0000	0.0000		
4.840	2.280	6.120					0.297	0.290
534.4								
534.4								
1.ThdEndRf	2	-13.901	4.					
2.7600	2.4060	0.0310	2.9021	0.0000	0.0000	0.0000		
2.360	1.530	2.150					0.297	0.290
534.4								
534.4								
1.SpIn Rf	3	-13.187	4.					
2.8800	2.4060	0.0470	3.0310	0.0000	0.0000	0.0000		
0.000	0.000	0.000					0.297	0.290
534.4								
534.4								
1.SpIn Rf	4	-11.846	4.					
2.8850	2.4060	0.0470	3.1221	0.0000	0.0000	0.0000		
0.000	0.000	0.000					0.297	0.290
534.4								
534.4								
2.AirHoles	5	-10.276	4.					
3.1214	2.4060	0.3830	4.	0.0000	0.0000	0.0000		
0.000	0.000	0.000					0.297	0.290
534.4								
534.4								
3.Oil Grve	6	-8.619	4.					
2.9600	2.4060	0.1200	3.1520	0.0000	0.0000	0.0000		
0.000	0.000	0.000					0.297	0.290
534.4								
534.4								
6.Oil Slot	7	-8.134	4.					
3.0200	2.4060	0.2600	4.	0.0000	0.0000	0.0000	0.020	3.152
0.000	0.000	0.000					0.297	0.290
534.4								
534.4								
6.Oil Slot	8	-7.755	4.					
2.9240	2.4060	0.1600	4.	0.0000	0.0000	0.0000	0.020	3.020
0.000	0.000	0.000					0.297	0.290
534.4								
534.4								
3.Grve	9	-6.246	4.					
2.8550	2.4060	0.02000	2.9440	0.0000	0.0000	0.0000		
0.000	0.000	0.000					0.297	0.290
534.4								
534.4								
1.Seal Rf	10	-5.398	4.					
2.8384	2.4060	0.0470	2.8780	0.0000	0.0000	0.0000		
0.000	0.000	0.000					0.297	0.290
534.4								
534.4								
2.AirFeed	11	-4.623	4.					
2.7000	2.2800	0.3980	5.	0.0000	0.0000	0.0000		
0.000	0.000	0.000					0.297	0.290
534.4								
534.4								
1.Shd Rf	12	-3.364	4.					
2.5200	2.2800	0.5160	2.8394	0.0000	0.0000	0.0000		
0.000	0.000	0.000					0.297	0.290
534.4								
534.4								
1.TperMid	13	0.508	4.					
2.5000	2.2800	99.9999	2.5000	0.0000	0.0000	0.0000		
1.000	1.000	1.000						

534.4						0.297	0.290
534.4							
1.TperEnd 14	4.380	4.					
2.4800	2.2800	99.9999	2.4800	0.0000	0.0000	0.0000	
1.000	1.000	1.000					
534.4						0.297	0.290
534.4							
1.Barrel 15	9.538	4.					
2.4800	2.2800	99.9999	2.4800	0.0000	0.0000	0.0000	
1.000	1.000	1.000					
534.4						0.297	0.290
534.4							
1.ShdIDrf 16	13.761	4.					
2.4800	2.2800	0.5000	2.0600	0.0000	0.0000	0.0000	
0.000	0.000	0.000					
534.4						0.297	0.290
534.4							
1.Step1 17	14.476	4.					
2.3150	2.0700	0.9690	2.4800	0.0000	0.0000	0.0000	
0.000	0.000	0.000					
534.4						0.297	0.290
534.4							
1.RvtLd 18	18.085	4.					
2.3150	2.0700	0.4840	2.4250	0.0000	0.0000	0.0000	
0.000	0.000	0.000					
762.6						0.297	0.290
762.6							
2.RvtHole 19	18.520	4.					
2.41500	2.0700	0.1000	2.	0.0000	0.0000	0.0000	
0.000	0.000	0.000					
762.6						0.297	0.290
762.6							
1.RvtLd 20	18.972	4.					
2.3150	2.0700	0.4840	2.4250	0.0000	0.0000	0.0000	
0.000	0.000	0.000					
762.6						0.297	0.290
762.6							
1.ShdIDrf 21	19.114	4.					
2.3150	2.0700	1.0000	1.4550	0.0000	0.0000	0.0000	
0.000	0.000	0.000					
762.6						0.297	0.290
762.6							
1.Step2 22	20.439	4.					
1.9015	1.4650	0.9690	2.3250	0.0000	0.0000	0.0000	
0.000	0.000	0.000					
762.6						0.297	0.290
762.6							
1.TprStd 23	26.681	4.					
1.9015	1.4650	99.9999	1.9015	0.0000	0.0000	0.0000	
1.000	1.000	1.000					
900.5						0.297	0.290
900.5							
1.TprEnd 24	31.476	4.					
1.9258	1.4650	0.5940	2.2205	0.0000	0.0000	0.0000	
0.000	0.000	0.000					
900.5						0.297	0.290
900.5							
1.SplUcut 25	32.350	4.					
1.9600	1.1400	0.0620	2.2205	0.0000	0.0000	0.0000	
0.000	0.000	0.000					
900.5						0.297	0.290
900.5							
3.SplGrve 26	34.017	4.					
1.7400	1.4460	0.0200	1.9800	0.0000	0.0000	0.0000	
0.000	0.000	0.000					
900.5						0.297	0.290
900.5							
2.AirHole 27	34.784	4.					
1.7610	1.4950	0.38300	4.	0.0000	0.0000	0.0000	
0.000	0.000	0.000					
928.6						0.297	0.290
928.6							
2.OilHole 28	36.231	4.					
1.7326	1.4850	0.0500	4.	0.0000	0.0000	0.0000	
0.000	0.000	0.000					
260.0						0.297	0.290

260.0									
1.5700	1.2510	37.017	4.	0.0000	0.0000	0.0000			
0.000	0.000	0.0310	1.7332						
260.0		0.000				0.297	0.290		
260.0									
1.6075	1.3480	37.319	4.	0.0000	0.0000	0.0000			
0.000	0.000	0.0094	1.6875						
260.0		0.000				0.297	0.290		
260.0									
7.									
1.	20000.	HDTO	Fn=5018#	.2 rad/sec,	23Jun02	10188.0	0.		
32754.0	0.0	830.5	15714.	0.				0.05	
32754.0	0.0	830.5	15714.	0.				0.05	
32754.0	38399.0	1131.6	15714.	0.				0.05	
32754.0	38399.0	1932.0	15714.	0.				0.05	
32754.0	38399.0	2179.8	15714.	0.				0.05	
32754.0	38399.0	2448.7	15714.	0.				0.05	
32754.0	38399.0	3467.4	15714.	0.				0.05	
7296.0	38399.0	3418.5	0.	0.				0.05	
7296.0	38399.0	3224.3	0.	0.				0.05	
7296.0	38399.0	3114.8	0.	0.				0.05	
7296.0	38399.0	3014.8	0.	0.				0.05	
7296.0	38399.0	2852.3	0.	0.				0.05	
7296.0	38399.0	2338.5	0.	0.				0.05	
7296.0	38399.0	1852.6	0.	0.				0.05	
7296.0	38399.0	1186.6	0.	0.				0.05	
7296.0	38399.0	641.6	0.	0.				0.05	
7296.0	38399.0	549.3	0.	0.				0.05	
7296.0	38399.0	103.9	0.	0.				0.05	
7296.0	38399.0	28.5	0.	0.				0.05	
7296.0	38399.0	30.9	0.	0.				0.05	
7296.0	38399.0	49.2	0.	0.				0.05	
7296.0	38399.0	220.3	0.	0.				0.05	
7296.0	38399.0	1026.1	0.	0.				0.05	
7296.0	38399.0	1645.1	0.	0.				0.05	
20200.0	38399.0	1547.1	18200.	0.				0.05	
20200.0	0.0	110.0	18200.	0.				0.05	
20200.0	0.0	39.6	18200.	0.				0.05	
20200.0	0.0	95.3	18200.	0.				0.05	
20200.0	0.0	136.0	18200.	0.				0.05	
20200.0	0.0	4.9	18200.	0.				0.05	
1.	20000.	HDTORev	Fn=5827#	.2 rad/sec,	23Jun02	9949.0	0.		
32754.0	0.	000.0	15714.	0.				0.05	
32754.0	0.	0000.0	15714.	0.				0.05	
32754.0	35165.	0000.0	15714.	0.				0.05	
32754.0	35165.	0000.0	15714.	0.				0.05	
32754.0	35165.	0000.0	15714.	0.				0.05	
32754.0	35165.	0000.0	15714.	0.				0.05	
7296.0	35165.	0000.0	0.	0.				0.05	
7296.0	35165.	0000.0	0.	0.				0.05	
7296.0	35165.	0000.0	0.	0.				0.05	
7296.0	35165.	0000.0	0.	0.				0.05	
7296.0	35165.	0000.0	0.	0.				0.05	
7296.0	35165.	0000.0	0.	0.				0.05	
7296.0	35165.	0000.0	0.	0.				0.05	
7296.0	35165.	0000.0	0.	0.				0.05	
7296.0	35165.	0000.0	0.	0.				0.05	
7296.0	35165.	0000.0	0.	0.				0.05	
7296.0	35165.	0000.0	0.	0.				0.05	
7296.0	35165.	0000.0	0.	0.				0.05	
7296.0	35165.	0000.0	0.	0.				0.05	
7296.0	35165.	0000.0	0.	0.				0.05	
7296.0	35165.	0000.0	0.	0.				0.05	
7296.0	35165.	0000.0	0.	0.				0.05	
7296.0	35165.	0000.0	0.	0.				0.05	
7296.0	35165.	0000.0	0.	0.				0.05	
20200.0	35165.	000.0	18200.	0.				0.05	
20200.0	0.	000.0	18200.	0.				0.05	
20200.0	0.	00.0	18200.	0.				0.05	
20200.0	0.	00.0	18200.	0.				0.05	
20200.0	0.	00.0	18200.	0.				0.05	
20200.0	0.	00.0	18200.	0.				0.05	
2.0	2482.	HDTO +2.0rad/s	23Jun02			9969.0	0.		
32754.0	0.0	8065.0							

32754.0	0.0	8065.0		
32754.0	38399.0	10957.4		
32754.0	38399.0	18648.1		
32754.0	38399.0	20437.6		
32754.0	38399.0	21398.0		
32754.0	38399.0	29587.5		
7296.0	38399.0	34253.9		
7296.0	38399.0	32431.6		
7296.0	38399.0	31404.6		
7296.0	38399.0	30465.7		
7296.0	38399.0	30035.9		
7296.0	38399.0	24119.0		
7296.0	38399.0	19559.0		
7296.0	38399.0	13308.1		
7296.0	38399.0	8193.3		
7296.0	38399.0	7327.0		
7296.0	38399.0	2890.4		
7296.0	38399.0	2412.0		
7296.0	38399.0	1882.5		
7296.0	38399.0	1710.0		
7296.0	38399.0	105.2		
7296.0	38399.0	7457.0		
7296.0	38399.0	13266.4		
20200.0	38399.0	12553.0		
20200.0	0.0	689.0		
20200.0	0.0	209.6		
20200.0	0.0	804.1		
20200.0	0.0	1188.0		
20200.0	0.0	43.3		
3.	1.Fan Blade-off 23Jun02		9952.0	0.
32754.0	26.2	85731.5		
32754.0	28.8	84797.5		
32754.0	51209.9	88632.6		
32754.0	51213.0	99272.2		
32754.0	52629.1	34737.4		
32754.0	48634.0	67083.0		
32754.0	59507.3	73659.4		
7296.0	59502.9	72541.2		
7296.0	59496.1	68421.1		
7296.0	59485.0	66149.3		
7296.0	59480.0	64197.9		
7296.0	59479.0	63312.5		
7296.0	59479.0	57282.0		
7296.0	59483.0	53600.0		
7296.0	59472.5	49783.8		
7296.0	59453.0	48128.4		
7296.0	59453.0	47574.0		
7296.0	54799.0	37282.6		
7296.0	58998.0	40099.6		
7296.0	59448.0	39381.1		
7296.0	59448.0	39007.0		
7296.0	59446.0	34992.3		
7296.0	59444.0	22561.0		
7296.0	59449.0	45112.5		
20200.0	43585.0	46394.1		
20200.0	5183.0	27977.0		
20200.0	25.0	16418.7		
20200.0	12.5	2213.8		
20200.0	5.0	6254.8		
20200.0	0.8	236.1		
3.	1.LPT Blade-off 23Feb02		9952.0	0.
32754.0	31.2	18001.8		
32754.0	33.9	18000.1		
32754.0	57974.0	24674.8		
32754.0	57977.2	42544.4		
32754.0	60147.9	49749.6		
32754.0	54058.0	58160.0		
32754.0	70718.5	79843.3		
7296.0	70721.0	76482.0		
7296.0	70723.0	63341.6		
7296.0	70730.0	56283.6		
7296.0	70733.0	50009.6		
7296.0	70733.0	47185.6		
7296.0	70723.0	11265.0		
7296.0	70700.0	20002.0		
7296.0	70652.6	42770.3		

7296.0	70630.0	52433.7		
7296.0	70636.0	53206.0		
7296.0	63547.9	46394.6		
7296.0	69994.6	51405.1		
7296.0	70688.7	51367.7		
7296.0	70690.0	51120.0		
7296.0	70703.0	48018.8		
7296.0	70716.0	18863.0		
7296.0	70723.0	33733.2		
20200.0	46435.7	36241.0		
20200.0	8005.3	18929.7		
20200.0	287.1	10958.0		
20200.0	142.9	2062.9		
20200.0	56.7	3922.1		
20200.0	12.3	154.2		
5.	1.80% hit, 2*1.5lb bird, 23Jun 02		9669.0	0.
41203.4	89.4	19884.3		
41208.7	96.7	19878.9		
41218.8	58585.0	24908.7		
41235.2	58579.0	38361.4		
41271.2	60790.7	36381.2		
41442.0	54482.0	40461.0		
43055.7	71558.4	55717.0		
26141.4	71547.7	54519.3		
26317.6	71528.1	49756.5		
26394.5	71496.3	47048.6		
26476.5	71479.8	44554.8		
26495.2	71476.2	43407.4		
26692.0	71430.0	27752.0		
26783.0	71413.0	23476.0		
26822.2	71345.6	25164.4		
26781.1	71285.0	25018.2		
26760.0	71295.0	24904.0		
26643.5	64079.8	19885.6		
26573.1	70665.8	21470.9		
26546.1	71376.7	21059.4		
26539.0	71379.0	20833.0		
26416.2	71408.0	20471.8		
25977.0	71476.0	19903.0		
25836.5	71506.8	32447.3		
38711.0	46562.0	31441.0		
30349.0	8159.2	9388.0		
28664.1	123.0	5240.3		
28657.0	62.2	1468.0		
28659.0	25.0	1834.1		
20224.3	4.9	78.4		
4.	1.80% hit, 2*1.5lb bird, 25Jun 02		9669.0	0.
44617.8	130.4	25744.0		
44616.1	140.4	25688.6		
44607.2	83876.1	31846.8		
44578.6	83851.6	48355.9		
44525.9	88808.4	44283.8		
44538.0	74569.0	52691.0		
58122.2	112897.5	70547.4		
32571.5	112868.2	69500.3		
32301.7	112819.2	65287.5		
32183.8	112744.5	62847.2		
32064.4	112709.5	60567.1		
32041.9	112702.3	59508.8		
31771.0	112670.0	44518.0		
31649.0	112605.0	38752.0		
31632.0	112476.6	37027.3		
31613.9	112351.2	31766.3		
31623.0	112314.0	30560.0		
31625.1	96002.0	22803.9		
31613.1	99610.8	26359.5		
31607.3	112348.6	27218.9		
31606.0	112352.0	27374.0		
31573.1	112389.9	28691.1		
31356.0	112474.0	34000.0		
31104.0	112489.0	43466.1		
43923.1	56644.0	41468.8		
33188.2	18233.2	10643.3		
31044.3	171.0	5736.3		
30978.7	84.3	2263.4		
30912.5	33.7	3455.5		

20229.0 7.4 137.2

Table with 13 columns showing stress and moment values for various components (e.g., 23 7296, 24 7296, 25 20200).

THE MAXIMUM LCF/HCF DESIGN FACTOR OF .78 OCCURRED AT SECTION 20
THE MINIMUM CYCLIC LIFE OF 98898. CYCLES OCCURRED AT SECTION 19

TABLE 6: GYROSCOPIC PRECESSION ; SHELLEY FATIGUE FACTORS ; CYCLES = 2482. ; MAXIMUM RPM = 9969. ; MINIMUM RPM = 0.
LOAD DESCRIPTION = HDTO +2.0rad/s 23Jum02

PROGRAM P0889 ; VERSION: 5.00

ENGINE MODEL: PW307A HOTD/Fn-REV
PART NUMBER: LP ShafteV2_1_t3az
SHAFT TYPE: 24K LCF 21/06/02

Table with 15 columns: SECT NUMB, AXIAL FORCE, SHAFT TORQUE, BENDING MOMENT, AXIAL STRESS, SHEAR STRESS, BENDING STRESS, CENTRIF STRESS, PLASTIC STRESS, MAX-PLAST STRESS, ULTIMATE STRESS, MAX-PLAST YIELD, MAX-PLAST ULTIMATE. Rows 1-30.

THE MAXIMUM LCF/HCF DESIGN FACTOR OF .93 OCCURRED AT SECTION 12
THE MINIMUM CYCLIC LIFE OF 4389. CYCLES OCCURRED AT SECTION 12
THE MAXIMUM ALLOWABLE GYROSCOPIC PRECESSION OCCURRED AT SECTION 12 AND IS 1.146 TIMES THE NOMINAL RATE

TABLE 7: COMPRESSOR BLADE-LOSS ; CYCLES = 1. ; MAXIMUM RPM = 9952. ; MINIMUM RPM = 0.
LOAD DESCRIPTION = Fan Blade-off 23Jum02

PROGRAM P0889 ; VERSION: 5.00

ENGINE MODEL: PW307A HOTD/Fn-REV
PART NUMBER: LP ShafteV2_1_t3az
SHAFT TYPE: 24K LCF 21/06/02

Table with 15 columns: SECT NUMB, AXIAL FORCE, SHAFT TORQUE, BENDING MOMENT, AXIAL STRESS, SHEAR STRESS, BENDING STRESS, CENTRIF STRESS, PLASTIC STRESS, MAX-PLAST STRESS, ULTIMATE STRESS, MAX-PLAST YIELD, MAX-PLAST ULTIMATE. Rows 1-30.

THE MAXIMUM (PLASTIC STRESS / ULT. STRESS) FACTOR OF .29 OCCURRED AT SECTION 14 AND THE STRESS IS 155.4 KSI
THE MAXIMUM (PLASTIC STRESS / YIELD STRESS) FACTOR OF 1.27 OCCURRED AT SECTION 14 AND THE STRESS IS 155.4 KSI

TABLE 8: COMPRESSOR BLADE-LOSS ; CYCLES = 1. ; MAXIMUM RPM = 9952. ; MINIMUM RPM = 0.
LOAD DESCRIPTION = LPT Blade-off 23Feb02

PROGRAM P0889 ; VERSION: 5.00

ENGINE MODEL: PW307A HOTD/Fn-REV
PART NUMBER: LP ShafteV2_1_t3az
SHAFT TYPE: 24K LCF 21/06/02

Table with 15 columns: SECT NUMB, AXIAL FORCE, SHAFT TORQUE, BENDING MOMENT, AXIAL STRESS, SHEAR STRESS, BENDING STRESS, CENTRIF STRESS, PLASTIC STRESS, MAX-PLAST STRESS, ULTIMATE STRESS, MAX-PLAST YIELD, MAX-PLAST ULTIMATE. Rows 1-9.

Table with columns for ID, Part No, Weight, etc. Rows 10-30 showing various parts like 7296, 70730, 56284, etc.

THE MAXIMUM (PLASTIC STRESS / ULT. STRESS) FACTOR OF 1.09 OCCURRED AT SECTION 16 AND THE STRESS IS 171.0 KSI
THE MAXIMUM (PLASTIC STRESS / YIELD STRESS) FACTOR OF 1.40 OCCURRED AT SECTION 16 AND THE STRESS IS 171.0 KSI
TABLE 9: MEDIUM BIRDSRIKE ; CYCLES = 1. ; MAXIMUM RPM = 9669. ; MINIMUM RPM = 0.
; LOAD DESCRIPTION = 80% hit, 2*1.51b bird, 23Jun 02

PROGRAM P0889 ; VERSION: 5.00

ENGINE MODEL: PW307A HOTO/Pn-REV
PART NUMBER: LP Shaftv21_t3az
SHAFT TYPE: 24K LCF 21/06/02

Main stress analysis table with columns: SECT NUMB, AXIAL FORCE, SHAFT TORQUE, BENDING MOMENT, AXIAL STRESS, SHEAR STRESS, BENDING STRESS, CENTRIF STRESS, MAXIMUM STRESS, YIELD STRESS, MAXIMUM STRESS, PLASTIC STRESS, MAX-PLAST YIELD, MAX-PLAST ULTIMATE, INNER STRESS, PROP LIMIT, INNER PROP-LIM.

THE MAXIMUM (PLASTIC STRESS / ULT. STRESS) FACTOR OF 1.02 OCCURRED AT SECTION 15 AND THE STRESS IS 160.1 KSI
THE MAXIMUM (PLASTIC STRESS / YIELD STRESS) FACTOR OF 1.31 OCCURRED AT SECTION 15 AND THE STRESS IS 160.1 KSI
THE MAXIMUM (OUTER STRESS / YIELD STRESS) FACTOR OF 1.41 OCCURRED AT SECTION 15 AND THE STRESS IS 172.6 KSI
THE MAXIMUM (INNER STRESS / PROP. LIMIT) FACTOR OF 1.56 OCCURRED AT SECTION 15 AND THE STRESS IS 160.1 KSI

TABLE 10: LARGE BIRDSRIKE ; CYCLES = 1. ; MAXIMUM RPM = 9669. ; MINIMUM RPM = 0.
; LOAD DESCRIPTION = 80% hit, 2*1.51b bird, 25Jun 02

PROGRAM P0889 ; VERSION: 5.00

ENGINE MODEL: PW307A HOTO/Pn-REV
PART NUMBER: LP Shaftv21_t3az
SHAFT TYPE: 24K LCF 21/06/02

Main stress analysis table with columns: SECT NUMB, AXIAL FORCE, SHAFT TORQUE, BENDING MOMENT, AXIAL STRESS, SHEAR STRESS, BENDING STRESS, CENTRIF STRESS, PLASTIC STRESS, MAX-PLAST STRESS, ULTIMATE STRESS, MAX-PLAST YIELD, MAX-PLAST ULTIMATE.

THE MAXIMUM (PLASTIC STRESS / ULT. STRESS) FACTOR OF 1.57 OCCURRED AT SECTION 14 AND THE STRESS IS 245.2 KSI
THE MAXIMUM (PLASTIC STRESS / YIELD STRESS) FACTOR OF 2.00 OCCURRED AT SECTION 14 AND THE STRESS IS 245.2 KSI

TABLE 11: DESIGN FACTOR SUMMARY

PROGRAM P0889 ; VERSION: 5.00

ENGINE MODEL: PW307A HOTO/Pn-REV
PART NUMBER: LP Shaftv21_t3az
SHAFT TYPE: 24K LCF 21/06/02

LOAD CASE 1 2 3 4 5 6 7
SECT LCF-HCF LCF-HCF GYROSCOPIC COMPRESSOR COMPRESSOR MEDIUM LARGE

NUNB	ANALYSIS	ANALYSIS	PRECESSION	BLADE-LOSS	BLADE-LOSS	BIRDSTRIKE	BIRDSTRIKE
1	.23	.15	.20	.52	.20	.36	.29
2	.19	.14	.23	.60	.24	.42	.33
3	.34	.30	.29	.49	.32	.48	.44
4	.38	.30	.35	.52	.36	.54	.48
5	.38	.31	.28	.24	.29	.42	.36
6	.34	.26	.31	.35	.33	.46	.39
7	.40	.30	.32	.33	.36	.50	.47
8	.46	.33	.39	.35	.38	.57	.54
9	.57	.37	.47	.40	.43	.65	.63
10	.43	.32	.46	.42	.43	.66	.66
11	.83	.63	.69	.63	.63	.99	.99
12	.84	.65	.93	.88	.87	1.34	1.38
13	.83	.70	.88	.92	.81	1.30	1.44
14	.89	.77	.89	.99	.92	1.39	1.57
15	.86	.77	.76	.97	1.03	1.41	1.56
16	.85	.77	.66	.95	1.09	1.41	1.53
17	.83	.76	.63	.91	1.05	1.36	1.46
18	.86	.78	.57	.83	.98	1.24	1.30
19	.80	.74	.40	.63	.76	.96	.95
20	.85	.78	.55	.89	1.08	1.35	1.50
21	.84	.77	.54	.89	1.08	1.35	1.50
22	.86	.78	.51	.81	1.00	1.32	1.41
23	.87	.78	.67	.77	.88	1.33	1.46
24	.88	.75	.74	.83	.88	1.36	1.40
25	.66	.55	.54	.50	.46	.77	.60
26	.09	.05	.21	.70	.55	.68	.61
27	.33	.31	.30	.74	.59	.76	.60
28	.25	.22	.23	.24	.24	.43	.35
29	.07	.04	.22	.29	.25	.38	.33
30	.05	.05	.20	.21	.20	.27	.20

1.TperEnd 14	4.380	4.				
2.4800 2.2950	99.9999	2.4800	0.0000	0.0000	0.0000	
1.000 1.000	1.000					
534.4					0.297	0.290
534.4						
1.Barrel 15	9.538	4.				
2.4800 2.2950	99.9999	2.4800	0.0000	0.0000	0.0000	
1.000 1.000	1.000					
534.4					0.297	0.290
534.4						
1.shdIDrf 16	13.761	4.				
2.4800 2.2950	0.5000	2.0600	0.0000	0.0000	0.0000	
0.000 0.000	0.000					
534.4					0.297	0.290
534.4						
1.Step1 17	14.476	4.				
2.3150 2.1100	0.9690	2.4800	0.0000	0.0000	0.0000	
0.000 0.000	0.000					
534.4					0.297	0.290
534.4						
1.RvtLd 18	18.085	4.				
2.3150 2.1100	0.4840	2.4250	0.0000	0.0000	0.0000	
0.000 0.000	0.000					
762.6					0.297	0.290
762.6						
2.RvtHole 19	18.520	4.				
2.41500 2.1100	0.1000	2.	0.0000	0.0000	0.0000	
0.000 0.000	0.000					
762.6					0.297	0.290
762.6						
1.RvtLd 20	18.972	4.				
2.3150 2.1100	0.4840	2.4250	0.0000	0.0000	0.0000	
0.000 0.000	0.000					
762.6					0.297	0.290
762.6						
1.shdIDrf 21	19.114	4.				
2.3150 2.1100	1.0000	1.4550	0.0000	0.0000	0.0000	
0.000 0.000	0.000					
762.6					0.297	0.290
762.6						
1.Step2 22	20.439	4.				
1.9015 1.5250	0.9690	2.3250	0.0000	0.0000	0.0000	
0.000 0.000	0.000					
762.6					0.297	0.290
762.6						
1.TprStd 23	26.681	4.				
1.9015 1.5250	99.9999	1.9015	0.0000	0.0000	0.0000	
1.000 1.000	1.000					
900.5					0.297	0.290
900.5						
1.TprEnd 24	31.476	4.				
1.9258 1.5250	0.5940	2.2205	0.0000	0.0000	0.0000	
0.000 0.000	0.000					
900.5					0.297	0.290
900.5						
1.spLUCut 25	32.350	4.				
1.9600 1.5250	0.0620	2.2205	0.0000	0.0000	0.0000	
0.000 0.000	0.000					
900.5					0.297	0.290
900.5						
3.spLGrve 26	34.017	4.				
1.7400 1.5250	0.0200	1.9800	0.0000	0.0000	0.0000	
0.000 0.000	0.000					
900.5					0.297	0.290
900.5						
2.AirHole 27	34.784	4.				
1.7610 1.5250	0.38300	4.	0.0000	0.0000	0.0000	
0.000 0.000	0.000					
928.6					0.297	0.290
928.6						
2.oilHole 28	36.231	4.				
1.7326 1.5250	0.0500	4.	0.0000	0.0000	0.0000	
0.000 0.000	0.000					
260.0					0.297	0.290
260.0						
1.Thducut 29	37.017	4.				

1.5700	1.2510	0.0310	1.7332	0.0000	0.0000	0.0000		
0.000	0.000	0.000						
260.0						0.297	0.290	
260.0								
	3.Thread 30	37.319	4.					
1.6075	1.3480	0.0094	1.6875	0.0000	0.0000	0.0000		
0.000	0.000	0.000						
260.0						0.297	0.290	
260.0								
7.								
1.	20000.	HDTO	Fn=5018#	.2 rad/sec	23Jun02	10188.0	0.	
32754.0	0.0	830.5	15714.					0.05
32754.0	0.0	830.5	15714.					0.05
32754.0	38399.0	1131.6	15714.					0.05
32754.0	38399.0	1932.0	15714.					0.05
32754.0	38399.0	2179.8	15714.					0.05
32754.0	38399.0	2448.7	15714.					0.05
32754.0	38399.0	3467.4	15714.					0.05
7296.0	38399.0	3418.5	0.					0.05
7296.0	38399.0	3224.3	0.					0.05
7296.0	38399.0	3114.8	0.					0.05
7296.0	38399.0	3014.8	0.					0.05
7296.0	38399.0	2852.3	0.					0.05
7296.0	38399.0	2338.5	0.					0.05
7296.0	38399.0	1852.6	0.					0.05
7296.0	38399.0	1186.6	0.					0.05
7296.0	38399.0	641.6	0.					0.05
7296.0	38399.0	549.3	0.					0.05
7296.0	38399.0	103.9	0.					0.05
7296.0	38399.0	28.5	0.					0.05
7296.0	38399.0	30.9	0.					0.05
7296.0	38399.0	49.2	0.					0.05
7296.0	38399.0	220.3	0.					0.05
7296.0	38399.0	1026.1	0.					0.05
7296.0	38399.0	1645.1	0.					0.05
20200.0	38399.0	1547.1	18200.					0.05
20200.0	0.0	110.0	18200.					0.05
20200.0	0.0	39.6	18200.					0.05
20200.0	0.0	95.3	18200.					0.05
20200.0	0.0	136.0	18200.					0.05
20200.0	0.0	4.9	18200.					0.05
	1.	20000.	HDTORev	Fn=5827#	.2 rad/sec	23Jun02	9949.0	0.
32754.0	0.0	000.0	15714.					0.05
32754.0	0.0	0000.0	15714.					0.05
32754.0	35165.	0000.0	15714.					0.05
32754.0	35165.	0000.0	15714.					0.05
32754.0	35165.	0000.0	15714.					0.05
32754.0	35165.	0000.0	15714.					0.05
32754.0	35165.	0000.0	15714.					0.05
7296.0	35165.	0000.0	0.					0.05
7296.0	35165.	0000.0	0.					0.05
7296.0	35165.	0000.0	0.					0.05
7296.0	35165.	0000.0	0.					0.05
7296.0	35165.	0000.0	0.					0.05
7296.0	35165.	0000.0	0.					0.05
7296.0	35165.	0000.0	0.					0.05
7296.0	35165.	0000.0	0.					0.05
7296.0	35165.	0000.0	0.					0.05
7296.0	35165.	0000.0	0.					0.05
7296.0	35165.	0000.0	0.					0.05
7296.0	35165.	0000.0	0.					0.05
7296.0	35165.	0000.0	0.					0.05
7296.0	35165.	0000.0	0.					0.05
7296.0	35165.	0000.0	0.					0.05
7296.0	35165.	0000.0	0.					0.05
7296.0	35165.	0000.0	0.					0.05
20200.0	35165.	000.0	18200.					0.05
20200.0	0.	000.0	18200.					0.05
20200.0	0.	00.0	18200.					0.05
20200.0	0.	00.0	18200.					0.05
20200.0	0.	00.0	18200.					0.05
20200.0	0.	00.0	18200.					0.05
	2.	2482.	HDTO	+2.0rad/s	23Jun02	9969.0	0.	
32754.0	0.0	8065.0						
32754.0	0.0	8065.0						
32754.0	38399.0	10957.4						

32754.0	38399.0	18648.1		
32754.0	38399.0	20437.6		
32754.0	38399.0	21398.0		
32754.0	38399.0	29587.5		
7296.0	38399.0	34253.9		
7296.0	38399.0	32431.6		
7296.0	38399.0	31404.6		
7296.0	38399.0	30465.7		
7296.0	38399.0	30035.9		
7296.0	38399.0	24119.0		
7296.0	38399.0	19559.0		
7296.0	38399.0	13308.1		
7296.0	38399.0	8193.3		
7296.0	38399.0	7327.0		
7296.0	38399.0	2890.4		
7296.0	38399.0	2412.0		
7296.0	38399.0	1882.5		
7296.0	38399.0	1710.0		
7296.0	38399.0	105.2		
7296.0	38399.0	7457.0		
7296.0	38399.0	13266.4		
20200.0	38399.0	12553.0		
20200.0	0.0	689.0		
20200.0	0.0	209.6		
20200.0	0.0	804.1		
20200.0	0.0	1188.0		
20200.0	0.0	43.3		
3.	1. Fan Blade-off 23Jun02		9952.0	0.
32754.0	26.2	85731.5		
32754.0	28.8	84797.5		
32754.0	51209.9	88632.6		
32754.0	51213.0	99272.2		
32754.0	52629.1	34737.4		
32754.0	48634.0	67083.0		
32754.0	59507.3	73659.4		
7296.0	59502.9	72541.2		
7296.0	59496.1	68421.1		
7296.0	59485.0	66149.3		
7296.0	59480.0	64197.9		
7296.0	59479.0	63312.5		
7296.0	59479.0	57282.0		
7296.0	59483.0	53600.0		
7296.0	59472.5	49783.8		
7296.0	59453.0	48128.4		
7296.0	59453.0	47574.0		
7296.0	54799.0	37282.6		
7296.0	58998.0	40099.6		
7296.0	59448.0	39381.1		
7296.0	59448.0	39007.0		
7296.0	59446.0	34992.3		
7296.0	59444.0	22561.0		
7296.0	59449.0	45112.5		
20200.0	43585.0	46394.1		
20200.0	5183.0	27977.0		
20200.0	25.0	16418.7		
20200.0	12.5	2213.8		
20200.0	5.0	6254.8		
20200.0	0.8	236.1		
3.	1. LPT Blade-off 23Feb02		9952.0	0.
32754.0	31.2	18001.8		
32754.0	33.9	18000.1		
32754.0	57974.0	24674.8		
32754.0	57977.2	42544.4		
32754.0	60147.9	49749.6		
32754.0	54058.0	58160.0		
32754.0	70718.5	79843.3		
7296.0	70721.0	76482.0		
7296.0	70723.0	63341.6		
7296.0	70730.0	56283.6		
7296.0	70733.0	50009.6		
7296.0	70733.0	47185.6		
7296.0	70723.0	11265.0		
7296.0	70700.0	20002.0		
7296.0	70652.6	42770.3		
7296.0	70630.0	52433.7		
7296.0	70636.0	53206.0		

7296.0	63547.9	46394.6		
7296.0	69994.6	51405.1		
7296.0	70688.7	51367.7		
7296.0	70690.0	51120.0		
7296.0	70703.0	48018.8		
7296.0	70716.0	18863.0		
7296.0	70723.0	33733.2		
20200.0	46435.7	36241.0		
20200.0	8005.3	18929.7		
20200.0	287.1	10958.0		
20200.0	142.9	2062.9		
20200.0	56.7	3922.1		
20200.0	12.3	154.2		
5.	1.80% hit, 2*1.5lb bird, 23Jun 02		9669.0	0.
41203.4	89.4	19884.3		
41208.7	96.7	19878.9		
41218.8	58585.0	24908.7		
41235.2	58579.0	38361.4		
41271.2	60790.7	36381.2		
41442.0	54482.0	40461.0		
43055.7	71558.4	55717.0		
26141.4	71547.7	54519.3		
26317.6	71528.1	49756.5		
26394.5	71496.3	47048.6		
26476.5	71479.8	44554.8		
26495.2	71476.2	43407.4		
26692.0	71430.0	27752.0		
26783.0	71413.0	23476.0		
26822.2	71345.6	25164.4		
26781.1	71285.0	25018.2		
26760.0	71295.0	24904.0		
26643.5	64079.8	19885.6		
26573.1	70665.8	21470.9		
26546.1	71376.7	21059.4		
26539.0	71379.0	20833.0		
26416.2	71408.0	20471.8		
25977.0	71476.0	19903.0		
25836.5	71506.8	32447.3		
38711.0	46562.0	31441.0		
30349.0	8159.2	9388.0		
28664.1	123.0	5240.3		
28657.0	62.2	1468.0		
28659.0	25.0	1834.1		
20224.3	4.9	78.4		
4.	1.80% hit, 2*1.5lb bird, 25Jun 02		9669.0	0.
44617.8	130.4	25744.0		
44616.1	140.4	25688.6		
44607.2	83876.1	31846.8		
44578.6	83851.6	48355.9		
44525.9	88808.4	44283.8		
44538.0	74569.0	52691.0		
58122.2	112897.5	70547.4		
32571.5	112868.2	69500.3		
32301.7	112819.2	65287.5		
32183.8	112744.5	62847.2		
32064.4	112709.5	60567.1		
32041.9	112702.3	59508.8		
31771.0	112670.0	44518.0		
31649.0	112605.0	38752.0		
31632.0	112476.6	37027.3		
31613.9	112351.2	31766.3		
31623.0	112314.0	30560.0		
31625.1	96002.0	22803.9		
31613.1	99610.8	26359.5		
31607.3	112348.6	27218.9		
31606.0	112352.0	27374.0		
31573.1	112389.9	28691.1		
31356.0	112474.0	34000.0		
31104.0	112489.0	43466.1		
43923.1	56644.0	41468.8		
33188.2	18233.2	10643.3		
31044.3	171.0	5736.3		
30978.7	84.3	2263.4		
30912.5	33.7	3455.5		
20229.0	7.4	137.2		

APPENDIX IV

Partial Output file for P0889 Shaft analysis program (Optimized Power Shaft)

TABLE 4: LCF-HCF ANALYSIS ; SHIGLEY FATIGUE FACTORS ; CYCLES = 20000 ; MAXIMUM RPM = 10188 ; MINIMUM RPM = 0.
 ; LOAD DESCRIPTION = HDT0 Fn=50188, .2 rad/sec, 23Jun02

PROGRAM P0889 ; VERSION: 5.00

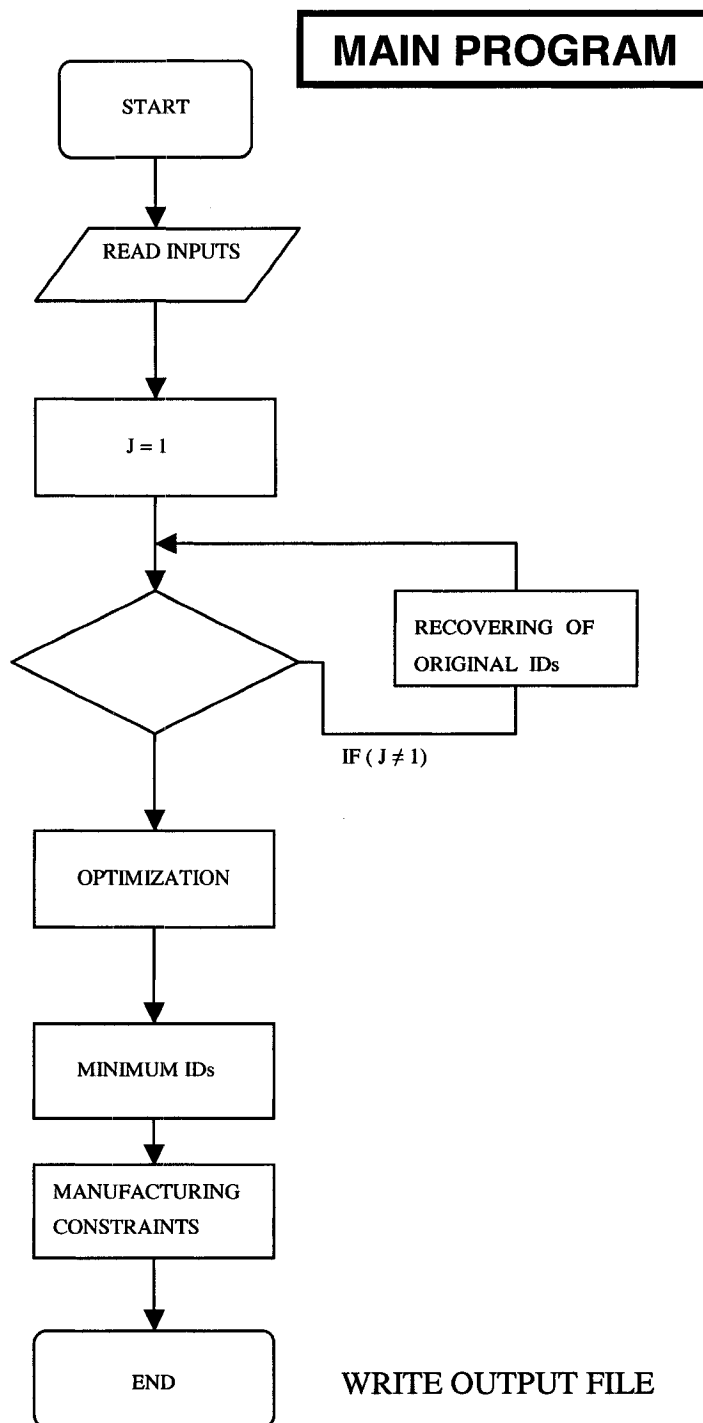
ENGINE MODEL: PW007A HDT0/Fn-REV
 PART NUMBER: LP ShaftVZil_E3ax
 SHAFT TYPE: 24K LCF 21/06/02

SECT NUMB (-)	AXIAL-FORCE		SHAFT-TORQUE		BENDING-MOMENT		AXIAL-STRESS		SHEAR-STRESS		LCF		C-F-STRESS		VON-MISES-STRESS		LCF BEND	HCF EQUIV	HCF EQUIV	HCF ALLOW	EQUIV ALLOW	MAXIMUM CYCLES	HOLE ANGLE (deg)
	MAX (lb)	MIN (lb)	MAX (lb-in)	MIN (lb-in)	LCF (lb-in)	HCF (lb-in)	MAX (ksi)	MIN (ksi)	MAX (ksi)	MIN (ksi)	BEND (ksi)	MAX (ksi)	MIN (ksi)	MAX (ksi)	MIN (ksi)	MAX (ksi)							
1	32754.	15714.	0.	0.	0.	831.	19.5	9.4	0.	0.	0.	1.3	0.	18.9	9.4	10.1	66.8	0.	2.5	11.0	.23	1000000.	-
2	32754.	15714.	0.	0.	0.	831.	51.8	24.8	0.	0.	0.	1.5	0.	51.0	24.8	31.1	86.1	2.0	8.4	17.7	.48	913763.	-
3	32754.	15714.	38399.	0.	0.	1132.	41.5	19.9	36.0	0.	0.	1.6	0.	74.5	19.9	62.5	92.2	2.1	19.6	23.3	.84	62125.	-
4	32754.	15714.	38399.	0.	0.	1932.	40.4	19.4	35.0	0.	0.	1.6	0.	72.4	19.4	60.5	90.5	3.5	17.9	19.8	.90	40572.	-
5	32754.	15714.	38399.	0.	0.	2180.	25.2	12.1	21.0	0.	0.	1.8	0.	43.8	12.1	39.6	79.8	2.4	11.3	13.6	.68	139930.	58.
6	32754.	15714.	38399.	0.	0.	2449.	41.5	19.9	34.9	0.	0.	1.7	0.	72.8	19.9	60.6	88.7	4.4	18.4	19.0	.97	25626.	-
7	32754.	15714.	38399.	0.	0.	3467.	28.7	13.8	23.9	0.	0.	1.7	0.	49.9	13.8	44.4	79.8	4.3	13.9	14.7	.85	53014.	63.
8	7296.	0.	38399.	0.	0.	3419.	7.1	0.	27.7	0.	0.	1.6	0.	48.4	0.	48.4	86.0	4.9	14.7	14.5	.90	43762.	61.
9	7296.	0.	38399.	0.	0.	3224.	6.7	0.	26.9	0.	0.	1.5	0.	47.0	0.	47.0	89.7	4.5	12.0	13.3	.91	45837.	-
10	7296.	0.	38399.	0.	0.	3115.	7.2	0.	28.9	0.	0.	1.5	0.	50.5	0.	50.5	101.7	4.7	18.4	26.3	.70	436770.	-
11	7296.	0.	38399.	0.	0.	3015.	6.2	0.	27.8	0.	0.	1.2	0.	48.6	0.	48.6	85.6	4.4	15.0	15.0	.85	58001.	58.
12	7296.	0.	38399.	0.	0.	2832.	8.6	0.	39.2	0.	0.	1.2	0.	68.3	0.	68.3	104.4	5.8	25.4	28.6	.89	63057.	-
13	7296.	0.	38399.	0.	0.	2339.	9.5	0.	43.2	0.	0.	1.2	0.	75.3	0.	75.3	105.9	5.3	33.7	38.3	.88	66829.	-
14	7296.	0.	38399.	0.	0.	1853.	10.5	0.	48.1	0.	0.	1.2	0.	83.9	0.	83.9	105.9	4.6	36.6	38.3	.95	30982.	-
15	7296.	0.	38399.	0.	0.	1187.	10.5	0.	48.1	0.	0.	1.2	0.	83.9	0.	83.9	105.9	3.0	35.5	38.3	.93	40409.	-
16	7296.	0.	38399.	0.	0.	642.	10.5	0.	48.1	0.	0.	1.2	0.	83.9	0.	83.9	105.9	1.6	34.8	38.3	.91	46902.	-
17	7296.	0.	38399.	0.	0.	549.	10.2	0.	50.9	0.	0.	1.0	0.	88.6	0.	88.6	105.1	1.5	35.4	36.4	.97	26034.	-
18	7296.	0.	38399.	0.	0.	104.	10.2	0.	50.9	0.	0.	1.0	0.	88.6	0.	88.6	101.5	.3	36.3	36.5	.99	21118.	-
19	7296.	0.	38399.	0.	0.	29.	6.9	0.	34.2	0.	0.	1.0	0.	59.6	0.	59.6	81.9	.1	16.7	10.4	.89	38934.	47.
20	7296.	0.	38399.	0.	0.	31.	10.2	0.	50.9	0.	0.	1.0	0.	88.6	0.	88.6	101.5	.1	36.3	36.6	.99	21182.	-
21	7296.	0.	38399.	0.	0.	49.	10.2	0.	50.9	0.	0.	1.0	0.	88.6	0.	88.6	102.9	.1	37.4	38.3	.98	23060.	-
22	7296.	0.	38399.	0.	0.	220.	7.2	0.	48.5	0.	0.	.6	0.	84.3	0.	84.3	101.8	.6	34.7	36.8	.94	33632.	-
23	7296.	0.	38399.	0.	0.	1026.	7.2	0.	48.5	0.	0.	.6	0.	84.3	0.	84.3	101.8	2.6	36.7	38.3	.96	30438.	-
24	7296.	0.	38399.	0.	0.	1645.	6.7	0.	45.1	0.	0.	.6	0.	78.4	0.	78.4	99.9	3.9	30.5	31.8	.96	30164.	-
25	20200.	18200.	38399.	0.	0.	1547.	17.0	15.3	41.0	0.	0.	.6	0.	72.9	15.3	64.3	91.8	3.3	20.3	22.1	.92	38907.	-
26	20200.	18200.	0.	0.	0.	110.	36.6	33.0	0.	0.	0.	.5	0.	36.4	33.0	4.3	64.6	.5	1.2	10.3	.12	1000000.	-
27	20200.	18200.	0.	0.	0.	40.	47.4	42.7	0.	0.	0.	.5	0.	47.1	42.7	25.7	73.4	.2	6.0	16.4	.36	793352.	90.
28	20200.	18200.	0.	0.	0.	95.	39.6	35.7	0.	0.	0.	.5	0.	39.3	35.7	21.3	81.7	.5	4.5	15.4	.29	1000000.	90.
29	20200.	18200.	0.	0.	0.	136.	28.6	25.8	0.	0.	0.	.4	0.	28.4	25.8	3.1	88.1	.6	1.2	17.8	.07	1000000.	-
30	20200.	18200.	0.	0.	0.	5.	33.5	30.2	0.	0.	0.	.4	0.	33.3	30.2	3.8	73.1	.0	.6	11.2	.05	1000000.	-

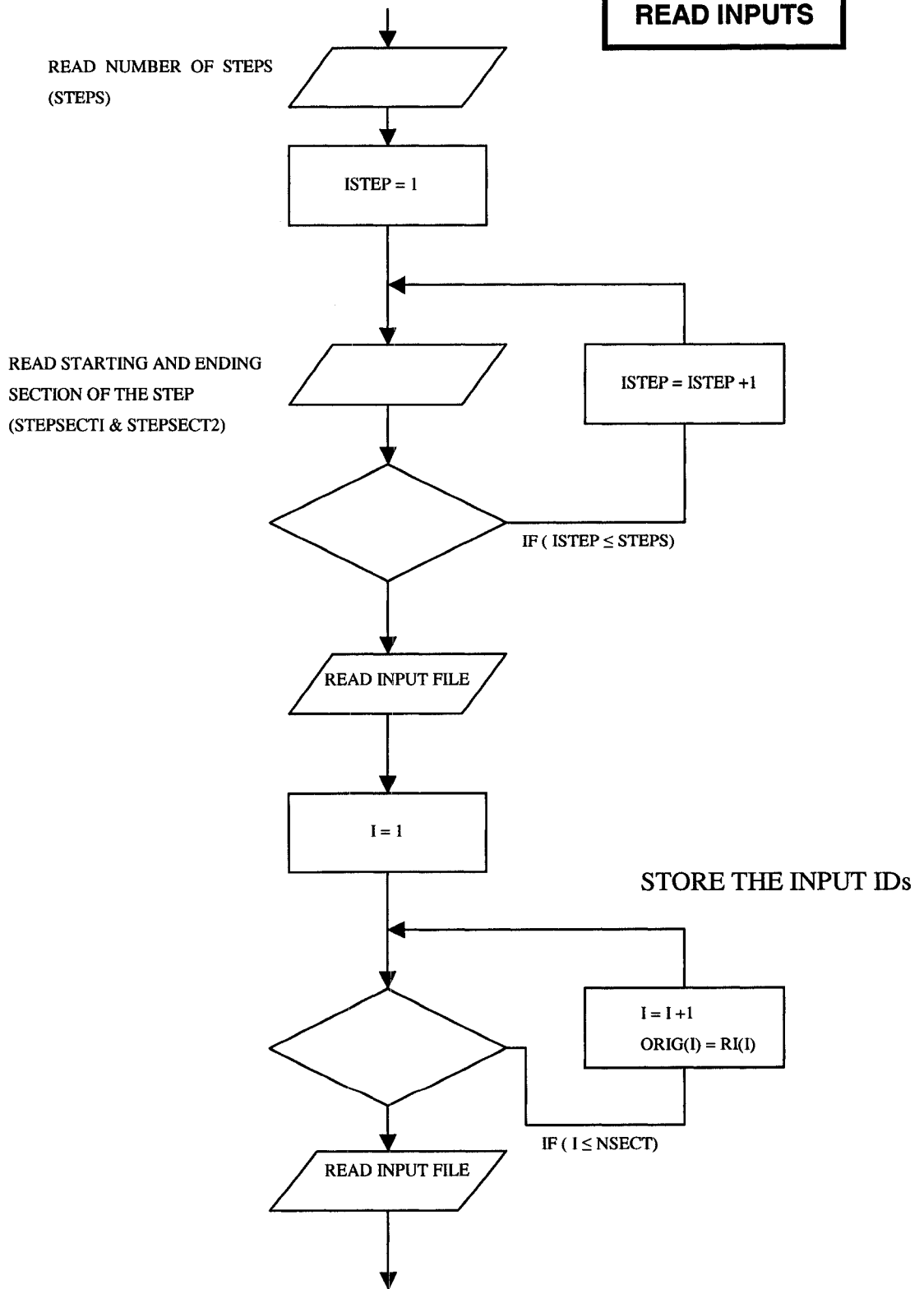
THE MAXIMUM LCF/HCF DESIGN FACTOR OF .99 OCCURRED AT SECTION 18
 THE MINIMUM CYCLIC LIFE OF 21118. CYCLES OCCURRED AT SECTION 18

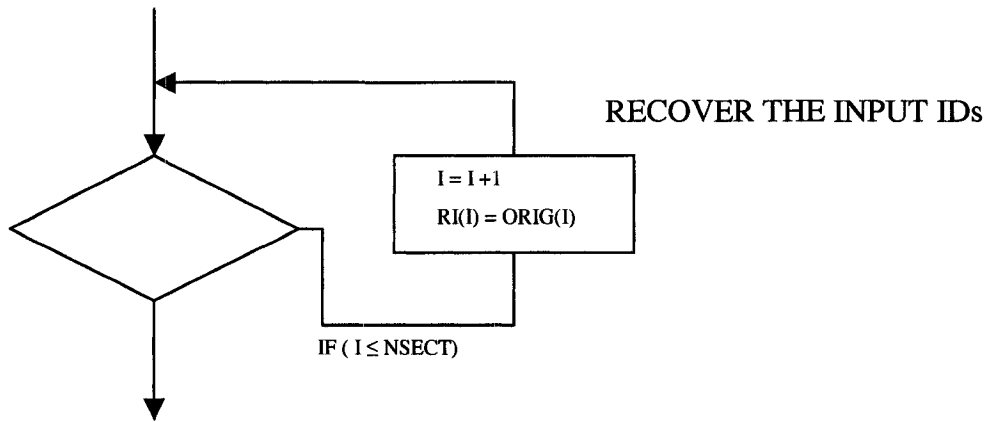
APPENDIX V

P0889opt Program Structure



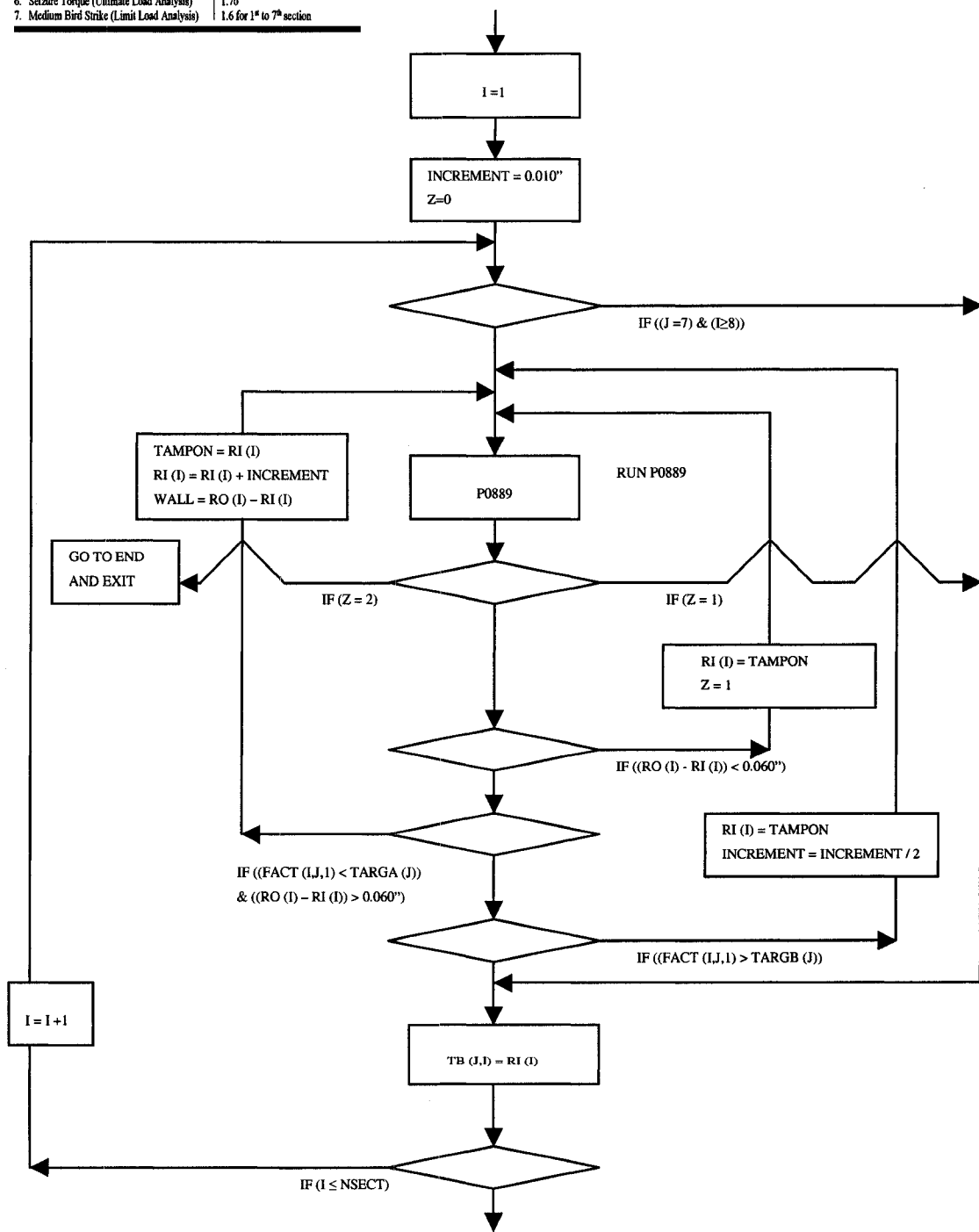
READ INPUTS



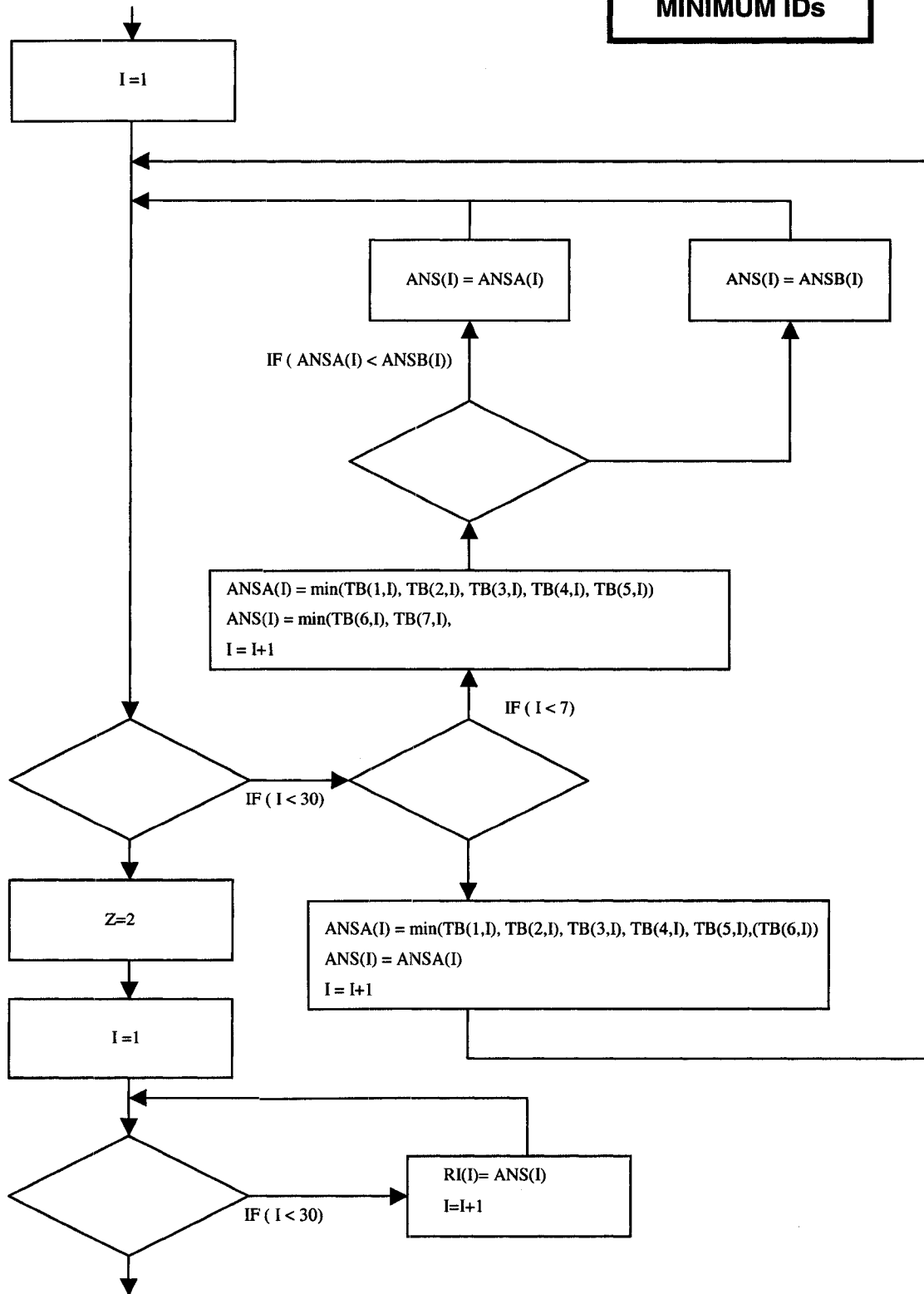
RECOVERING OF ORIGINAL IDs

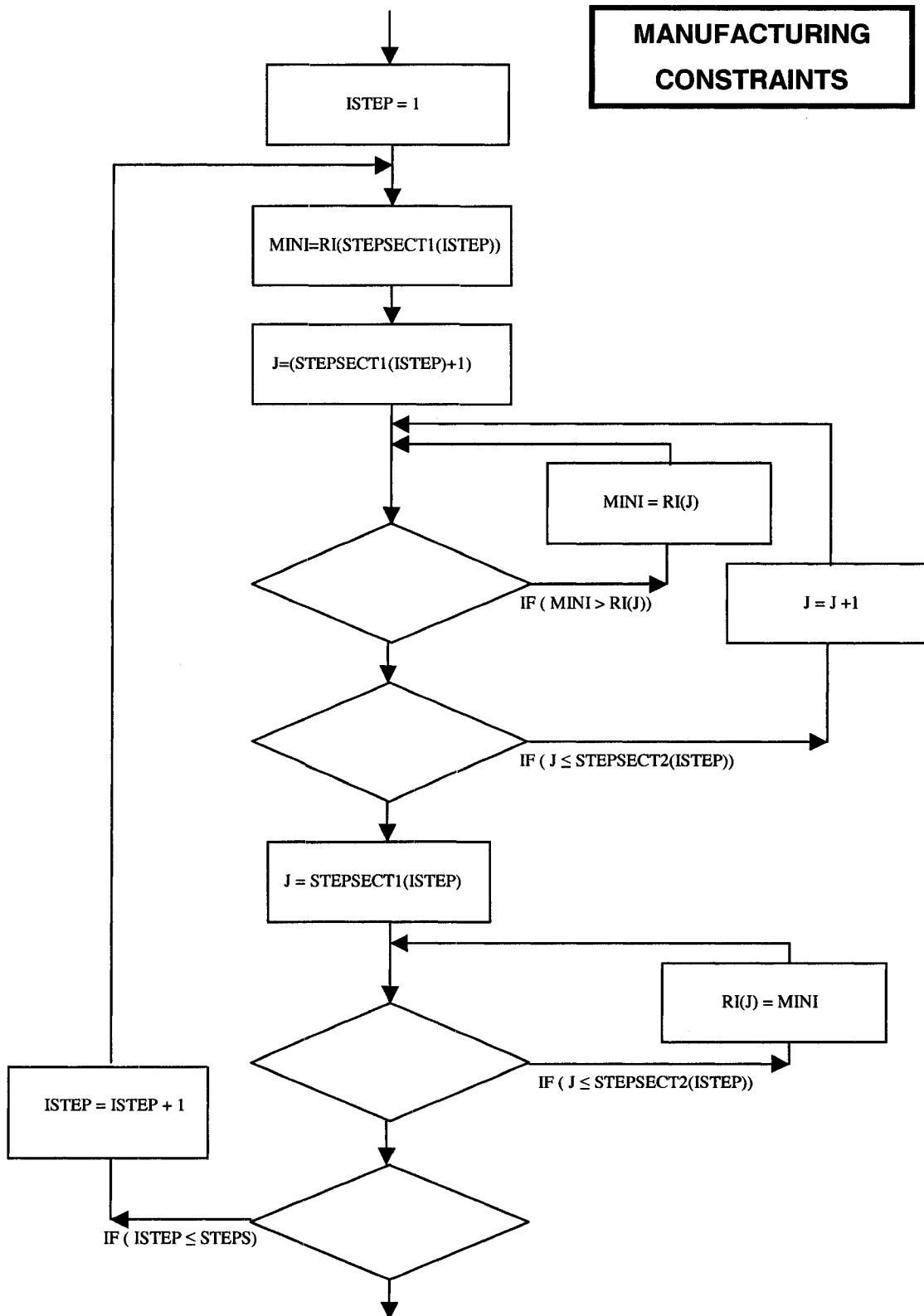
TYPES OF ANALYSIS	TARGETED VALUES PW307
1. LCF-HCF Analysis	1.0
2. Gyroscopic Precession	1.0
3. Fan Blade-Loss (Ultimate Load Analysis)	1.0
4. Large Bird Strike (Ultimate Load Analysis)	1.34
5. Turbine Blade-Loss (Ultimate Load Analysis)	1.34
6. Seizure Torque (Ultimate Load Analysis)	1.70
7. Medium Bird Strike (Limit Load Analysis)	1.6 for 1 st to 7 th section

OPTIMIZATION



MINIMUM IDs





APPENDIX VI

P0889opt Code

```
PROGRAM P0889OPT
C
C Program: P0889OPT
C Name: Geometry Optimizer for Shaft Strength Analysis Program
C
C P0889OPT Programmer: R. Grassi
C
C Description:
C
C IMPLICIT NONE
C
C include 'include'
C
C INTEGER I, J, Z
C
C REAL*8 TAMPON, INCREMENT, WALL, TB(1:7, 1:30), ORIG(1:30), ANS(1:30)
C
C REAL*8 TARGA(1:7), TARGB(1:7), ANSA(1:30), ANSB(1:30), MINI
C
C INTEGER STEPS, SEC1, SEC2, SEC3, SEC4, SEC5, SEC6
C
C TARGA(1) = 0.950
C TARGA(2) = 0.950
C TARGA(3) = 0.950
C TARGA(4) = 1.290
C TARGA(5) = 1.290
C TARGA(6) = 1.650
C TARGA(7) = 1.550
C
C TARGB(1) = 0.990
C TARGB(2) = 0.990
C TARGB(3) = 0.990
C TARGB(4) = 1.330
C TARGB(5) = 1.330
C TARGB(6) = 1.690
C TARGB(7) = 1.590
C
C TAMPON = 0
C
C VERSION = 5.00
C NUMAT = 0 ! initialize to ensure it starts at zero
```

C

```

WRITE(6,*) 'INPUT NUMBER OF STEPS : '
READ(5,100) STEPS
100 FORMAT(I1)
WRITE(6,*) 'ENTER THE STARTING SECTION FOR STEP1 : '
READ(5,110) SEC1
110 FORMAT(I2)
WRITE(6,*) 'ENTER THE ENDING SECTION FOR STEP1 : '
READ(5,120) SEC2
120 FORMAT(I2)
WRITE(6,*) 'ENTER THE STARTING SECTION FOR STEP2 : '
READ(5,130) SEC3
130 FORMAT(I2)
WRITE(6,*) 'ENTER THE ENDING SECTION FOR STEP2 : '
READ(5,140) SEC4
140 FORMAT(I2)
WRITE(6,*) 'ENTER THE STARTING SECTION FOR STEP3 : '
READ(5,150) SEC5
150 FORMAT(I2)
WRITE(6,*) 'ENTER THE ENDING SECTION FOR STEP3 : '
READ(5,160) SEC6
160 FORMAT(I2)

WRITE(6,*) 'ENTERED DATA : '
WRITE(6,*) 'NB OF STEPS=', STEPS
WRITE(6,*) 'STEP1= SEC. ', SEC1, ' TO SEC. ', SEC2
WRITE(6,*) 'STEP2= SEC. ', SEC3, ' TO SEC. ', SEC4
WRITE(6,*) 'STEP3= SEC. ', SEC5, ' TO SEC. ', SEC6

```

C

C Reading the p0889 input file
CALL READIN

C Store the values of original ID in memory

```

DO I=1,NSECT
    ORIG(I)= RI(I)
END DO

```

```

DO J=1,7

```

C For each analysis, what follows is repeated.

C

C Once the first analysis is done, the value of the IDs changes,
 therefore each
 C time we start over an analysis, we recover the original IDs of the
 input file

```

IF (J.NE.1) THEN
  DO I=1,NSECT
    RI(I)= ORIG(I)
  END DO
END IF

```

C For each section, what follows is repeated.
 C _____

```

DO I=1,NSECT

IF((J.EQ.7).AND.(I.GE.8)) THEN
  GO TO 399
END IF

```

C The value of the variable INCREMENT is defined.
 C The value of the variable Z is set to zero.

```

INCREMENT= 0.010

Z= 0

```

C Calculating stresses and life

```

398 IF ( JTYP .EQ. 1 ) THEN      ! Main Shaft Analysis
    CALL MSHAFT
ELSE
    WRITE(6,*) 'ERROR: INVALID ANALYSIS SHAFT TYPE = ',JTYP

```

```
        CALL KILLIT(' ')
    ENDIF
```

C Sends the program to the end.
C

```
        IF (Z.EQ.2) THEN
            GO TO 400
        END IF
```

C Sends the program to the next section.
C

```
        IF (Z.EQ.1) THEN
            GO TO 399
        END IF
```

C In case the wall thickness is less than 0.060" the program recovers
C the RI (interior radius) of the previous iteration and gives the
C variable Z the value of 1 which, after having re computed P0889 with
C the previous RI, will send the program to the next section.

```
        IF ((RO(I)-RI(I)).LT.0.060) THEN
            RI(I)= TAMPON
            Z= 1
            GO TO 398
        END IF
```

C If the value of the stress factor (Equiv/allow) is lower than TARGA
and
C the thickness of the wall is more than 0.060", the program will keep
C in memory RI in the variable TAMPON, increment RI by an amount
C that is stored in the variable INCREMENT and goes back to run P0889.

```
        IF ((FACT(I,J,1).LT.TARGA(J)).AND.((RO(I)-RI(I)).GE.0.060)) THEN
            TAMPON= RI(I)
            RI(I)= RI(I)+INCREMENT
```

```
WALL= RO(I)-RI(I)
```

```
GO TO 398
```

```
END IF
```

```
C In case the stress factor (Equiv/allow) is greater then TARGB, the  
C program recovers RI from the variable TAMPON, splits the value in  
C the variable INCREMENT in 2, and goes back to run P0889.
```

```
IF (FACT(I,J,1).GT.TARGB(J)) THEN
```

```
RI(I)= TAMPON
```

```
INCREMENT = INCREMENT / 2
```

```
GO TO 398
```

```
END IF
```

```
C The optimized ID for each section and each analisys are stored in  
C the array TB.
```

```
399     TB(J,I)= RI(I)
```

```
END DO
```

```
C _____
```

```
C  
C End of sections.
```

```
END DO
```

```
C _____
```

```
C  
C End of analysis.
```

```
C Printing on screen of optimized ID for each section and each
```

C analysis.

```

      DO I=1,30
          WRITE(6,79) TB(1,I),TB(2,I),TB(3,I),TB(4,I)
79  FORMAT(' ',F6.4,' ',F6.4,' ',F6.4,' ',F6.4)
      END DO

      DO I=1,30
          WRITE(6,76) TB(5,I),TB(6,I),TB(7,I)
76  FORMAT(' ',F6.4,' ',F6.4,' ',F6.4)
      END DO

```

C For each section we find the minimum ID of the IDs generated by the
 C analysis and we place them in the array ANS.
 C There is one exception for the sections going from 8 until the end,
 C the IDs of the analysis 7 are not taken in consideration.

```

      DO I=1,30

          IF (I.LE.7) THEN
C_____
          ANSA(I)=min(TB(1,I),TB(2,I),TB(3,I),TB(4,I),TB(5,I))
          ANSB(I)=min(TB(6,I),TB(7,I))

          IF (ANSA(I).LT.ANSB(I)) THEN
              ANS(I)=ANSA(I)
          ELSE
              ANS(I)=ANSB(I)
          END IF

C_____

          ELSE

          ANSA(I)=min(TB(1,I),TB(2,I),TB(3,I),TB(4,I),TB(5,I),TB(6,I))
          ANS(I)=ANSA(I)

```

```
END IF
```

```
WRITE(6,66) I,ANSA(I),ANSB(I),ANS(I)
```

```
66 FORMAT('Section ',I2,' ID ',F6.4,' ',F6.4,' ',F6.4)
```

```
END DO
```

```
DO I=1,30
```

```
WRITE(6,83) I, ANS(I)
```

```
83 FORMAT('Section ',I2,' ID ',F6.4)
```

```
END DO
```

C We place the minimum IDs from the array ANS in the array RI and run
 C P0889 for the last time to get the final answer. We give a value of
 C 2 to the variable Z in order for the program to go directly at the
 C end when the last calculation of P0889 is done.

```
Z=2
```

```
DO I=1,30
```

```
RI(I)= ANS(I)
```

```
END DO
```

C Find the minimum in each step and give that dimension to the rest of
 C the sections in within that step.

```
C_____
```

```
MINI = RI(SEC1)
```

```
DO J=(SEC1+1),SEC2
```

```
      IF (MINI .GT. RI(J)) THEN
          MINI = RI(J)
      END IF
  END DO

  DO J=SEC1, SEC2
      RI(J)=MINI
  END DO
```

C_____

```
      MINI = RI(SEC3)
  DO J=(SEC3+1), SEC4
      IF (MINI .GT. RI(J)) THEN
          MINI = RI(J)
      END IF
  END DO

  DO J=SEC3, SEC4
      RI(J)=MINI
  END DO
```

C_____

```
      MINI = RI(SEC5)
  DO J=(SEC5+1), SEC6
      IF (MINI .GT. RI(J)) THEN
          MINI = RI(J)
      END IF
  END DO

  DO J=SEC5, SEC6
      RI(J)=MINI
```

END DO

C_____

DO I=1,30

WRITE(6,13) I, RI(I)

13 FORMAT('Section ',I2,' ID ',F6.4)

END DO

GO TO 398

C_____

C Writing the p0889 output file

400 CALL WRITEOUT

CALL EXIT(0)

END

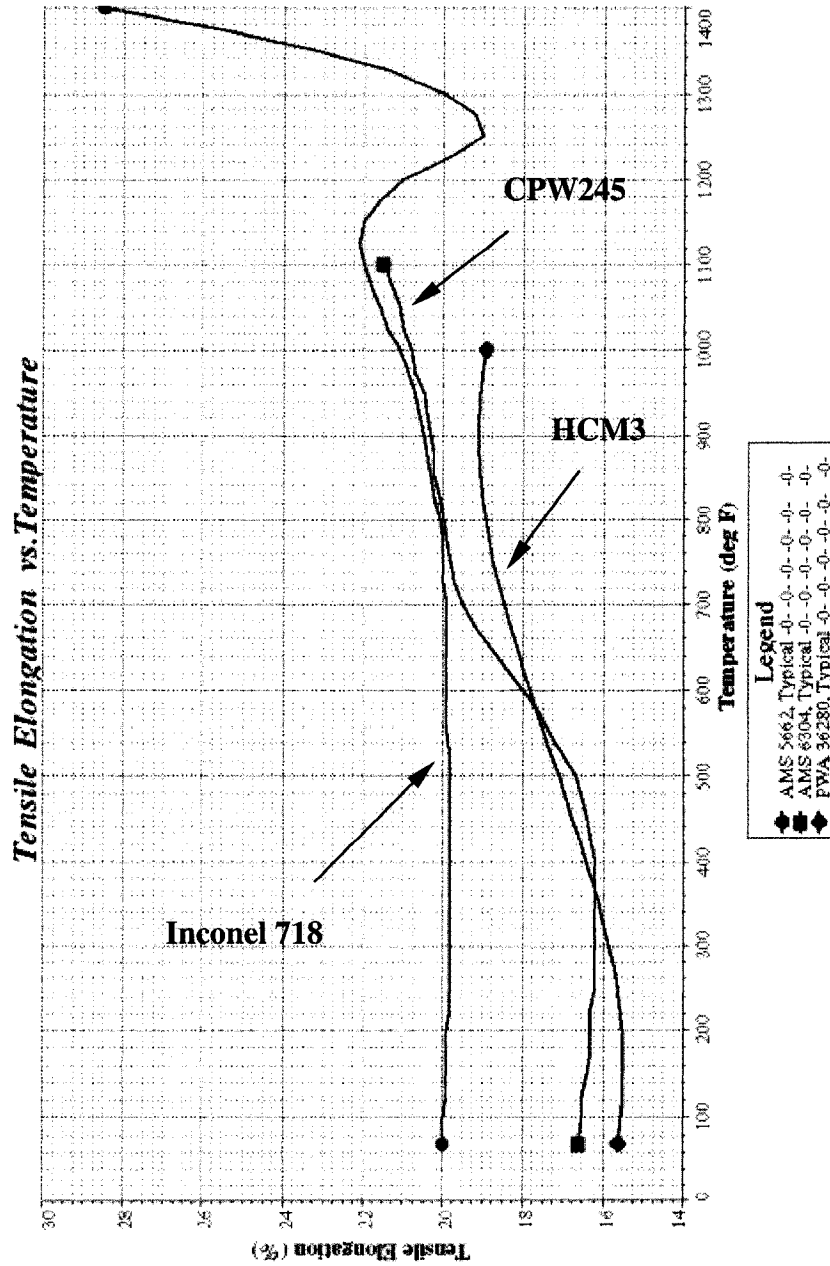
APPENDIX VII

Materials Graphs



-- For P&WC Internal Use Only --

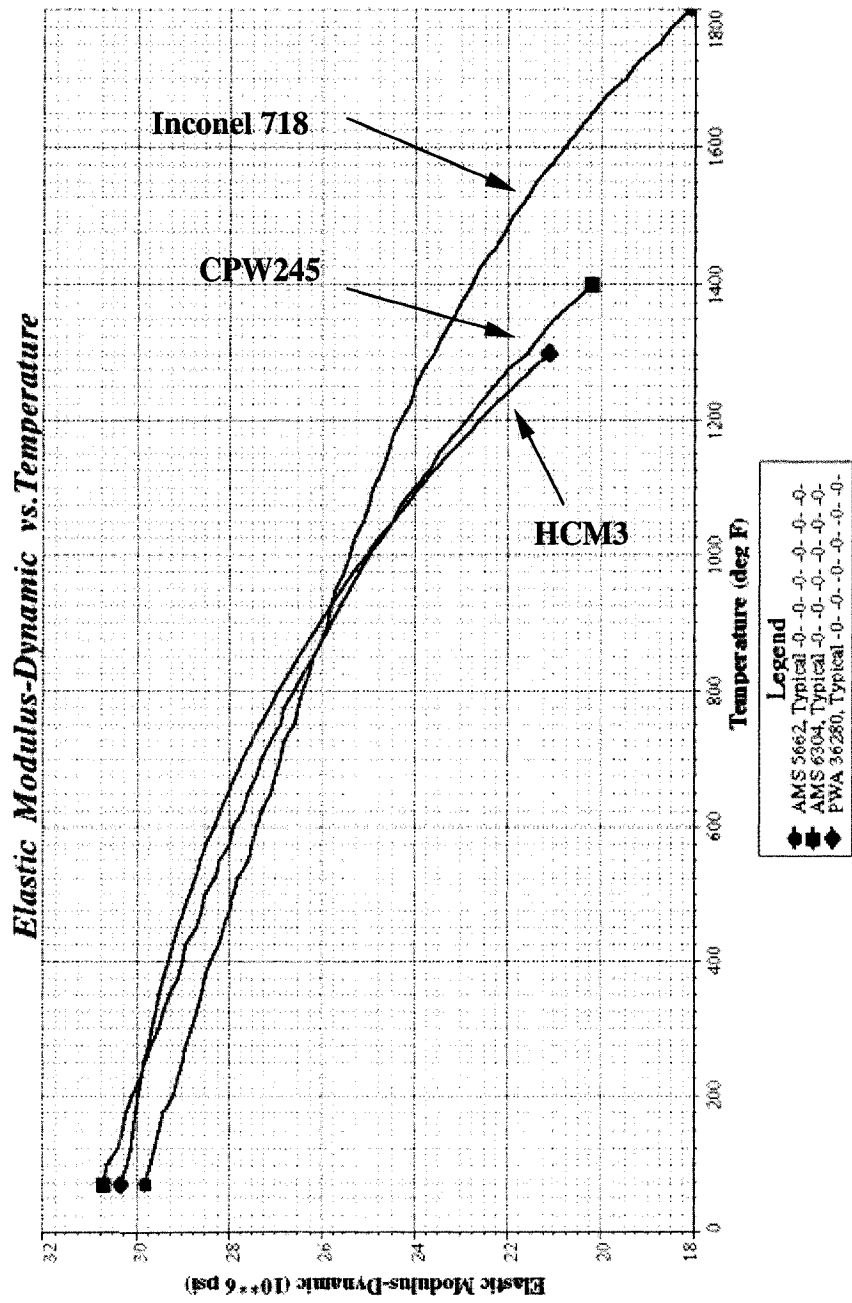
WARNING - This document is the property of United Technologies Corporation (UTC). You may not publish, use, copy or disclose the document or any information contained therein, in any form, without UTC's express written permission. Neither receipt nor possession of this document shall, from any source, constitute such permission. Processing, use, copying or disclosure by anyone without UTC's express written permission is not authorized and may result in criminal (and/or civil) liability.





... For P&WC Internal Use Only ...

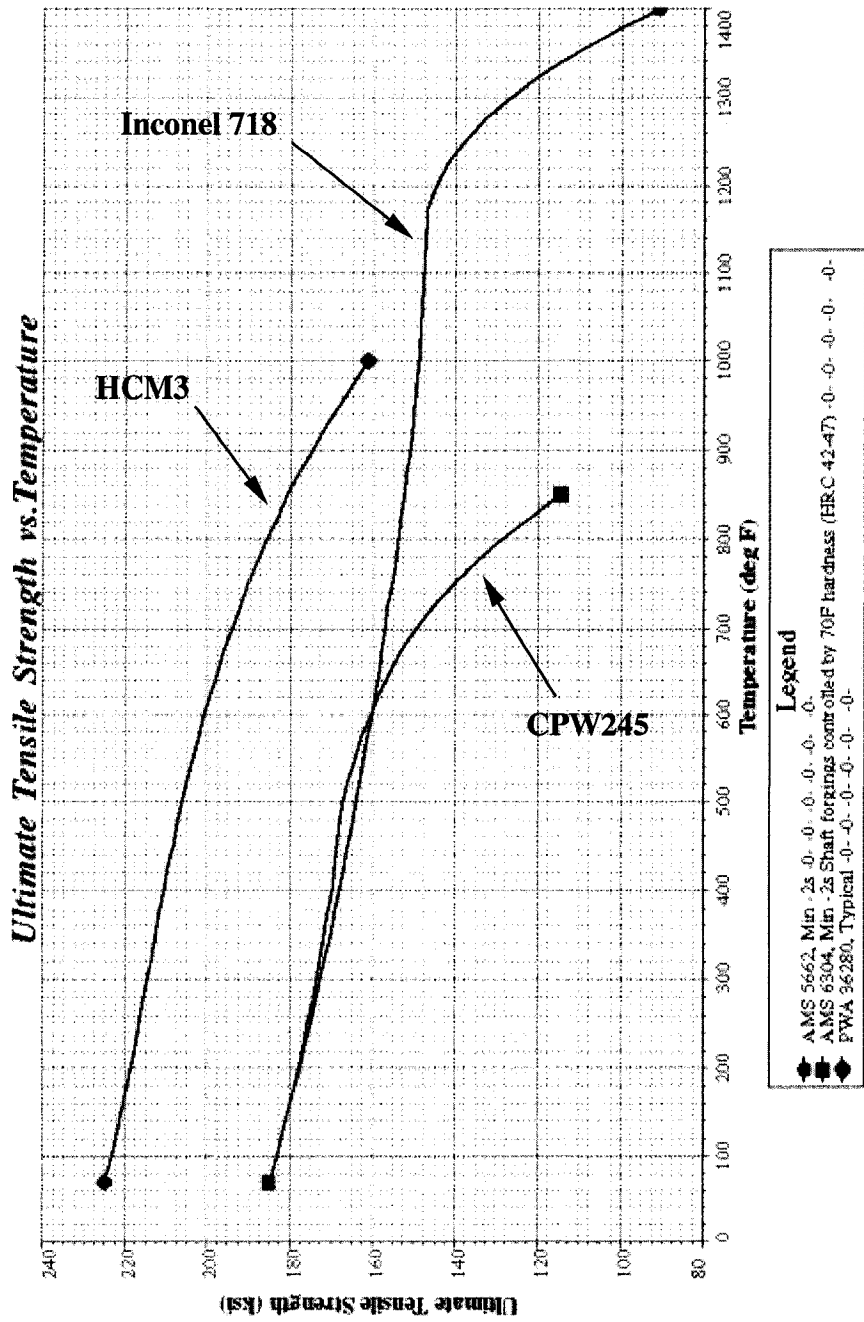
WARNING - This document is the property of United Technologies Corporation (UTC). You may not permit, use, copy or disclose this document or any information in it, for any purpose, including without limitation to design, manufacturing, operation, maintenance, repair, or other use, without the prior written permission of UTC. Any unauthorized use, copying, or disclosure by anyone without UTC's express written permission is not authorized and may result in criminal and/or civil liability.



-- For P&WC Internal Use Only --



WALSHRHC. This document is the property of Walsh Technologies Corporation (WTC). Verbatim or partial use, copy or disclosure of this document or any information contained herein is strictly prohibited without the prior written permission of Walsh Technologies Corporation. Reproduction or use of this document or any information contained herein is prohibited without the prior written permission of Walsh Technologies Corporation. Reproduction or use of this document or any information contained herein is prohibited without the prior written permission of Walsh Technologies Corporation. Reproduction or use of this document or any information contained herein is prohibited without the prior written permission of Walsh Technologies Corporation.



APPENDIX VIII

Partial Output file for P0571 Whirl speed analysis of coaxial shafts

ENERGY CALCULATIONS

TOTALS S.E. = .7365006E-06 K.E. = .7331516E-06 P.E. = .3464568E-05
 TOTALS BENDING S.E. = .5828313E-06 SHEAR S.E. = .1536692E-06

	PERCENT SHEAR	PERCENT BENDING	PERCENT TOTAL	PERCENT K.E.
SHAFT 1	10.7897	66.3745	77.1641	.102E+03
SHAFT 2	3.3362	6.2450	9.5812	-.725E+00
SHAFT 3	1.9959	.6049	2.6007	.254E+00
SHAFT 4	.2517	3.8965	4.1482	-.152E-04
SHAFT 5	.5459	.1018	.6477	-.127E+01

BEARING

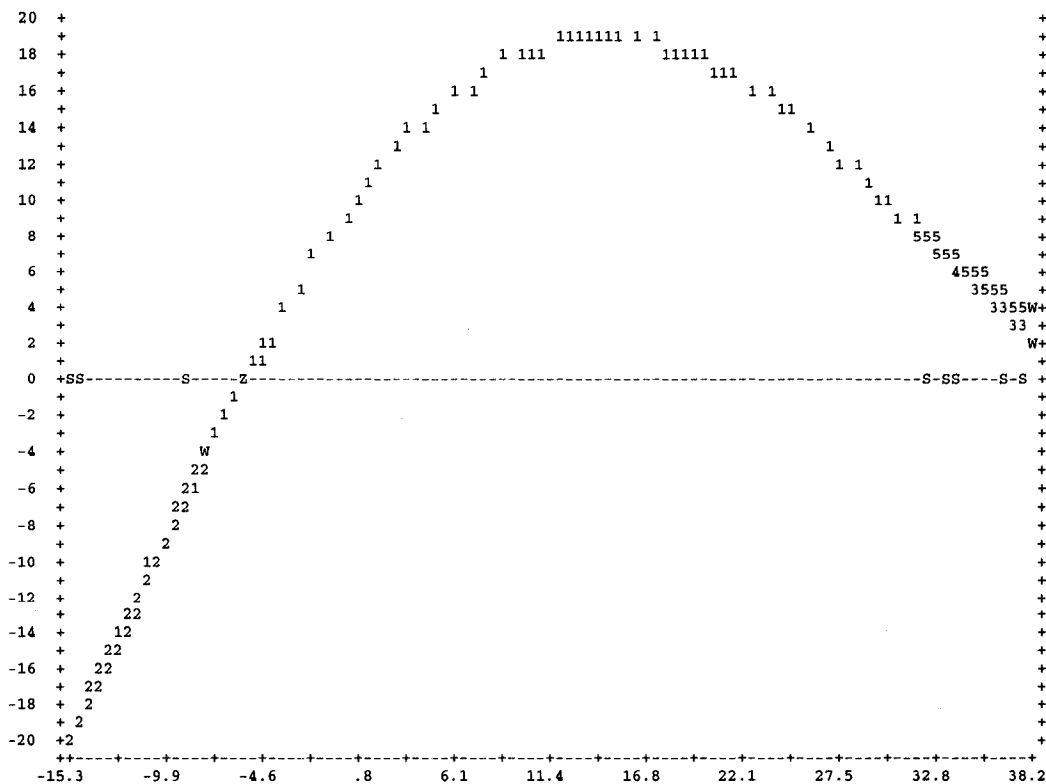
0 1	.0000	.0000	.0000	
0 8	.0000	.0000	.0000	
0 20	.0000	.0000	.0000	
0 11	3.1982	.0000	3.1982	
0 16	.7224	.0000	.7224	
2 9	.0002	.8073	.8076	
3 10	.0070	.6508	.6578	
4 12	.0093	.0000	.0093	
5 14	.0011	.3115	.3126	
6 15	.0001	.0000	.0001	
7 17	.0000	.0000	.0000	
13 18	.0036	.0474	.0510	
19 21	.0036	.0954	.0990	

0

1

Brg Stiffness = 350/150/150/100 fwd modes gear =100,000

5070. RPM



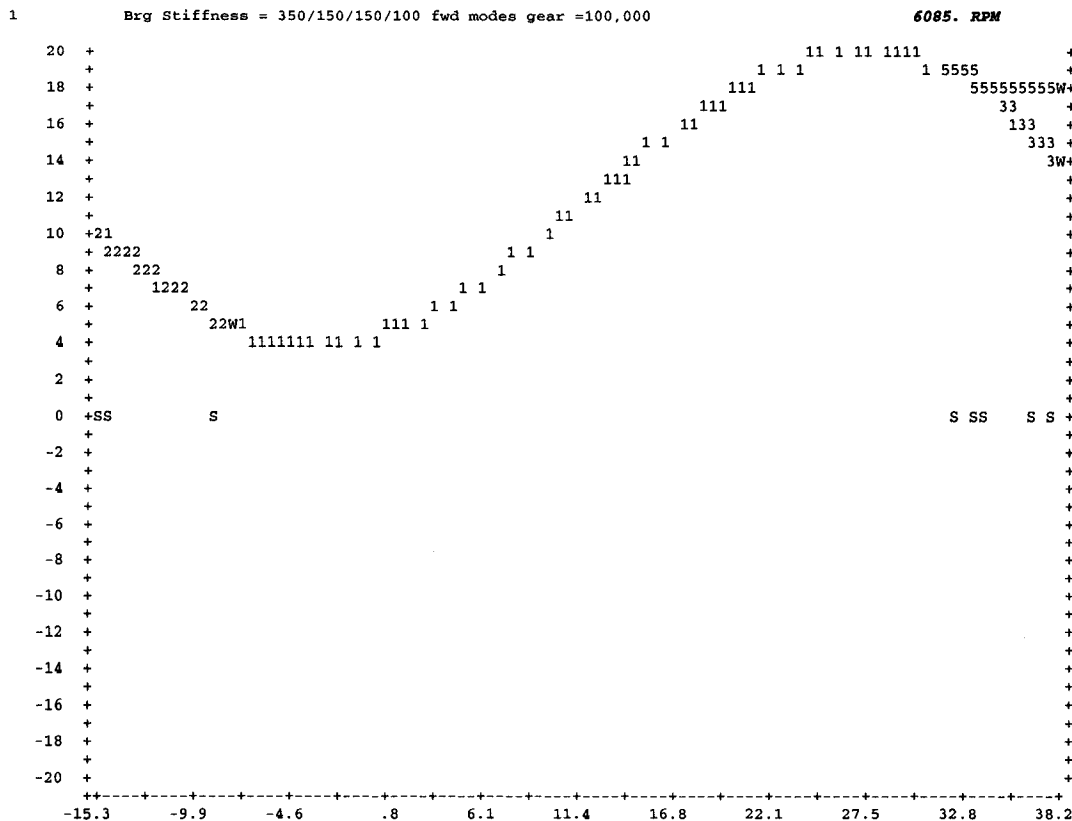
ENERGY DISTRIBUTION

TOTALS S.E. = .2719118E-05 K.E. = .2712213E-05 P.E. = -.6114259E-03
 PERCENTAGES

	SHEAR	BENDING	TOTAL	K.E.
SHAFT 1	.8699	27.6161	28.4860	14.8674
SHAFT 2	3.8495	3.2197	7.0692	76.7612
SHAFT 3	.7037	.8232	1.5269	.0995
SHAFT 4	.0558	1.0887	1.1444	.0002
SHAFT 5	.0239	.0092	.0332	8.2718
BEARING				
0 1	.0029	.0000	.0029	
0 8	.0029	.0000	.0029	
0 20	.0005	.0000	.0005	
0 11	48.2914	.0000	48.2915	
0 16	12.4280	.0000	12.4280	
2 9	.0008	.7513	.7521	
3 10	.0010	.1895	.1905	
4 12	.0003	.0000	.0003	
5 14	.0005	.0425	.0430	
6 15	.0001	.0000	.0001	
7 17	.0000	.0000	.0000	
13 18	.0008	.0184	.0192	
19 21	.0008	.0086	.0094	

Strain energy on shaft: Total = 38.2534%
The strain energy on the power shaft is less then 50% for the first mode.

Strain energy on the bearings



LENERGY DISTRIBUTION
 0TOTALS S.E. = .1066594E-05 K.E. = .1066182E-05 P.E. = .6078030E-03
 0PERCENTAGES

	SHEAR	BENDING	TOTAL	K.E.
SHAFT 1	1.1041	8.9015	10.0055	7.5465
SHAFT 2	.5493	.2294	.7787	15.6511
SHAFT 3	2.7394	3.2932	6.0326	.6754
SHAFT 4	.4988	2.4468	2.9456	.0008
SHAFT 5	.2647	.0135	.2782	76.1282
BEARING				
0 1	.0002	.0000	.0002	
0 8	.0002	.0000	.0002	
0 20	.0000	.0000	.0000	
0 11	12.8411	.0000	12.8411	
0 16	66.7547	.0000	66.7547	
2 9	.0004	.0858	.0862	
3 10	.0007	.1503	.1511	
4 12	.0000	.0000	.0000	
5 14	.0011	.0543	.0554	
6 15	.0008	.0000	.0008	

Strain energy on shaft: Total = 20.0406%
The strain energy on the power shaft is less then 50% for the second mode.

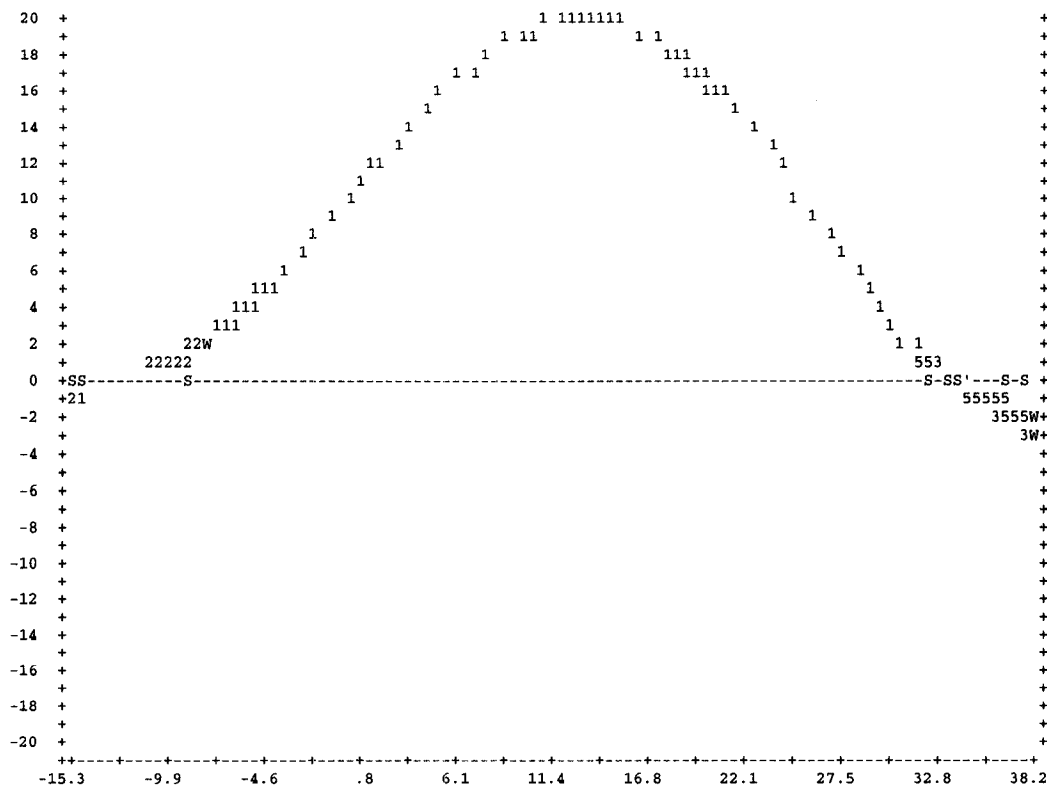
Strain energy on the bearings

```

7 17 .0000 .0000 .0000
13 18 .0071 .0469 .0540
19 21 .0071 .0078 .0149
    
```

1 Brg Stiffness = 350/150/150/100 fwd modes gear =100,000

13691. RPM

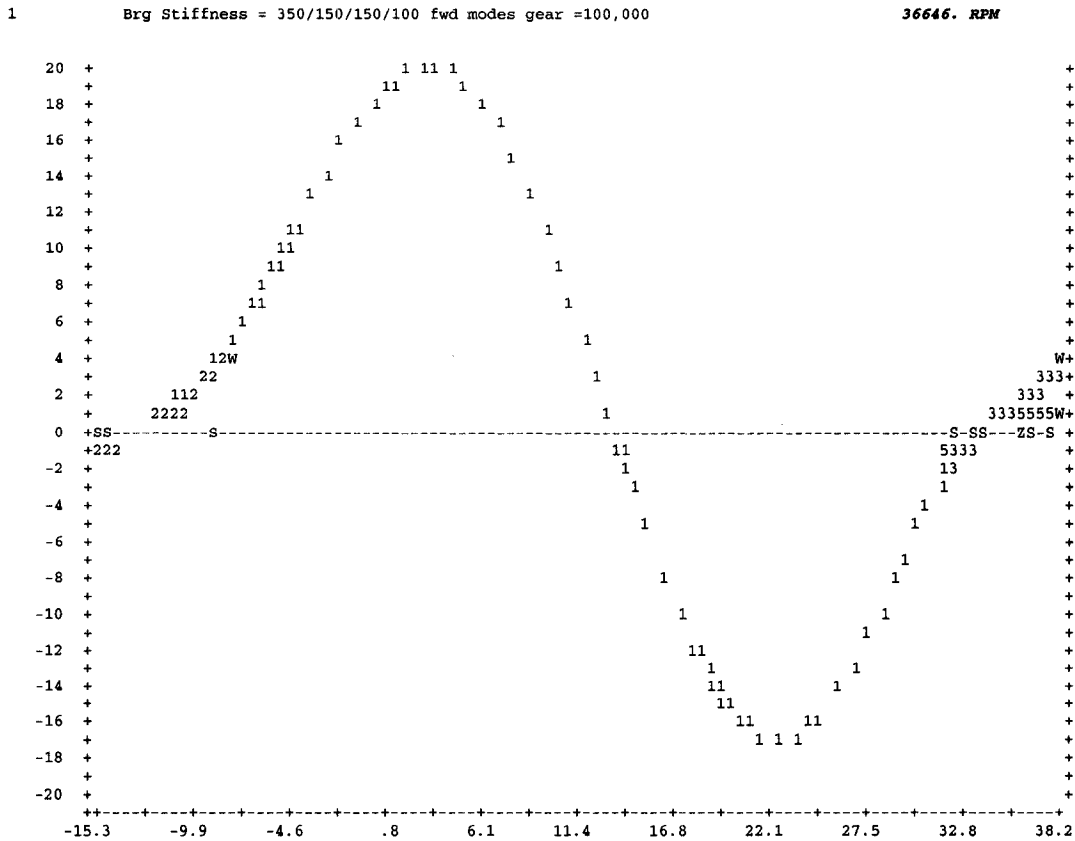


ENERGY DISTRIBUTION
 OTOTALS S.E. = .5098744E-06 K.E. = .5087223E-06 P.E. = .7321757E-05
 OPERCENTAGES

	SHEAR	BENDING	TOTAL	K.E.
SHAFT 1	7.0003	71.1016	78.1019	*****
SHAFT 2	1.0196	3.2007	4.2203	-6.9544
SHAFT 3	1.9343	.4478	2.3821	.1953
SHAFT 4	.2302	3.2087	3.4389	.0000
SHAFT 5	.3335	.0853	.4188	-7.9541
BEARING				
0 1	.0000	.0000	.0000	
0 8	.0000	.0000	.0000	
0 20	.0000	.0000	.0000	
0 11	5.7186	.0000	5.7186	
0 16	4.0655	.0000	4.0655	
2 9	.0008	.2629	.2637	
3 10	.0044	.8971	.9015	
4 12	.0088	.0000	.0088	
5 14	.0018	.3522	.3541	
6 15	.0001	.0000	.0001	
7 17	.0000	.0000	.0000	
13 18	.0033	.0386	.0419	
19 21	.0033	.0805	.0838	

Strain energy on shaft: Total = 88.562
 The engine is not supposed to reach the third mode therefore, even if the strain energy is over 50% it does not matter.

Strain energy on the bearings



ENERGY DISTRIBUTION
 OTOTALS S.E. = .7365006E-06 K.E. = .7331516E-06 P.E. = .3464568E-05
 OPERCENTAGES

	SHEAR	BENDING	TOTAL	K.E.
SHAFT 1	10.7897	66.3745	77.1641	*****
SHAFT 2	3.3362	6.2450	9.5812	-.7249
SHAFT 3	1.9959	.6049	2.6007	.2540
SHAFT 4	.2517	3.8965	4.1482	.0000
SHAFT 5	.5459	.1018	.6477	-1.2714
BEARING				
0 1	.0000	.0000	.0000	
0 8	.0000	.0000	.0000	
0 20	.0000	.0000	.0000	
0 11	3.1982	.0000	3.1982	
0 16	.7224	.0000	.7224	
2 9	.0002	.8073	.8076	
3 10	.0070	.6508	.6578	
4 12	.0093	.0000	.0093	
5 14	.0011	.3115	.3126	
6 15	.0001	.0000	.0001	
7 17	.0000	.0000	.0000	
13 18	.0036	.0474	.0510	
19 21	.0036	.0954	.0990	

1 Brg Stiffness = 350/150/150/100 fwd modes gear =100,000

RPM = 36646. DRPM = 1000. RPML = 40000. RPMA = 1.000 NO. OF MODES = 4.

PRECESSION FACTORS VS SPEED

SPEED	1000.00
SHAFT 1	1.0000
SHAFT 2	1.0000
SHAFT 3	1.0000
SHAFT 4	1.0000
SHAFT 5	1.0000

BEARING STIFFNESSES			BEARING ISOTROPIC FACTOR	
RADIAL	ANGULAR	NODES	RADIAL	ANGULAR
.10000E+01	.10000E+01	19 21	.0000	.0000

.10000E+01	.10000E+01	19	21	.0000	.0000
.10000E+01	.10000E+01	19	21	.0000	.0000
.20000E+06	.10000E+01	19	21	.0000	.0000
.11500E+06	.10000E+01	19	21	.0000	.0000
.10000E+10	.10000E+08	19	21	.0000	.0000
.10000E+10	.10000E+08	19	21	.0000	.0000
.10000E+10	.00000E+00	19	21	.0000	.0000
.10000E+10	.10000E+08	19	21	.0000	.0000
.10000E+10	.00000E+00	19	21	.0000	.0000
.10000E+10	.00000E+00	19	21	.0000	.0000
.10000E+10	.10000E+10	19	21	.0000	.0000
.10000E+10	.10000E+10	19	21	.0000	.0000

0

RPM	DETERMINANT		PRECESSION FACTORS				
36646.48	-.46283E-01	73	1.00	1.00	1.00	1.00	1.00
36746.48	-.48809E-01	73	1.00	1.00	1.00	1.00	1.00
37746.48	-.81700E-01	73	1.00	1.00	1.00	1.00	1.00
37846.48	-.85884E-01	73	1.00	1.00	1.00	1.00	1.00
38846.48	-.13945E-01	74	1.00	1.00	1.00	1.00	1.00
38946.48	-.14616E-01	74	1.00	1.00	1.00	1.00	1.00
39946.48	-.23070E-01	74	1.00	1.00	1.00	1.00	1.00
40046.48	-.24115E-01	74	1.00	1.00	1.00	1.00	1.00

0

APPENDIX IX

Output File for P0889opt Automated Shaft analysis program (Input file used was the one of the actual power shaft)

```

ENTERED DATA :
NB OF STEPS= 3
STEP 1 = SECT 11 TO SECT 16
STEP 2 = SECT 17 TO SECT 21
STEP 3 = SECT 22 TO SECT 27
1.3275 1.3275 1.3275 1.3200
1.3130 1.3130 1.3130 1.3030
1.3630 1.3705 1.3730 1.3580
1.3580 1.3730 1.3680 1.3555
1.4480 1.4705 1.4830 1.4930
1.3930 1.4130 1.4055 1.4130
1.4080 1.4380 1.4330 1.4430
1.3580 1.3930 1.3780 1.3930
1.3080 1.3555 1.3330 1.3630
1.3380 1.3530 1.3305 1.3530
1.1800 1.2300 1.2100 1.2600
1.1600 1.1850 1.1450 1.1825
1.1600 1.1750 1.1500 1.1750
1.1500 1.1625 1.1500 1.1650
1.1525 1.1625 1.1450 1.1675
1.1550 1.1625 1.1750 1.1687
1.0550 1.0650 1.0825 1.0750
1.0500 1.0600 1.0900 1.0825
1.0700 1.0850 1.1450 1.1300
1.0500 1.0600 1.0950 1.0775
1.0550 1.0650 1.0950 1.0775
.7725 .7925 .8575 .8275
.7625 .7925 .8225 .8375
.7625 .8025 .8025 .8325
.7800 .8250 .8300 .8650
.8030 .8030 .8030 .7980
.8175 .8175 .8175 .8100
.8025 .8025 .8025 .8025
.7155 .7155 .7155 .7155
.7340 .7340 .7340 .7340
1.3275 1.3275 1.3275
1.3130 1.3130 1.3130
1.3730 1.3730 1.3730
1.3730 1.3730 1.3730
1.4930 1.4905 1.4930
1.4130 1.4130 1.4130
1.4430 1.4405 1.4355
1.3930 1.3905 1.2030
1.3630 1.3518 1.2030
1.1530 1.1443 1.2030
1.2600 1.2400 1.1400
1.1825 1.1650 1.1400
1.1850 1.1675 1.1400
1.1712 1.1575 1.1400
1.1625 1.1575 1.1400
1.1575 1.1575 1.1400
1.0600 1.0600 1.0350
1.0675 1.0700 1.0350
1.1150 1.1175 1.0350
1.0575 1.0625 1.0350
1.0575 1.0625 1.0350
.7925 .7925 .7325
.8175 .7925 .7325
.8225 .7925 .7325
.8750 .8500 .5700
.8030 .8030 .7230
.8175 .8175 .7475
.8025 .8025 .7425
.7155 .7155 .6255
.7340 .7340 .6740
Section 1 ID 1.3200 1.3275 1.3200
Section 2 ID 1.3030 1.3130 1.3030
Section 3 ID 1.3580 1.3730 1.3580
Section 4 ID 1.3555 1.3730 1.3555
Section 5 ID 1.4480 1.4905 1.4480
Section 6 ID 1.3930 1.4130 1.3930
Section 7 ID 1.4080 1.4355 1.4080
Section 8 ID 1.3580 .0000 1.3580
Section 9 ID 1.3080 .0000 1.3080
Section 10 ID 1.3305 .0000 1.3305
Section 11 ID 1.1800 .0000 1.1800
Section 12 ID 1.1450 .0000 1.1450
Section 13 ID 1.1500 .0000 1.1500
Section 14 ID 1.1500 .0000 1.1500
Section 15 ID 1.1525 .0000 1.1525
Section 16 ID 1.1550 .0000 1.1550
Section 17 ID 1.0550 .0000 1.0550
Section 18 ID 1.0500 .0000 1.0500
Section 19 ID 1.0700 .0000 1.0700
Section 20 ID 1.0500 .0000 1.0500
Section 21 ID 1.0550 .0000 1.0550
Section 22 ID .7725 .0000 .7725
Section 23 ID .7625 .0000 .7625
Section 24 ID .7625 .0000 .7625
Section 25 ID .7800 .0000 .7800
Section 26 ID .7980 .0000 .7980
Section 27 ID .8100 .0000 .8100
Section 28 ID .8025 .0000 .8025
Section 29 ID .7155 .0000 .7155
Section 30 ID .7340 .0000 .7340
Section 1 ID 1.3200
Section 2 ID 1.3030
Section 3 ID 1.3980
Section 4 ID 1.3555
Section 5 ID 1.4480
Section 6 ID 1.3930
Section 7 ID 1.4080
Section 8 ID 1.3580
Section 9 ID 1.3080
Section 10 ID 1.3305
Section 11 ID 1.1800
Section 12 ID 1.1450
Section 13 ID 1.1500
Section 14 ID 1.1500
Section 15 ID 1.1525
Section 16 ID 1.1550
Section 17 ID 1.0550
Section 18 ID 1.0500
Section 19 ID 1.0700
Section 20 ID 1.0500
Section 21 ID 1.0550

```


Table with columns: NUMB, OUTER TEMP, ULTIM STRESS, YIELD STRESS, ENDUR, S-N-CURVE-CORNERS, REFR, NOTCH RADIUS, FACTORS, MAT-L, POISSON, INNER, ULTIM, PROP, FATIGUE-CONCENTRATION-FACTORS, LCF-STRESS. Rows 23-30.

AXIAL SLOT; SHOULDER DIAMETER = DIAMETER TO BOTTOM OF SLOT; # OF HOLES = # OF SLOTS; HOLE DIAMETER = SLOT WIDTH

TABLE 3: SECTION MATERIAL DESCRIPTION

Table with columns: SECT, OUTER TEMP, ULTIM STRESS, YIELD STRESS, ENDUR, S-N-CURVE-CORNERS, REFR, NOTCH RADIUS, FACTORS, MAT-L, POISSON, INNER, ULTIM, PROP, FATIGUE-CONCENTRATION-FACTORS, LCF-STRESS. Rows 1-30.

TABLE 4: LCF-HCF ANALYSIS; SHIGLEY FATIGUE FACTORS; CYCLES = 20000; MAXIMUM RPM = 10188; MINIMUM RPM = 0.

Table with columns: SECT, AXIAL-FORCE, SHAFT-TORQUE, BENDING-MOMENT, AXIAL-STRESS, SHEAR-STRESS, LCF, C-F-STRESS, VON-MISES-STRESS, LCF, HCF, HCF, HCF, EQUIV, MAXIMUM, HOLE. Rows 1-30.

THE MAXIMUM LCF/HCF DESIGN FACTOR OF .97 OCCURRED AT SECTION 6 THE MINIMUM CYCLIC LIFE OF 24536 CYCLES OCCURRED AT SECTION 5

TABLE 5: LCF-HCF ANALYSIS; SHIGLEY FATIGUE FACTORS; CYCLES = 20000; MAXIMUM RPM = 9949; MINIMUM RPM = 0.

Table with columns: SECT, AXIAL-FORCE, SHAFT-TORQUE, BENDING-MOMENT, AXIAL-STRESS, SHEAR-STRESS, LCF, C-F-STRESS, VON-MISES-STRESS, LCF, HCF, HCF, HCF, EQUIV, MAXIMUM, HOLE. Rows 1-14.

Table with columns for section number, axial force, shaft torque, bending moment, axial stress, shear stress, bending stress, centrifugal stress, v-mises stress, cyc-bend stress, equiv stress, allow stress, max life, max rate, and hole angle. Rows 15-30 show stress data for various sections.

THE MAXIMUM LCF/MCF DESIGN FACTOR OF .87 OCCURRED AT SECTION 20
THE MINIMUM CYCLIC LIFE OF 60362. CYCLES OCCURRED AT SECTION 5

ITABLE 6: GYROSCOPIC PRESSION ; SHIGLEY FATIGUE FACTORS ; CYCLES = 2482 ; MAXIMUM RPM = 9969 ; MINIMUM RPM = 0.
LOAD DESCRIPTION = HOTO +2.0rad/# 23Jun02

PROGRAM P0889 ; VERSION: 5.00

ENGINE MODEL: PW307A HOTO/Fn-REV
PART NUMBER: LP ShaftV21L33az
SHAFT TYPE: 24K LCF 21/06/02

Table with columns for sect numb, axial force, shaft torque, bending moment, axial stress, shear stress, bending stress, centrifugal stress, v-mises stress, cyc-bend stress, equiv stress, allow stress, max life, max rate, and hole angle. Rows 1-30 show stress data for various sections.

THE MAXIMUM LCF/MCF DESIGN FACTOR OF .97 OCCURRED AT SECTION 10
THE MINIMUM CYCLIC LIFE OF 3108. CYCLES OCCURRED AT SECTION 10
THE MAXIMUM ALLOWABLE GYROSCOPIC PRESSION OCCURRED AT SECTION 10 AND IS 1.058 TIMES THE NOMINAL RATE

ITABLE 7: COMPRESSOR BLADE-LOSS ; CYCLES = 1 ; MAXIMUM RPM = 9952 ; MINIMUM RPM = 0.
LOAD DESCRIPTION = Fan Blade-off 23Jun02

PROGRAM P0889 ; VERSION: 5.00

ENGINE MODEL: PW307A HOTO/Fn-REV
PART NUMBER: LP ShaftV21L33az
SHAFT TYPE: 24K LCF 21/06/02

Table with columns for sect numb, axial force, shaft torque, bending moment, axial stress, shear stress, bending stress, centrifugal stress, plastic stress factor, max-plast stress, ultimate stress, max-plast yield, and max-plast ultimate. Rows 1-30 show stress data for various sections.

THE MAXIMUM (PLASTIC STRESS / ULT. STRESS) FACTOR OF 1.33 OCCURRED AT SECTION 1 AND THE STRESS IS 207.4 KSI
THE MAXIMUM (PLASTIC STRESS / YIELD STRESS) FACTOR OF 1.69 OCCURRED AT SECTION 1 AND THE STRESS IS 207.4 KSI

ITABLE 8: COMPRESSOR BLADE-LOSS ; CYCLES = 1 ; MAXIMUM RPM = 9952 ; MINIMUM RPM = 0.
LOAD DESCRIPTION = LPT Blade-off 23Feb02

PROGRAM P0889 ; VERSION: 5.00

ENGINE MODEL: PW307A HOTO/Fn-REV
PART NUMBER: LP ShaftV21L33az
SHAFT TYPE: 24K LCF 21/06/02

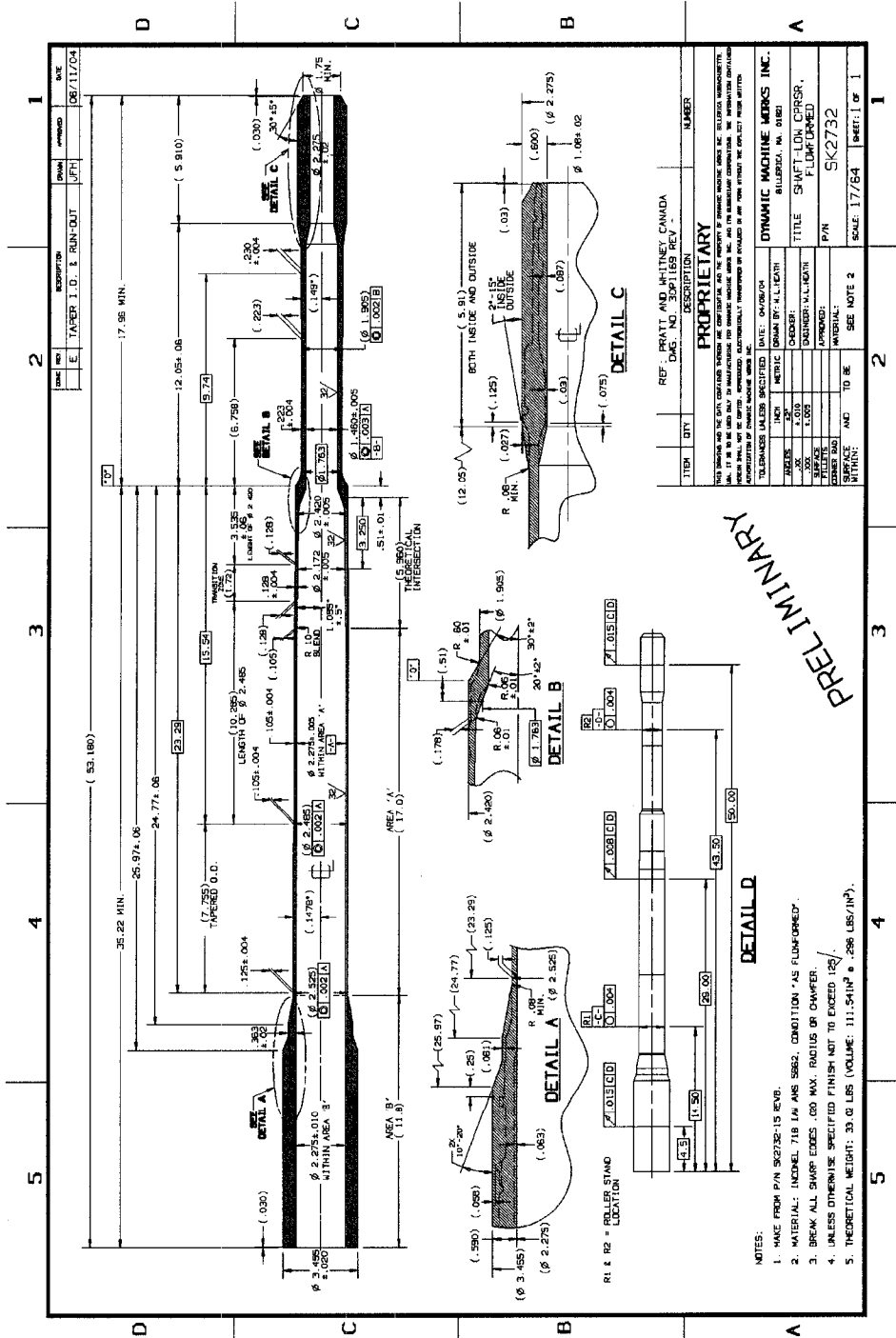
Table with columns for sect numb, axial force, shaft torque, bending moment, axial stress, shear stress, bending stress, centrifugal stress, plastic stress factor, max-plast stress, ultimate stress, max-plast yield, and max-plast ultimate. Row 1 shows stress data for section 1.

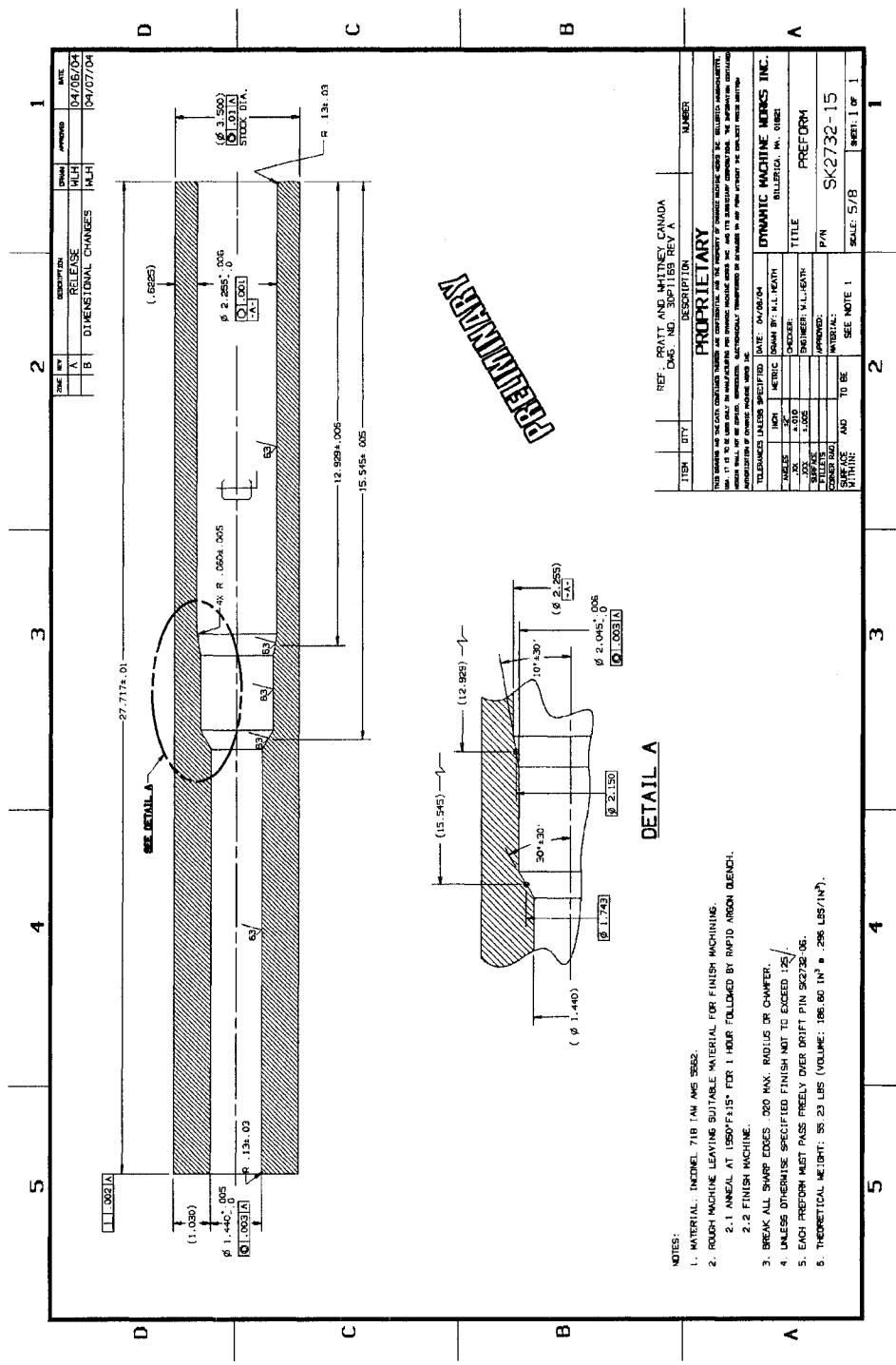
PART NUMBER: LP Shaftv2:1_t3az
 SHAFT TYPE: 24K LCF 21/06/02

LOAD CASE	1	2	3	4	5	6	7
SECT NUMB	LCF-MCF ANALYSIS	LCF-MCF ANALYSIS	GYROSCOPIC PRECESSION	COMPRESSOR BLADE-LOSS	COMPRESSOR BLADE-LOSS	MEDIUM BIRDSTRIKE	LARGE BIRDSTRIKE
1	.64	.47	.52	1.33	.54	.92	.75
2	.46	.35	.30	1.30	.53	.90	.73
3	.92	.81	.73	1.30	.83	1.22	1.16
4	.96	.77	.83	1.31	.90	1.31	1.20
5	.96	.79	.70	.65	.78	1.07	.98
6	.97	.74	.83	.98	.94	1.25	1.10
7	.96	.71	.75	.83	.91	1.21	1.19
8	.96	.69	.82	.76	.84	1.20	1.18
9	.96	.62	.79	.71	.74	1.11	1.11
10	.91	.68	.97	.93	.95	1.43	1.47
11	.84	.64	.70	.64	.64	1.01	1.01
12	.87	.67	.96	.91	.90	1.39	1.44
13	.86	.73	.92	.96	.85	1.36	1.50
14	.93	.81	.93	1.04	.97	1.46	1.64
15	.90	.81	.80	1.01	1.08	1.48	1.63
16	.89	.81	.69	1.00	1.15	1.47	1.61
17	.93	.85	.71	1.02	1.18	1.52	1.64
18	.95	.87	.63	.93	1.10	1.38	1.46
19	.85	.79	.43	.68	.82	1.03	1.03
20	.95	.87	.61	1.00	1.22	1.51	1.69
21	.94	.86	.60	1.00	1.22	1.51	1.69
22	.94	.86	.56	.91	1.12	1.46	1.58
23	.96	.86	.74	.86	.99	1.47	1.63
24	.96	.82	.82	.92	.98	1.50	1.56
25	.92	.75	.75	.76	.71	1.12	.92
26	.12	.07	.28	.91	.72	.89	.81
27	.16	.15	.33	.82	.65	.84	.66
28	.46	.41	.43	.45	.45	.79	.66
29	.17	.10	.46	.61	.52	.81	.70
30	.12	.12	.36	.37	.37	.48	.37

APPENDIX X

Dynamics Machine Works Contract Proposal



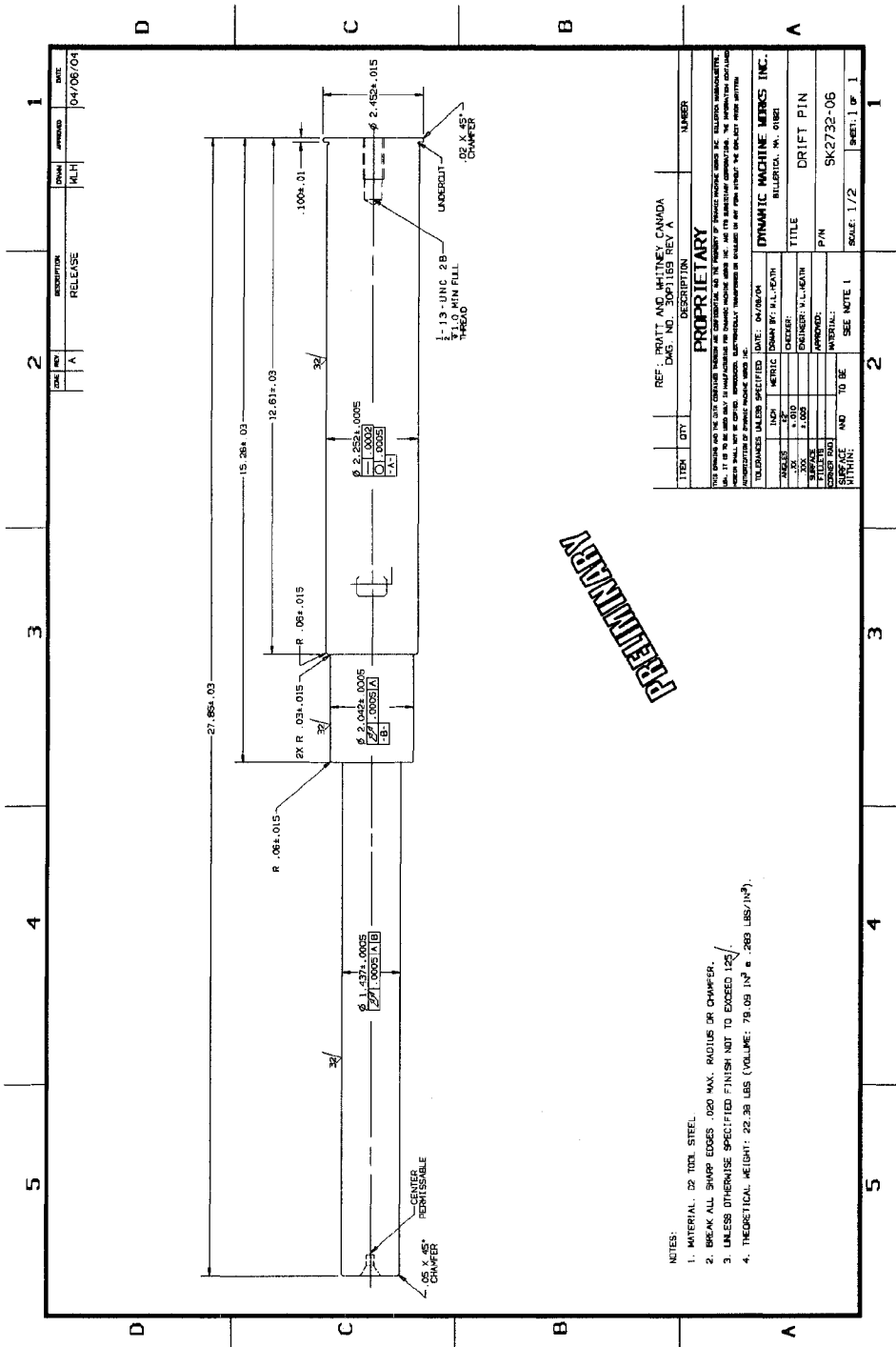


DETAIL A

- NOTES:
1. MATERIAL: INCONEL 718 (AW AMS 5642)
 2. ROUGH MACHINE LEAVING SUITABLE MATERIAL FOR FINISH MACHINING.
 - 2.1 ANNEAL AT 1350°F ± 15° FOR 1 HOUR FOLLOWED BY RAPID AIR COOL.
 - 2.2 FINISH MACHINE.
 3. BREAK ALL SHARP EDGES .020 MAX. RADIUS OR CHAMFER.
 4. UNLESS OTHERWISE SPECIFIED FINISH NOT TO EXCEED 125.
 5. EACH PREFORM MUST PASS FREELY OVER DRAFT PIN SK2732-06.
 6. THEORETICAL WEIGHT: 98.23 LBS (VOLUME: 106.60 IN³ @ .296 LBS/IN³).

ITEM	QTY	DESCRIPTION	NUMBER
PROPRIETARY			
THIS DRAWING AND THE DATA CONTAINED THEREIN ARE CONFIDENTIAL AND THE PROPERTY OF DYNAMIC MACHINE WORKS INC. IT IS TO BE KEPT SECRET AND NOT REPRODUCED OR TRANSMITTED IN ANY FORM OR BY ANY MEANS, ELECTRONIC OR MECHANICAL, INCLUDING PHOTOCOPYING, RECORDING, OR BY ANY INFORMATION STORAGE AND RETRIEVAL SYSTEM. UNLESS OTHERWISE SPECIFIED, DIMENSIONS UNLESS OTHERWISE SPECIFIED ARE IN INCHES AND DECIMALS THEREOF. UNLESS OTHERWISE SPECIFIED, DIMENSIONS UNLESS OTHERWISE SPECIFIED ARE IN MILLIMETERS AND DECIMALS THEREOF.			
UNITS	INCH	METRIC	MILLIMETER
DESIGN	BY: S.L.P. (S)	DATE:	04/06/04
DRWING	NO: 1.000	REVISED:	
SURFACE	FINISH:	BY: S.L.P. (S)	
TOLERANCE	± .0005	BY: S.L.P. (S)	
SCALE	AS SHOWN	BY: S.L.P. (S)	
TITLE	DYNAMIC MACHINE WORKS INC.		
P/N	SK2732-15		
SCALE	5/8	SEE NOTE 1	SHEET 1 OF 1

DATE	APPROVED	DATE
04/06/04	[Signature]	04/07/04
DESCRIPTION	CHG. NO.	
RELEASE	HLH	
DIMENSIONAL CHANGES	HLH	



- NOTES:
1. MATERIAL: D2 TOOL STEEL.
 2. BREAK ALL SHARP EDGES .020 MAX. RADIUS OR CHAMFER.
 3. UNLESS OTHERWISE SPECIFIED FINISH NOT TO EXCEED 125.
 4. THEORETICAL WEIGHT: 22.36 LBS (VOLUME: 78.09 IN³ @ .283 LBS/IN³).

ITEM	CITY	REF.	PRATT AND WHITNEY CANADA	NUMBER
		DWG. NO.	SK2732-06	
		DESCRIPTION	DRIFT PIN	
		RELEASE	1/24	
		DATE	04/06/04	

TITLE	DRIFT PIN
PIN	SK2732-06
SCALE	1/2
SHEET	1 OF 1

INCH	MM
1/16	1.5875
1/8	3.175
3/16	4.7625
1/4	6.35
5/16	7.9375
3/8	9.525
7/16	11.1125
1/2	12.7
9/16	14.2875
5/8	15.875
11/16	17.4625
3/4	19.05
13/16	20.6375
7/8	22.225
15/16	23.8125
1	25.4

PRELIMINARY